INVESTIGATION OF CIRCULAR MICROSTRIP ANTENNA WITH IMPROVED INPUT AND RADIATION CHARACTERISTICS

A THESIS SUBMITTED IN PARTIAL FULFILLMENT OF THE REQUIREMENTS FOR THE DEGREE OF DOCTOR OF PHILOSOPHY

ZONUNMAWII

MZU REGN NO: 1904972

PH.D. REGN NO: MZU/Ph.D./ 1618 of 26.07.2019

DEPARTMENT OF ELECTRONICS & COMMUNICATION ENGINEERING
SCHOOL OF ENGINEERING AND TECHNOLOGY

AUGUST 2022

INVESTIGATION OF CIRCULAR MICROSTRIP ANTENNA WITH IMPROVED INPUT AND RADIATION CHARACTERISTICS

BY

Zonunmawii
Department of Electronics & Communication Engineering

Name of Supervisor : Dr. Abhijyoti Ghosh
Name of Joint Supervisor : Prof. Sudipta Chattopadhyay

Submitted

In partial fulfillment of the requirement of the Degree of Doctor of Philosophy in Electronics and Communication Engineering of Mizoram University, Aizawl

Department of Electronics and Communication Engineering
School of Engineering and Technology
MIZORAM UNIVERSITY
(*A Central University*)
Tanhril**,** Aizawl - 796 004, Mizoram

CERTIFICATE

This is to certify that the thesis entitled "**Investigation of Circular Microstrip Antenna with Improved Input and Radiation Characteristics"** submitted to Mizoram University for the award of the degree of **Doctor of Philosophy Electronics and Communication Engineering** by **Zonunmawii**, Ph.D. Registration No. **MZU/Ph.D./1618 of 26.07.2019**, is Ph.D. scholar in the Department of Electronics and Communication Engineering, under our guidance and supervision and has not been previously submitted for the award of any degree in any Indian or foreign University. She has fulfilled all criteria prescribed by the UGC (Minimum Standard and Procedure governing Ph.D. Regulations). She has fulfilled the mandatory publication (Publication enclosed) and completed Ph.D course work. It is also certified that the scholar has been admitted in the Department through an entrance test, followed by an interview as per UGC Regulation of 2016.

Date: (Dr. Abhijyoti Ghosh)
Place: Aizawl Supervisor

(Prof. Sudipta Chattopadhyay)
Joint Supervisor

MIZORAM UNIVERSITY
Aizawl -796 004

(August 2022)

DECLARATION

I, **Zonunmawii,** hereby declare that the subject matter of this thesis entitled "**Investigation of Circular Microstrip Antenna with Improved Input and Radiation Characteristics"** is the record of work done by me, that contents of this thesis did not form basis of the award of any previous degree to me or to do the best of my knowledge to anybody else, and that the thesis has not been submitted by me for any research degree in any other University/Institute.

This is being submitted to the Mizoram University for the degree of Doctor of Philosophy in **Electronics and Communication Engineering.**

(Zonunmawii)
Candidate

(Dr. Abhijyoti Ghosh)
Supervisor

(Prof. (Dr.) Sudipta Chattopadhyay)
Joint Supervisor

Head of the Department

Acknowledgement

Praise be to **GOD** for his uncountable blessings and for the wisdom he has bestowed upon me, the strength and good health in order to finish this research work.

I would like to express my deepest appreciation and indebtedness to my supervisor, **Dr. Abhijyoti Ghosh**, Assistant Professor, Department of Electronics and Communication Engineering, Mizoram University and joint supervisor, **Prof. Sudipta Chattopadhyay,** Dean of School of Engineering and Technology, Mizoram University, for their support, effective guidance, timely motivation, constant encouragement and valuable suggestions throughout the course of this research work. I am also thankful to **Dr. Reshmi Maity**, Head of the Department of Electronics and Communication Engineering, Mizoram University, Aizawl, Mizoram. I am grateful to **Prof. L. Lolit Kumar Singh**, Professor, Department of Electronics and Communication Engineering, Mizoram University, for his sincere guidance during the course of my research work.

I thank my doctoral committee members **Prof. N.P. Maity** and **Dr. Achinta Baidya** for their suggestions and comments that have enabled me to complete the research work. I am also thankful to **Mr. Sarath Kumar Annavarapu** for his help and support.

I appreciate the love, support, effort and sacrifices of my parents, **Mr. Zothantluanga** and **Mrs. Lalbiakmawii** for educating me preparing me for my future. I owe thanks to my husband, **Mr. Lalmuankima** for his support, understanding and prayers during the course of research work. I dedicate this work to my children, who made me stronger, better and motivates me to keep moving forward. You are my everything.

Lastly, I would like to convey special thanks to one and all those who have directly or indirectly extended their helping hand in this endeavor.

ZONUNMAWII

Table of Contents

Acknowledgement			i
Table of Contents			ii
List of Figures			v
List of Tables			ix
Chapter 1	**Introduction and Literature Review**		1 - 13
	1.1	Introduction	1
	1.2	Basics of Microstrip Antenna	2
		1.2.1 Basic Structure	2
		1.2.2 Advantages and Limitations	4
	1.3	Feeding Techniques	4
	1.4	Existing Techniques to Improve the Radiation Characteristics of a Microstrip Antenna	8
	1.5	Conclusion	13
Chapter 2	**Improvement of Polarization Performance and Gain Properties with Shorting and Strip Loading Approach of Circular Microstrip Antenna**		14 - 30
	2.1	Introduction	14
	2.2	Shorted Circular Microstrip Antenna Approach to Improve the Cross Polarization Performance	15
		2.2.1 Design Technique	16
		2.2.2 Parametric Studies	17
		2.2.3 Optimum Structure	20
		2.2.4 Simulated Results	20
	2.3	Strip Loading Approach to Improve the Cross Polarization Performance of Circular Microstrip Antenna	24
		2.3.1 Evolution of Optimum Structure	24
		2.3.2 Performance from Optimized Antenna Structure	27
	2.4	Conclusion	29
Chapter 3	**Wideband Circular Microstrip Antenna with Improved Polarization Purity using Defected Ground Structure Approach**		31-47
	3.1	Introduction	31
	3.2	Curved Shaped Defected Ground Structure: A way to	33

achieve high Polarization Purity, Wide Bandwidth and Stable Gain

3.2.1 Theoretical Background and Parametric Studies 33

3.2.2 Optimum Structure 38

3.2.3 Simulated Result and Discussion from Optimized Structure 38

3.3 Rectangular Shaped Defected Ground Structure Integrated CMA: A Way to Enhance Impedance Bandwidth and Polarization Purity 40

3.3.1 Theoretical Background and Parametric Studies 41

3.3.2 Optimum Structure 44

3.2.3 Results and Discussions 45

3.4 Conclusion 47

Chapter 4 Reduced Surface Wave Approach with Modulation of Fringing Field to Yield Concurrent Improvement in Radiation Properties of Circular Microstrip Antenna 48 - 74

4.1 Introduction 48

4.2 Theoretical Insight 51

4.2.1 Excited Mode 51

4.2.2 Effective Permittivity and Resonant Frequency 55

4.2.3 Gain and Efficiency 58

4.2.4 Cross Polarized Radiation in Principal Planes 62

4.2.5 Cross Polarized Radiation in Diagonal Planes 63

4.3 Parametric Studies and Optimization 66

4.4 Proposed Structure 69

4.5 Experimental Results and Discussions 70

4.6 Conclusion 74

Chapter 5 Modulation of Cavity Field Under Circular Microstrip Antenna for Reduced Horizontal Radiation with Omni-Present Improvement of Radiation Properties 75 - 98

5.1 Introduction 75

5.2 Antenna Evolution and Analysis 77

5.2.1 Structural Evolution 77

5.2.2 Evolution Analysis: Resonant Frequency 79

5.2.3 Evolution Analysis: Cavity Field Modulation with Modulating Patch Surface Geometry 82

5.2.4 Evolution Analysis: Radiation Characteristics 86
5.2.5 Circuit Model Approach 90
5.3 Proposed Structure 92
5.4 Results and Discussions 92
5.5 Conclusion 98
Chapter 6 Conclusion and Scope of Future Studies 99 - 101
References 102 - 116
Brief Bio-data of candidate 117
List of Publications 118
Particulars of the candidate 119

List of Figures

Fig. 1.1	Basic structure of microstrip patch antenna	3
Fig. 1.2	Different shapes of a microstrip patch antenna (a) square (b) rectangle (c) dipole (d) circular (e) rectangular (f) circular ring.	3
Fig. 1.3	Coaxial probe feeding technique (a) top view (b) side view	5
Fig. 1.4	Microstrip line feeding technique	6
Fig. 1.5	Aperture coupled feeding technique	7
Fig. 1.6	Proximity coupled feeding technique	7
Fig. 2.1	Shorting Walls integrated circular patch (a) view from top (b) cross sectional view	16
Fig. 2.2	Co-polar peak gain variation with respect to the short angle for different substrate width (a) 0.787mm (b) 1.58 mm	17
Fig. 2.3	Polarization purity variation with respect to the short angle for different substrate (a) FR4 (b) glass with different substrate thickness	18
Fig. 2.4	Resonant frequency variation of the proposed structure for different shorting angles (θ) (a) FR4 substrate (b) Glass substrate.	19
Fig. 2.5	Simulated S_{11}versus frequency of the CMA and present antenna with $\theta = 100^0$ (a) FR4 (b) Glass substrate.	21
Fig. 2.6	Simulated radiation pattern of the proposed antenna ($\theta = 100°$) (a) FR4 substrate with thickness 0.787 mm (b) FR4 substrate with thickness 1.58 mm (c) Glass substrate with thickness 0.787 mm (d) Glass substrate with thickness 1.58 mm.	23
Fig. 2.7	Surface current distribution over patch for $\theta = 100^0$	23
Fig. 2.8	Schematic representation of (a) traditional CMA (b) proposed rectangular strip loaded CMA.	24
Fig. 2.9	Variation of CP-XP separation with respect to length of the rectangular strip with different values of rectangular strip width.	25
Fig. 2.10	Variation of co polarization gain with respect to length of the rectangular strip with different values of rectangular strip width.	26
Fig. 2.11	Simulated S_{11} profile of conventional CMA and proposed rectangular strip loaded CMA.	27

Fig. 2.12	E-plane gain profile of the conventional CMA and rectangular strip loaded CMA (optimum).	28
Fig. 2.13	H-plane gain profile of the conventional CPA and rectangular strip loaded CMA (optimum).	28
Fig. 2.14	Field distribution over the substrate of the proposed structure (optimum).	29
Fig. 3.1	Top view of the proposed structure with curved dumbbell shape DGSs at the non-radiating edges.	33
Fig. 3.2	Electric field and current distribution over the patch surface (a) Fundamental dominant TM_{11} mode (b) Next higher-order TM_{21} mode.	34
Fig. 3.3	Simulated plot of CP-XP isolation with respect to variation of CD-DGS rectangular head slot width (*sw*). (Keeping d = 0.5 mm, sl = 4 mm fixed).	35
Fig. 3.4	Simulated plot of CP-XP isolation with respect to variation of dumbbell arc (*d*) of CD-DGS. (*sw* = 1 mm (optimized), *sl* = 4 mm (fixed)).	35
Fig. 3.5	Simulated plot of CP-XP isolation with respect to variation of CD-DGS rectangular head slot length (*sl*). (*sw* = 1 mm (optimized), d = 0.5 mm (optimized).	36
Fig. 3.6	H plane cross-polarization radiation with respect to CDDGS rectangular head slot length (*sl*).	37
Fig. 3.7	Variation of gain of the proposed CD-DGS structure with respect to CD-DGS rectangular head slot length (*sl*).	37
Fig. 3.8	Simulated S_{11} profile of conventional and proposed CDDGS integrated CMA.	38
Fig. 3.9	E plane radiation pattern of the conventional and proposed structure.	39
Fig. 3.10	Normalized H plane radiation pattern of the conventional and proposed structure.	40
Fig. 3.11	Schematic representation of proposed Rectangular defective ground structure (RDGS) integrated CMPA (a) top view (b) side view.	41
Fig. 3.12	Variation of impedance bandwidth (%) as a function of RDGS width with RDGS length (*sl*) fixed at 14 mm.	42
Fig. 3.13	Reflection coefficient profile for conventional CMA and RDGS incorporated CMA with RDGS length (*sl*) fixed at 14 mm.	43
Fig. 3.14	Variation of H plane XP level as a function of RDGS width (*sw*) with RDGS length (*sl*) fixed at 14 mm.	44
Fig. 3.15	Simulated reflection coefficient profile of conventional and	45

	proposed rectangular DGS integrated CMA.	
Fig. 3.16	Normalized E plane radiation pattern of conventional and proposed rectangular DGS integrated CMA.	46
Fig. 3.17	Simulated conventional and proposed structure radiation pattern in H plane.	46
Fig. 4.1	The schematic representation of patch (a) conventional CMA and (b) the proposed antenna with field distribution at lower radiating slots for conventional and proposed antenna.	50
Fig. 4.2	Electric surface current vector on patch surface (a) conventional circular patch, (b) Proposed patch, Electric field magnitude over patch surface (c) conventional circular patch, (d) Proposed patch, Electric field vector within substrate (e) conventional circular patch, (f) Proposed patch, [All figures are in same scale which is provided at left of each row]	52
Fig. 4.3	The effect of shorting strip on modes	54
Fig. 4.4	Plot for solution of equations (4.4) and (4.7): Variation of $(\varepsilon_r)_N$ and NPC as a function of shorting angle ψ.	57
Fig. 4.5	Computed and simulated variations of resonant frequency as a function of shorting angle ψ for two different substrate thickness.	58
Fig. 4.6	Variation of (a) peak gain and (b) efficiency of the proposed antenna as a function of shorting angle ψ for two substrate thicknesses.	60
Fig. 4.7	Variation of BG-HG isolation of the proposed antenna as a function of shorting angle ψ for two substrate thickness.	61
Fig. 4.8	Simulated H plane radiation patterns of the proposed antenna for shorting angle $\psi = 70^0$.	62
Fig. 4.9	Comparison of diagonal plane radiation pattern of conventional CMA and proposed shorted circular patch at same frequency.	63
Fig. 4.10	Comparison of diagonal plane radiation pattern of conventional CMA and proposed shorted circular patch at same frequency.	64
Fig. 4.11	Simulated electric field magnitude distribution within substrate at excited mode (a) conventional CMA (b) proposed CMA.	65
Fig. 4.12	Simulated radiation patterns (a) E plane and (b) H plane for the conventional CMA and the proposed antenna for different shorting angle ψ.	67
Fig. 4.13	Surface current distribution over patch for (a) $\psi = 70^\circ$ and (b) $\psi = 100^\circ$.	68
Fig. 4.14	Photo of fabricated prototype (a)Top view, (b) bottom view.	69

Fig. 4.15	Simulated and measured reflection coefficient profile of the proposed antenna.	70
Fig. 4.16	Comparison of measured radiation patterns for conventional CMA and proposed antenna (a) E plane, (b) H plane (f = 9.13 GHz).	72
Fig. 5.1	Antenna Evolution (a) Ant#1, (b) Ant#2 (c) Ant#3	78
Fig. 5.2	Schematic representation of electric surface current path on patch (a) Antenna#2, (b) Antenna#3	80
Fig. 5.3	Simulated electric surface current path on patch (a) Antenna#2, (b) Antenna#3	81
Fig. 5.4	Simulated electric field magnitude over substrate (a) Antenna#1, (b) Antenna#2, (c) Antenna#3	83
Fig. 5.5	Simulated electric field vector over substrate (a) Antenna#1, (b) Antenna#2, (c) Antenna#3	85
Fig. 5.6	Comparison of H plane radiation pattern(a) Antenna#1 and Antenna#2 (b)Antenna#1 and Antenna#3, (c) Comparison of E plane radiation patterns of Antenna#1, Antenna#2 and Antenna#3.	88
Fig. 5.7	Effect of polarization current in horizontal radiation at E plane	89
Fig. 5.8	Approximate circuit model (a) Conventional CMA, (b) proposed antenna	90
Fig. 5.9	Fabricated prototype (a) Top view (b) bottom view	92
Fig. 5.10	Simulated and measured reflection coefficient profiles of proposed Antenna#3	93
Fig. 5.11	Comparison of simulated and measured radiation patterns of conventional Antenna#1 and proposed Antenna#3 (a) H plane, (b) E plane.	94
Fig. 5.12	Simulated electric field magnitude over substrate in proposed Antenna#3.	95
Fig. 5.13	Variation of gain of proposed antenna at both principal planes within it's 3 dB beam widths	96
Fig. 5.14	Variation of gain and efficiencies of proposed antenna as function of frequency in the operating band.	97

List of Tables

Table2.1	The detailed parameters of the proposed rectangular strip loaded CMA (Substrate thickness h = 1.575 mm)	27
Table 3.1	The detailed parameters of the proposed rectangular DGS loaded CMA (Substrate thickness h = 1.575 mm)	44
Table 4.1	The detailed parameters of the proposed and conventional antenna (Substrate permittivity ε_r = 2.33, thickness h = 0.787 mm)	70
Table 4.2	Radiation properties of the proposed Antenna.	73
Table 4.3	Comparison of the proposed work with recently published works.	73
Table 5.1	Comparison of simulated and computed resonance frequency using proposed theory	84
Table 5.2	Performance comparison of the present antenna with recently reported relevant works	97

CHAPTER

1

Introduction and Literature Review

1.1 Introduction

The beginning of communication can be traced back to 1844 when Morse successfully transmitted a message over a single wire. The age of wireless communication started in 1886 when German scientist Heinrich Hertz discovered radio waves. In 1988 the first antenna was built by Heinrich Hertz for his experiment to prove the existence of radio waves. Antenna is a radiator by which radio frequency waves are transmitted or received. Antennas have wide range of configuration and can be classified to understand their functionality and physical structure. Some of the common configuration of antenna includes wire antennas, aperture antennas, lens antennas and microstrip antennas. Significant efforts have been made by scientists and researchers to explore different types of antennas for use in the wireless world. Initially communication happens at very low radio frequency so the size of the antennas was gigantic. As time goes by, requirement of smaller antennas increases as the demand for wireless world shifts towards higher spectrum operations. In the present wireless world, mobility of wireless device is imperious and has become an essential constraint for developing the antennas compatible with handheld communication devices. This demands for light weight, low profile, compact and low-cost antennas. In this context, microstrip antenna emerges as the best choice to meet all the requirements of the modern wireless world.

In the kilomegacycle range, the first concept of microstrip antenna as a new transmission technology is introduced by Greig and Engleman [1] in the year 1952. In 1953, Deschamps [2] first proposed the concept of microstrip antenna as a radiator. The concept of microstrip antenna was patented by Gutton and Bassinot [3] in 1955. The concept of microstrip antenna was proposed by Deschamps but it came into

existence in 1970's when Howell [4] and Munson [5] practically proposed it. In 1960, Lewin [6] investigated and reported the radiation from strip line discontinuities. During the year 1955 to almost 1969, research has been carried out for radiation from discontinuities of strip line and researchers brought forward different perspectives [7-9]. The inherent advantage of microstrip antenna like light weight, structural simplicity, low cost and easy to fabricate attract many antenna researchers. Researchers reported theoretical analysis and practical implementation of different geometry of microstrip antenna [10-20]. Two well cited and famous books were published in the early 1980's by Bahl and Bhatia [21] and James, Hall and Wood [22]. These two books cover all the achievements in the field of microstrip antennas. Nearly after a decade, James et. al published the first handbook [23] in 1989. Balanis in 1997 published a book which covers the fundamental antenna theory and design related issues of microstrip antenna [24]. The microstrip antennas are gaining popularity day by day but they also have some inherent limitations which need to be addressed and overcome.

This chapter deals with the basic historical background of microstrip antenna in section 1.1. In section 1.2 basic structure, advantages and limitations are covered. In section 1.3 different feeding techniques of microstrip antenna is discussed. In section 1.4 a survey on the existing techniques to improve the radiation characteristics of microstrip antenna has been documented. Lastly, section 1.6 presents the summary of the chapter.

1.2 Basics of Microstrip Antenna

Microstrip antenna (MA) consist of a patch which is a conducting metal strip on one side of a dielectric substrate and a ground plane which is another conducting metal plate of bigger size on the other side of the substrate. The following subsection covers the basic structure, basic operation, advantages and limitations of a microstrip antenna.

1.2.1 Basic Structure

In its most basic form, a microstrip antenna consists of a thin dielectric substrate which is sandwiched between two conducting plates. The lower conducting plate acts

as the ground plane and the other conducting plate acts as the patch. The length of the upper metallic plate geometry approaches a half-wavelength long of its operating frequency. Conducting materials such as gold and copper are generally used as the patch. The basic structure of a circular microstrip antenna is shown in Fig. 1.1.

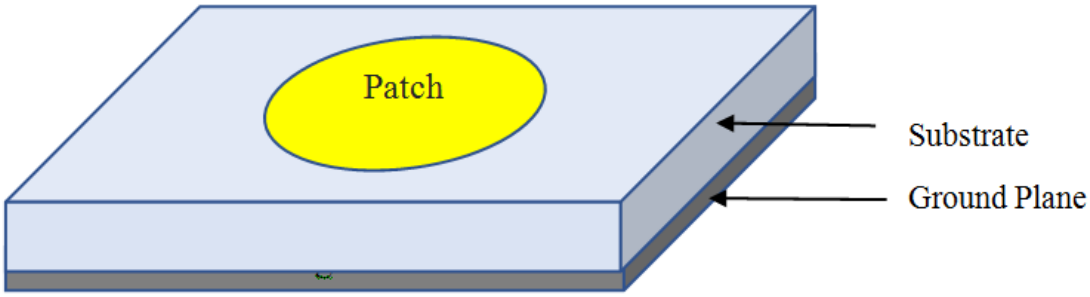

Fig. 1.1 Basic structure of microstrip antenna

A microstrip antenna can come in various shapes. Some common shapes of microstrip antenna are shown in Fig. 1.2. To simplify the analysis and predict the performance, the patch is generally rectangular, circular, elliptical and triangular.

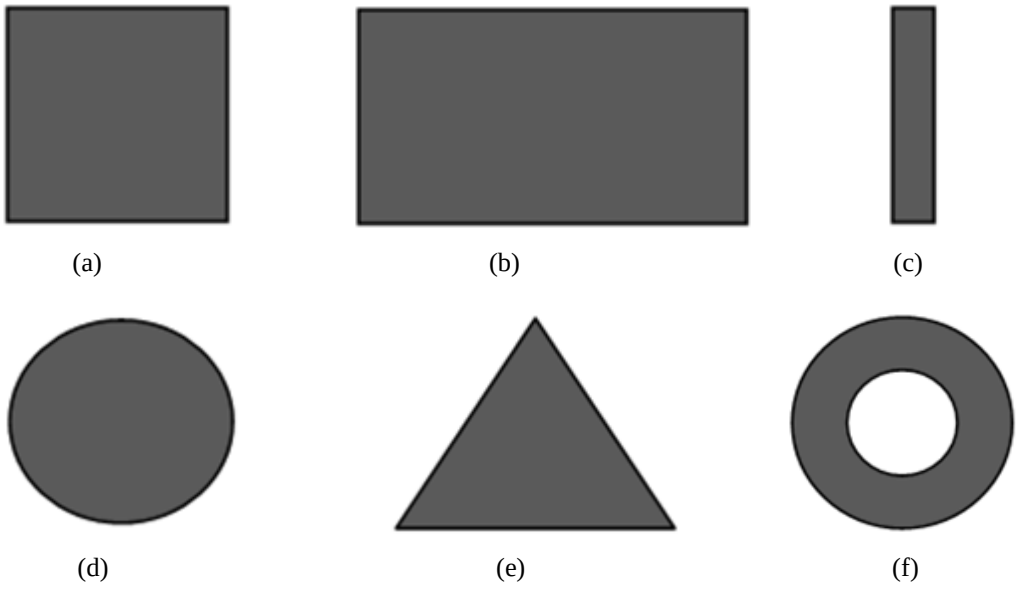

Fig. 1.2 Different shapes of a microstrip antenna (a) square (b) rectangle (c) dipole (d) circular (e) rectangular (f) circular ring

1.2.2 Advantages and Limitations

Microstrip antennas are gaining attention for use in wireless application, handheld wireless devices, military applications and commercial sectors. The principal advantage which makes the microstrip antenna popular are low profile, light weight, small in size, ease of mass production as the fabrication cost is low, both circular and linear polarization can be obtained from a single MA. The MA can work in multiband frequency i.e., they are capable of dual, triple or further more frequency operation. The MA are flexible, can be mounted to any curved surface and can be molded to any shape. They can be easily integrated with microwave monolithic integrated circuits (MMICs) [25-28].

Besides the many advantages mentioned above, microstrip antenna has some limitations like narrow impedance bandwidth (typically less than 5%), low efficiency, low gain, low power handling capacity, excitation of surface waves, less co-polarization to cross polarization isolation (polarization purity), large ohmic losses, and design complexity due to small size [25-28].

The different techniques employed for improving the radiation characteristics are discussed in section 1.4.

1.3 Feeding Techniques

Variety of feeding techniques is available for feeding microstrip antennas. To get efficient radiation from the patch, the antenna should fed properly. Feeding mechanisms available for microstrip antenna are broadly classified into two categories namely contacting and non-contacting. In the contacting method, contacting elements such as microstrip line is used to feed RF power directly to the radiating patch. In the non-contacting method, power transfer between the radiating patch and the microstrip line is done by electromagnetic field coupling. Microstrip line feeding, coaxial cable feeding, proximity coupling and aperture coupling are the four most common feeding techniques used in microstrip antenna. The two most popular contacting method used for feeding are coaxial cable feeding and microstrip line feeding whereas proximity coupling and aperture coupling are the two extensively used non-contacting type of feeding.

The coaxial probe feeding is one of the most common feeding techniques used for feeding microstrip antenna. The basic arrangement of coaxial probe feed is shown in Fig. 1.3. The inner material of the coaxial cable extends through the substrate which is a dielectric material and is connected and soldered to the patch. The outer material of the coaxial cable is connected to the ground plane. The probe or the feed point can be placed at any desired contact point on the patch so that impedance matching is maximized. This feed method is easy to fabricate. If it is properly soldered, spurious radiation from the probe is very less and this makes the feeding mechanism more versatile and most efficient. However, it has some limitations such as narrow bandwidth, high cross polarization radiation due to asymmetries in feed position, impedance matching problem and inappropriate with array structures.

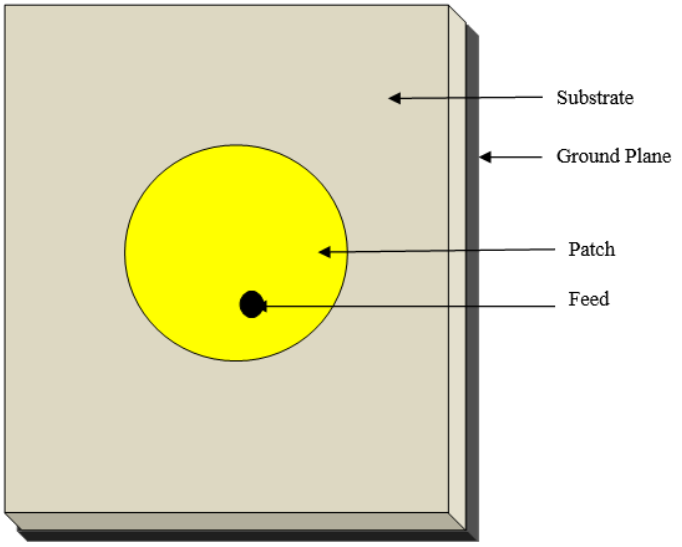

(a)

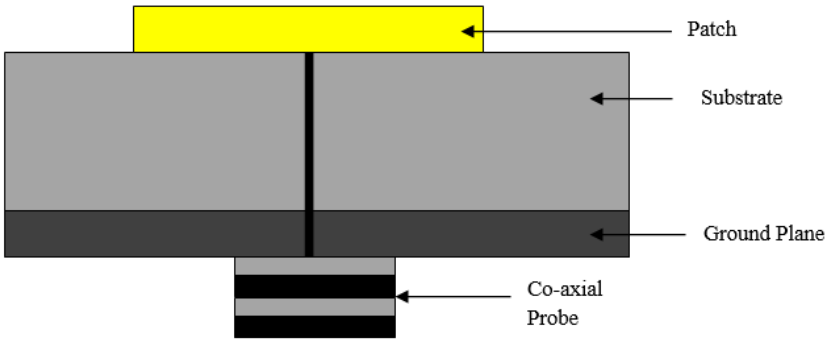

(b)

Fig. 1.3 Coaxial probe feeding technique (a) top view (b) side view

In microstrip line feeding a microstrip line or strip is directly connected to the edge of the microstrip patch. The basic arrangement of this type of feed is shown in Fig. 1.4. Compared to the width of the patch, the conducting strip is smaller. The advantage of this type of feed arrangement is that the feed can be etched on the same substrate so as to provide a planar structure. It is an easy feeding technique that provides ease of fabrication, simplicity in analysis and modeling and provides good impedance matching. The increase in thickness of the dielectric substrate hampers the bandwidth of the antenna. This is due to the increase in surface waves and increase in spurious feed radiation as the thickness of the substrate increases. The increase in spurious feed radiation result in undesirable cross polarized radiation.

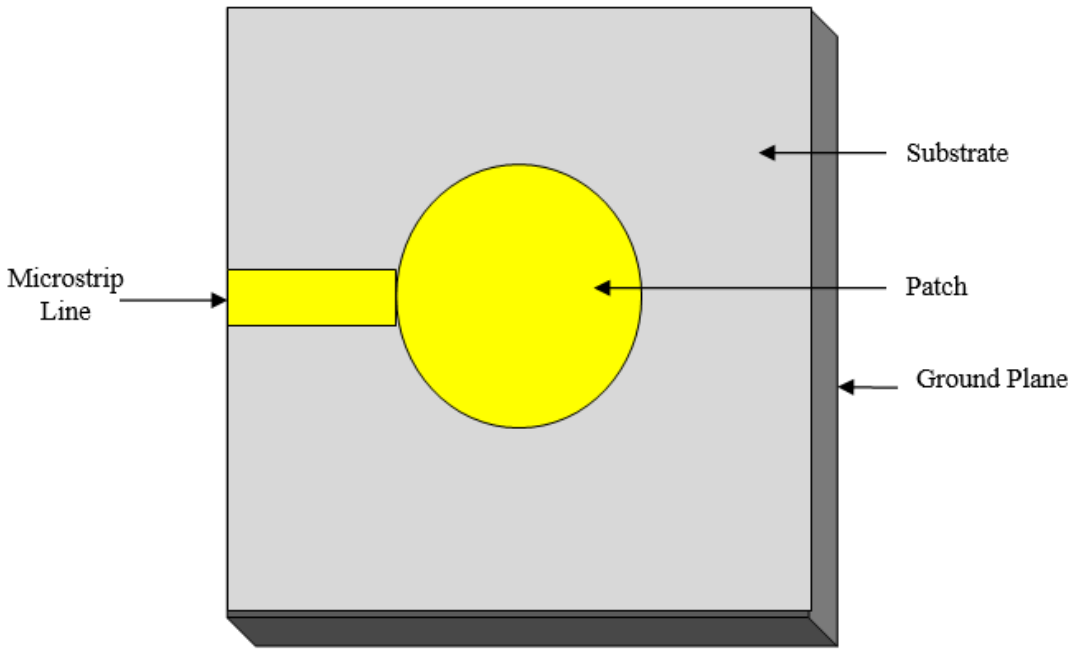

Fig. 1.4 Microstrip line feeding technique

Aperture couple feeding is another type of feeding technique. In this type of feeding arrangement, the ground plane is sandwiched by two substrates as shown in Fig. 1.5. The two substrates have different height and different dielectric constant. The microstrip antenna is etched on top of the upper substrate and the microstrip line is etched on the lower substrate. A slot or an aperture is made for coupling the patch and the feed. To lower cross polarization the coupling aperture is usually centered under the patch. The shape, size and location of the aperture determine the amount of coupling from the feed line to the patch. Spurious feed radiation is minimized since

the patch and the feed line are separated by the ground plane. This results in improved bandwidth. The major drawback of this feeding arrangement is that it is difficult to fabricate due to the multi-layers and narrow bandwidth.

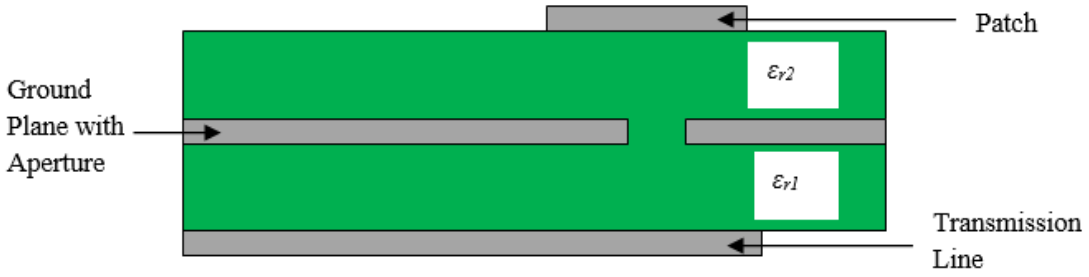

Fig. 1.5 Aperture coupled feeding technique

Proximity coupled feeding is non-contact type of feeding mechanism and shown in Fig. 1.6, It is also called as electromagnetic coupling scheme. Two dielectric substrates of different height are used and the feed line is between the two substrates. The patch is placed on top of the upper substrate. The major advantage of this feed technique is elimination of spurious feed radiation which provides a very high bandwidth. The main drawback of this scheme is that it is difficult to fabricate. This is due to the two dielectric layers which need proper alignment making the fabrication process complex.

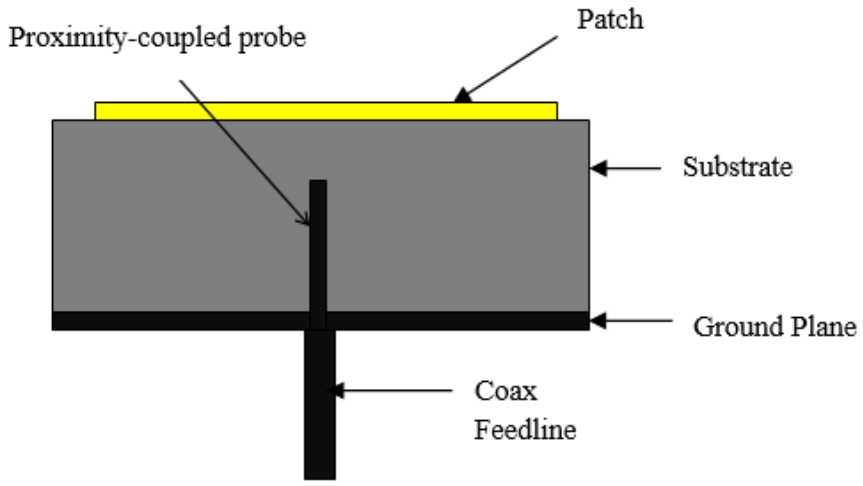

Fig. 1.6 Proximity coupled feeding technique

1.4. Existing Techniques to Improve the Radiation Characteristics of a Microstrip Antenna

The radiation characteristics of a basic MA suffers from several significant flaws; for instance, narrow bandwidth, low gain, low efficiency, poor polarization purity and low power handling capability. Thereupon, over the last few years, substantial attention is given by antenna researchers to enhance various characteristics of MA. Several techniques like the use of electromagnetic bandgap surface [29], air substrate [30], laminated ground plane [31], frequency selective surface absorbing layer [32], and dielectric covers [33] are investigated to improve the radiation characteristics of a MA. The basic radiation characteristics of circular microstrip antenna is discussed in [34]. The effects of finite ground plane have been used to analyze the radiation characteristics of a CMA in [35].

Recently, numerous researches have been carried out to improve the gain of a MA. The demand for fast and reliable connectivity with minimum path loss leads to the increasing demand for high gain antennas. The improvement of bandwidth and gain by incorporating the resonator structure is presented in [36]. Adding a metamaterial resonating structure [37 - 38] is one technique used to enhance the gain of a MA. Gain enhancement is achieved by using several techniques like using of electronic band gap structure (EBG) [39-43] and polarization rotation metasurface (PRMS) [44]. Superstrate materials [45 - 47], metallic reflectors [48], artificial magnetic conductors (AMC) [49] and frequency selective surface (FSS) [50 - 51] are also employed to increase the gain. Loading of shorting pins or shorting slots are proposed in [52 - 55] to enhance the gain a microstrip antenna. Other methods that have been proposed to improve the gain are partial removal of substrate [56 - 57] and defected ground surface (DGS) in [58 - 59].

Narrow bandwidth of a microstrip antenna is one of its major drawbacks. The increasing demand of high-rate data transfer motivates researchers to find a way to improve the bandwidth of a microstrip antenna. Different techniques have been used by various researchers to improve the bandwidth [60 - 86]. Modification in the patch shape like S- shape [62], stacked stair-case patch [63], E- shape [64], multiple notches

on the patch [65], and different types of slots in the patch [66 - 69] are investigated for improvement of bandwidth. Enhancement in bandwidth is achieved by modifying the ground plane and is reported in [70 -74]. In [70] modification of ground plane to partial ground plane is proposed. Partial DGS of hexagonal periodic array [71], ridge ground plane [72], W- shaped ground plane [73] and inserting multiple slots in the ground plane [74] has been employed for improving the bandwidth. Addition of parasitic patch is also proposed in [75-77]. The parasitic patch that is added couples with the main radiating patch and this causes a multiple resonance frequency which creates bandwidth enhancement. In [78-80] air gap technique for bandwidth improvement is reported. Use of multiple feeding techniques [81], metamaterials [82-85] and different liquid crystal polymer substrates [86] are proposed to improve the gain and bandwidth of a microstrip antenna.

A MA emits linearly polarized radiation (Co polar (CP) radiation) in its broadside direction in its dominant mode. Cross polarized (XP) radiation are also emitted in the orthogonal direction. The XP radiation are not desirable. The E-plane XP radiation is always lower than -40 dB so it is not that significant. But the H-plane XP radiation is quite significant which limits the application of the microstrip antenna in the modern wireless world. So, the cross polarized radiation of a microstrip antenna is another aspect that needs to be considered. Researchers have documented many techniques for enhancement of CP-XP isolation.

Non-contact type fed patch for the improvement of CP-XP isolation (polarization purity) in H-plane is reported in [87-89]. CP-XP isolation of -23 dB is reported in [87] using a T-shaped microstrip feed line and an annular ring slot exited by aperture coupling feed. In [88], a broad-band dual-polarized aperture coupled stacked patches provides 30 dB of CP-XP isolation. A differential rat-race feeding structure achieves an excellent CP-XP isolation of 22.5 dB and has been reported in [89].

Improvement of CP-XP isolation in the H-plane can be achieved by modifying the feed structure and this technique is documented in [90-94]. A wideband microstrip antenna fed by meandering strip [90] achieves XP level below -20 dB in both E-plane and H-plane. In [91], a differentially fed patch achieves cross polarization levels lower than 20 dB. A broadband suspended plate antenna [92], dual polarized single antenna

fed by two hybrid input ports [93] and dual-feed dual polarized microstrip antenna [94] have been experimentally studied to improve the polarization purity.

Stacked offset microstrip antenna [95] and two-layer shorted square microstrip antenna [96] are designed and experimented to enhance the CP-XP isolation. In [97], XP radiation of below -16 dB over all angles in both the principal planes using stacked patch structure is reported. A mirrored pair feeding technique of an 8×2 element L band dual polarization stacked microstrip antenna which achieves around 15-20 dB of cross polarized radiation is reported in [98].

Modification of the ground plane of a microstrip antenna is another technique that is reported in [73, 99] to reduce XP radiation. A 3-dimensional U- shaped ground plane for a broadband probe fed microstrip antenna is investigated in [99]. This proposed antenna provides 10-15 dB of XP isolation. In [73] 14 dB CP-XP isolation is attained with a W-shaped ground plane.

Shorted patch configuration for improvement of CP-XP isolation is reported in [100 - 106]. A rectangular patch which is short circuited to the ground plane for use in UMTS application is reported in [100]. A square patch shorted to the ground plane via two shorting walls [101] and a shorted microstrip antenna which is fed by a folded ramp patch suspended by shorting pins [102] are utilized for broad banding. The impedance and radiation characteristics of a classic shorted quarter wavelength microstrip antenna for wide bandwidth are reported in [103]. Shorting the non-radiating edge of a rectangular microstrip antenna [104], a rectangular patch antenna with shorted plate [105] and a microstrip patch with near-field edge-shorted slot [106] are also investigated for reduced cross polarized radiation.

There has been an increasing interest in the use of defected ground surface (DGS) to reduce the cross polarized radiation from a patch. In this technique defect which can be of different forms and dimensions are created on the ground plane to achieve improvement in the radiation characteristics. The concept of DGS for improving the CP-XP isolation is reported in [107-123]. A rectangular patch with bracketed DGS provides around 13 dB of XP suppression in the H-plane [107]. Integrated DGS triangular patches [108-109], Elliptical DGS [110] and circular headed dumbbell DGS

[111] are investigated to address the issues of XP radiation. In [112] a symmetric non-proximal DGS employed with a square confirms up to 8-10 dB improvement in cross polarization level in the H-plane. Significant improvement in CP-XP isolation is achieved using a Dumbbell shaped DGS employed with a rectangular microstrip antenna [113]. A rectangular microstrip antenna with a simple slot type DGS is proposed in [114] which provide 15-25 dB of XP suppression. An asymmetrically shaped DGS has been explored for the first time in [115] and this technique is capable of suppressing over 10 dB. Around 25-28 dB of CP-XP isolation is achieved using a cross type DGS integrated microstrip antenna [116]. Cross polarization reduction in a square microstrip antenna is done based on gap analysis with DGS and suppression of cross polarization level ranges from 10-20 dB [117]. In [118] a compact hexagonal patch antenna with DGS structure is investigated. Suppression of Xp level from -10 dB to -34.6 dB in the boresight direction is achieved with an arc shaped DGS etched in the ground plane under each patch [119]. A Z shaped DGS [120] is investigated for improving impedance matching and cross polarization performance and it provides around 22 dB of XP reduction. In [121] 18-22 dB of polarization purity is achieved using a rectangular microstrip antenna with triangular slotted ground plane. Linear shaped defected ground structure, fractal defected ground structure [122] and F-shaped DGS [123] have been investigated to suppress the cross polarization.

Defected patch surface is a new and simple technique used for improving XP radiation without affecting the back radiation performance. The concept of DPS is almost similar to that of DGS. In the concept of DGS, defects are made on the ground plane whereas in DPS defects are introduced on the patch surface. The concept of DPS for improving cross polarization has been investigated in [124-130]. In [124] more than 28 dB of cross polarization isolation is achieved using a simple compact rectangular microstrip antenna with cross headed dumbbell defected patch surface. Linear slot defects on the patch surface [125] and D- shaped defected patch structure [126] has been designed for suppression of cross polarized radiation. Circular arc defected patch surface on a rectangular microstrip antenna is proposed in [127] and around 25 dB of XP radiation isolation is revealed. Rectangular patch with a circular defect on the patch surface [128], rectangular microstrip antenna with dumbbell shaped

defected patch surface [129] and a wideband slot dipole loaded shorted rectangular patch with defected patch surface [130] is investigated to address the issues of XP radiation.

The different techniques to miniaturized the microstrip antenna have been documented in [131]. In [132 - 133] gain enhancement of a compact circular microstrip antenna is achieved using electromagnetically coupled parasitic ring. An analytical method for gain enhancement by replacing the dielectric substrate with air substrate is proposed in [134-135]. A dual-frequency selective surface (FSS) superstrate layer with a circularly shaped microstrip antenna is implemented to optimize the gain and is reported in [136]. Shorting pin loading technique for gain enhanced circular microstrip antenna is reported in [137]. Bandwidth enhancement technique for a CMA is investigated in [138-140]. Characteristic mode analysis [138], introduction of modified microstrip feed [139] and introduction of different feeding techniques [140] are discussed to enhance the bandwidth of a CMA.

Cross polarization suppression technique of a CMA is investigated in [141-147]. Guha et. al. proposed the concept of DGS for minimizing XP radiation for a CMA in 2005 141]. 5-8 dB of XP suppression is achieved in the broadside direction. In [142] arc-shaped DGS and ring-shaped DGS are reported to improve the cross polarized radiation. Around 12 dB improvement is achieved for an arc-shaped DGS whereas the ring-shaped DGS achieves about 7 dB improvement over a conventional MA. A new arc-shaped DGS [143] is again designed and it achieves a significant improvement in suppressing the XP radiation. Dot DGS, annular ring DGS and arc DGS for XP suppression is compared in [144]. From the comparison arc- shaped DGS is the best choice followed by annular ring DGS. 10-12 dB of XP level suppression is achieved using an arc-shaped DGS. A new arc-cornered microstrip antenna with a circular shaped and rectangular shaped microstrip antenna is investigated in [145]. Wide impedance bandwidth and 20-25 dB of CP-XP isolation is achieved. The concept of defected patch surface for improved polarization purity of a circular microstrip antenna is proposed in [146]. About 27-28 dB XP isolation is achieved with circular cut defects placed at the non-radiating edge of a CMA. A pair of symmetric clusters of shorting pins peripherally located along the radius of the patch [147] is also investigated foe

cross polarization reduction in a CMA. Around 51 dB of XP isolation at the boresight and an average of 30 dB around $\pm 60^\circ$ on either side of boresight is achieved.

1.5 Conclusion

In this literature survey, existing techniques to improve the radiation characteristics of a circular microstrip antenna has been investigated and documented. In this thesis, a circular microstrip antenna has been investigated theoretically and experimentally for the improvement of the input and radiation characteristics.

In **Chapter 2**, two different approach namely shorting of non-radiating side of CMA and rectangular strip loading aa the radiating side of a CMA have been studied for improvement of co-polarization gain as well as the polarization purity. The study of the shorting of the non-radiating side of CMA has been investigated using two different substrate materials like FR4 (ε_r = 4.4) and glass (ε_r = 5) with two different substrate thickness of 0.787 mm and 1.58 mm.

In **Chapter 3**, two different defected ground surface structure namely curved dumbbell shape DGS (CDDGS) structures and rectangular DGS (RDGS) structure have been investigated for improvement of impedance bandwidth as well as the polarization purity.

In **Chapter 4**, a simple circular microstrip antenna with a pair of shorting strips loaded at the non-radiating sides has been successfully investigated analytically and experimentally based on the reduced surface wave theorem to improve co-polarization gain, efficiency, and polarization purity simultaneously.

In **Chapter 5**, a symmetrically modified circular microstrip antenna with a pair of thin strips has been proposed and investigated theoretically as well as experimentally. Excellent improvement in radiation performance like high co-polarization gain, polarization purity, efficiency have been obtained. Notably, a new feature of reduced horizontal radiation compare to the co-polarization gain has been achieved which is undeniably helpful for modern array or 5G MIMO configuration.

Finally in **chapter 6**, a conclusion of all the investigations that have been carried out in this thesis is presented along with future scope of research in the particular area.

CHAPTER

2

Improvement of Polarization Performance and Gain Properties with Shorting and Strip Loading Approach of Circular Microstrip Antenna

2.1 Introduction

In the present scenario, tiny, compatible and affordable antennas are very much crucial to design. A circular microstrip antenna (CMA) is a good contender in this field due to its inherent advantages such as light weight, small size, low profile, planar structure and ease of fabrication. All these advantages have made it very popular as an attractive radiator for the modern wireless world [26, 147-148]. However, conventional microstrip antennas have several shortcomings such as narrow impedance bandwidth, poor polarization purity (co-polar radiation (CP) to cross-polar radiation (XP) isolation), poor gain and less efficiency. The circular microstrip antenna (CMA) emits broad side field in TM_{11} mode, which is the dominant mode of CMA. When CMA emits these broad side fields, a small number of orthogonal fields are also emitting which is undesirable. These unwanted fields are called cross polarized radiation (XP). Due to these XP the separation between co-polarization radiation and cross polarization radiation becomes very less which limits the application of patch antenna in full elevation angle. H plane XP is always higher than the E plane XP. The higher order mode i.e., TM_{21} is mainly responsible for this high XP [149].

Researchers have carried out handful number of investigations to improve the input and radiation performance of a conventional microstrip antenna.

Around 7.8 dBi gain in circular patches have been investigated using different techniques like aperture coupling [150], slot and short loaded stacked ground plane [151] without any improvement in polarization purity (PP). The employment of shorting vias with branch line couplers in annular ring antenna [152], numerous

shorting vias beneath the circular patch [137, 153] have been employed to achieve maximum 7.2 dBi to 9 dBi gain with polarization purity of around 18 dB only. Hence, the investigations [137, 150 - 153] fail to address all the main antenna parameters concurrently such as gain and polarization purity. Although the gain is good in [137], still it suffers from poor polarization purity. Furthermore, the radiation pattern obtained in [137] suffers from much distortion with high side lobe level. The use of multi-layered circular substrate patch [154], hexadecagon circular geometry [155], patch with graphene-based materials [156] are investigated for high gain and around 6.8 to 8 dBi gain has been achieved without any enhancement in polarization purity.

Nevertheless, the upgradation in polarization purity is always important for modern wireless applications. Numerous efforts such as use of defected patch surface (DPS) [157 - 158], defected ground surface (DGS) [141-144] have been reported by different research groups to improve polarization purity of CMA. Maximum 20-22 dB of polarization purity is achieved with no enhancement in co-polarization gain.

Therefore, to discourse the limitations of previously investigated structures and for the simultaneous enhancement in co-polarized gain and polarization purity, two approaches are discussed in the following sections.

The chapter has been arranged in the following way. In section 2.2 shorting of non-radiating periphery of conventional CMA is explained in details including design technique (section 2.2.1), parametric studies to obtain optimum structure (section 2.2.2), final proposed structure obtain through parametric studies (section 2.2.3), and results obtained from the optimum structure (section 2.2.4). In section 2.3 detail investigations of a strip loaded CMA is presented which includes evolution of the optimum structure through parametric studies (section 2.3.1), results obtained from the optimum structure (section 2.3.2). The conclusion of the proposed works is documented in section 2.4.

2.2 Shorted Circular Microstrip Antenna Approach to Improve the Cross Polarization Performance

Four CMAs, two with FR4 substrate and another two with glass substrate with different substrate thickness and a pair of shorting walls in the non-radiating periphery

of CMA has been proposed in this section. The schematic representation of the proposed antenna is shown in Fig. 2.1.

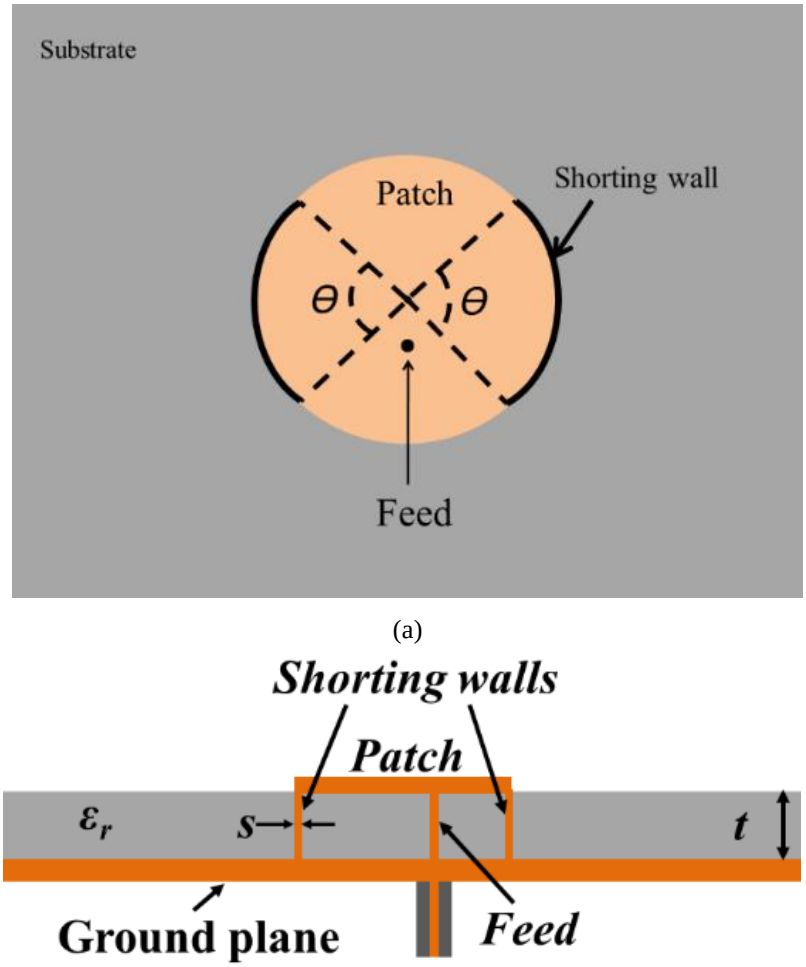

Fig. 2.1 Shorting walls integrated circular patch (a) view from top (b) cross sectional view.

2.2.1 Design Technique

The conventional CMA has been designed on two types of substrates having different thickness. The radius of the patch has been determined by the equation as

$$f_r = \frac{1.84c}{2\pi a\sqrt{\epsilon_r}} \tag{2.1}$$

Then, shorting walls are placed along non-radiating sides of the patch with an intension to reduce the cross polarized field radiation from that side so to improve the polarization purity.

2.2.2 Parametric Studies

To find out the structure that provides best possible outcome in terms antenna performance, robust parametric studies have been carried out with the support of [159]. At first, four conventional CMA with FR4 and glass substrates with different thicknesses of 0.787 mm and 1.58 mm has been designed for X-band frequencies. The parametric studies have been started by placing pair of shorting strips of copper at the non-radiating edge along the periphery of CMA for both structures with FR4 and glass substrate.

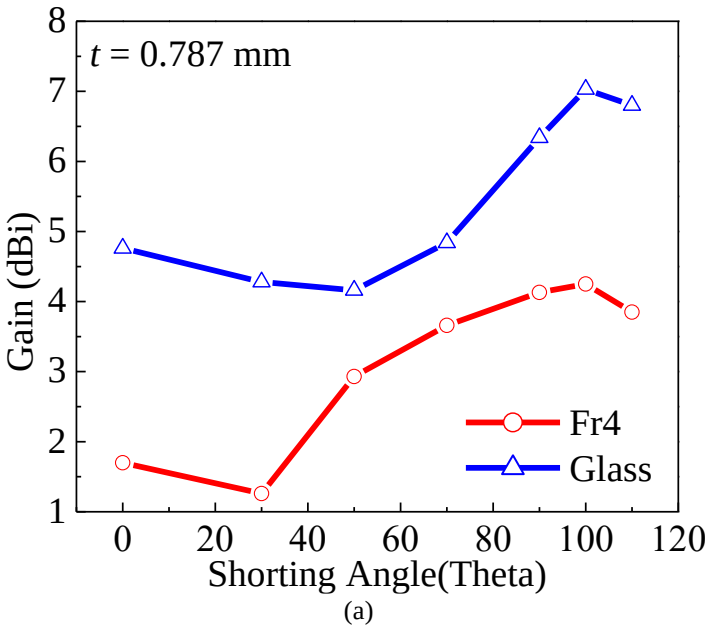

(a)

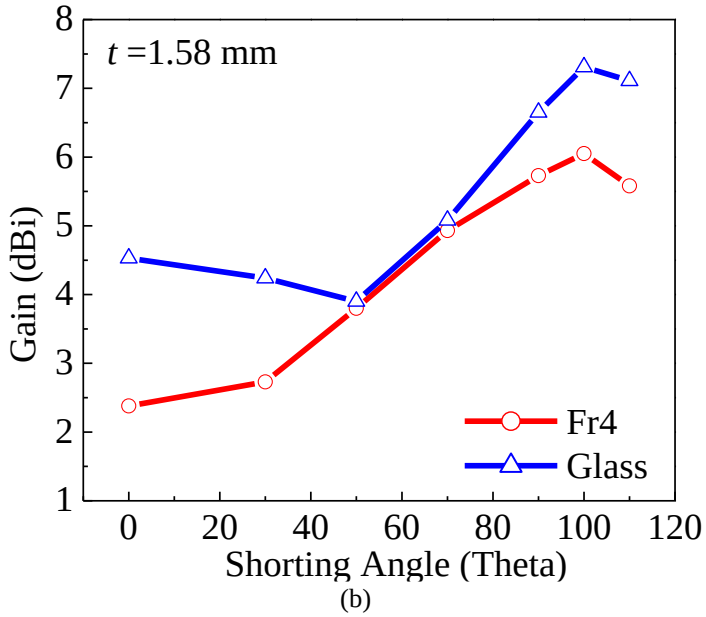

(b)

Fig. 2.2 Co-polar peak gain variation with respect to the short angle for different substrate width (a) 0.787mm (b) 1.58 mm.

Figure 2.2 shows the gain profile of the proposed models for different shorting angles (θ). It is detected that the co-polar (CP) gain increases as the shorting angle (θ) is increased for all four structures and attains maximum peak at $\theta = 100°$. Further increase of the short angle reduces the CP gain.

For further confirmation about the best possible structure the parametric studies on polarization purity have also been done and presented in Fig. 2.3.

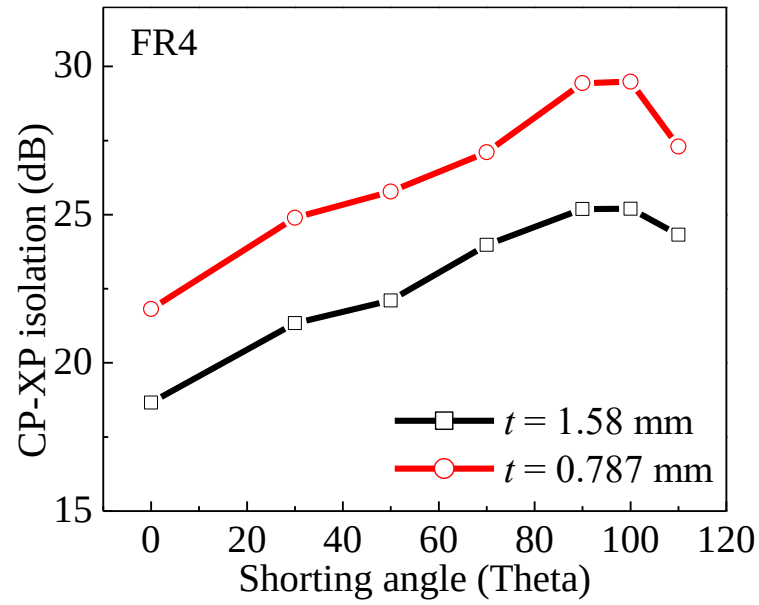

(a)

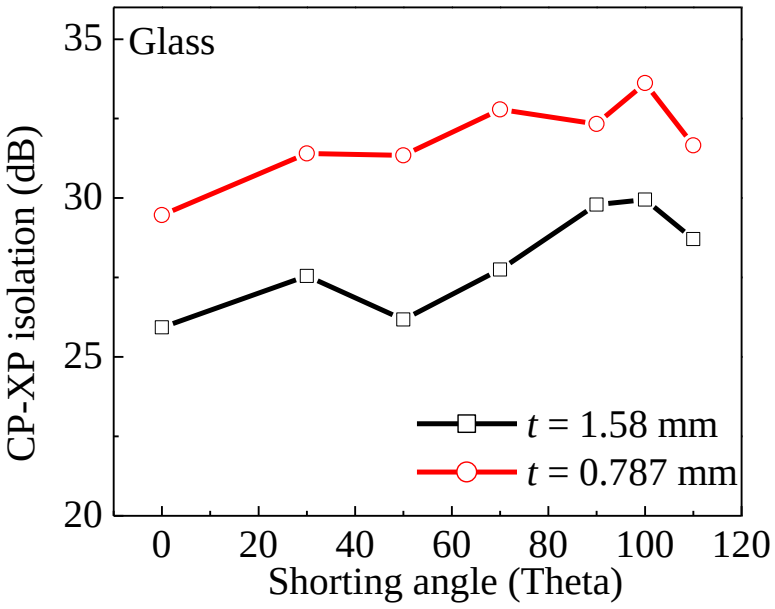

(b)

Fig. 2.3 Polarization purity variation with respect to the short angle for different substrate (a) FR4 (b) glass with different substrate thickness.

For the conventional structure i.e., $\theta = 0°$ the polarization purity is 18 dB and 22 dB for FR4 substrate with substrate thickness of 0.787 mm and 1.58 mm respectively while it is around 26 dB and 29 dB in case of glass substrate with substrate thickness of 0.787 mm and 1.58 mm respectively. As soon as the shorting strips have been introduced at the non-radiating sides of the patch the polarization purity starts increasing in all the structure as seen from Fig. 2.3. The CP - XP isolation (PP) keeps on increasing as the short angle rises and attains a maximum value at $\theta = 100^0$.

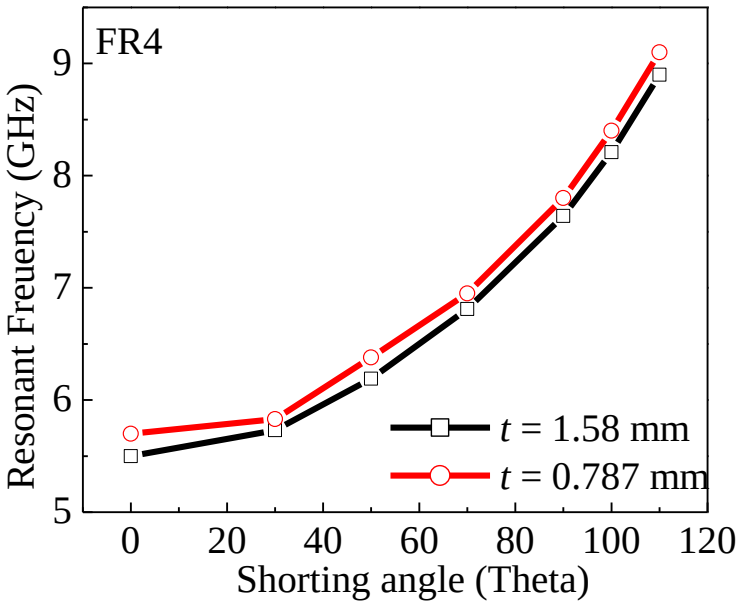

(a)

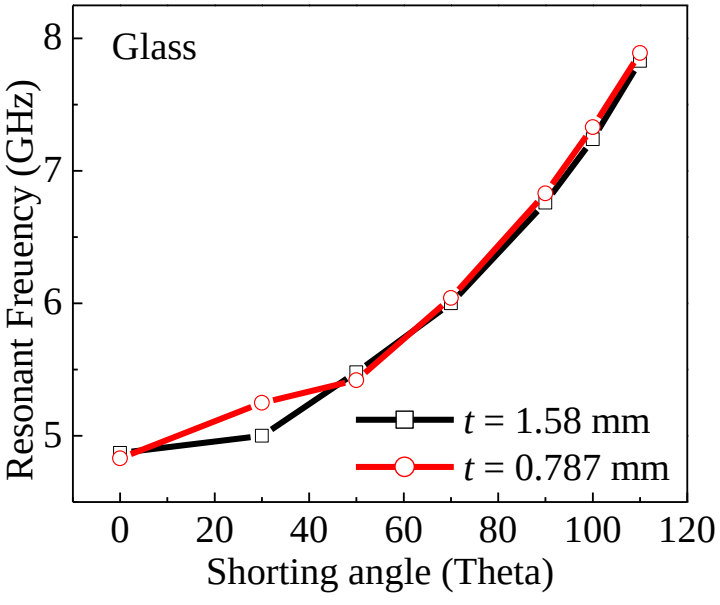

(b)

Fig. 2.4 Resonant frequency variation of the proposed structure for different shorting angles (θ) (a)FR4 substrate (b) Glass substrate.

Figure 2.4 shows the resonance frequency profile of the structures under study. In all the cases for different substrate with different substrate thickness the resonance frequency increases linearly as the shorting angle increases.

2.2.3 Optimum Structure

At the beginning four conventional circular patch antenna of radius 7 mm has been designed on the top of FR4 (ε_r = 4.4) and glass (ε_r = 5) substrate out of which two structures are with substrate thickness (t) of 0.787 mm and other two are with substrate thickness (t) 1.58 mm. The dimensions of the ground plane are 60 x 60 mm^2. After that a pair of grooves with thickness (s) 0.1 mm have been made at both non-radiating periphery of the CMA and a pair of metal strips of same width are inserted in the grooves. In this way the final proposed structure (Fig. 2.1) i.e., shorted circular microstrip antenna has been designed. The shorting angle (θ) has been varied from 30^0 to 110^0 gradually.

2.2.4 Simulated Results

The results achieved with the optimum structure i.e., with shorting angle (θ) 100^0 with the help of [159] is documented in this section. The S_{11} profile of the conventional CMA and present optimum structure with two different substrate and thickness is shown in Fig. 2.5.

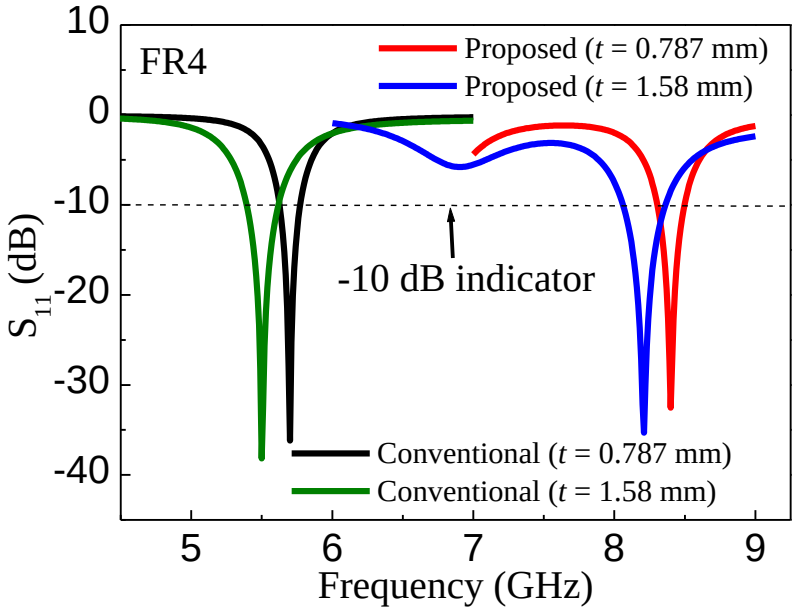

(a)

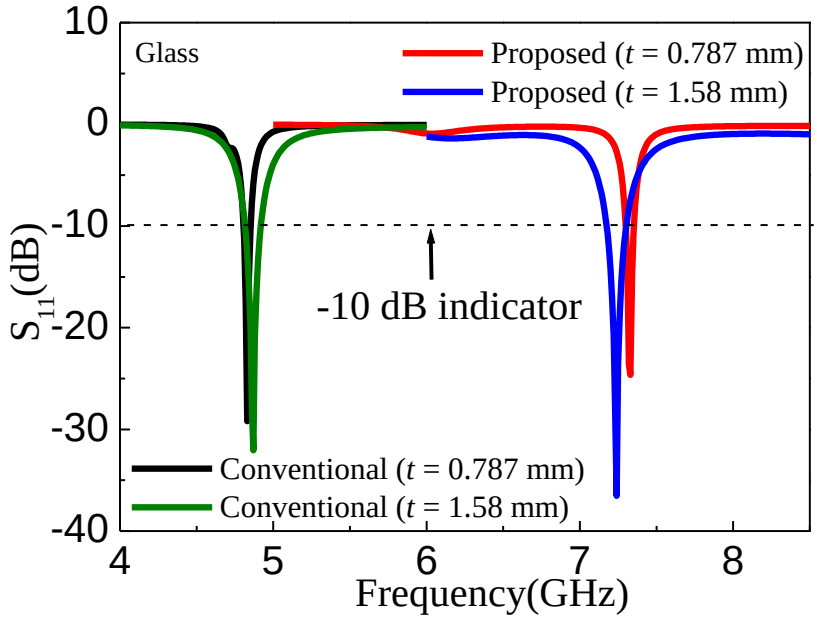

(b)

Fig. 2.5 Simulated S_{11} versus frequency of the CMA and present antenna with $\theta = 100^0$ (a) FR4 (b) Glass substrate.

For all the proposed structures the resonant frequency shifted towards higher side of spectrum in comparison to traditional CMA. Figure 2.5 also shows that all the structure is having good impedance matching.

The simulated radiation pattern of the proposed antenna ($\theta = 100^0$) with FR4 and glass substrate is shown in the Fig. 2.6. All the figures show improved polarization purity as compared to the conventional CMA.

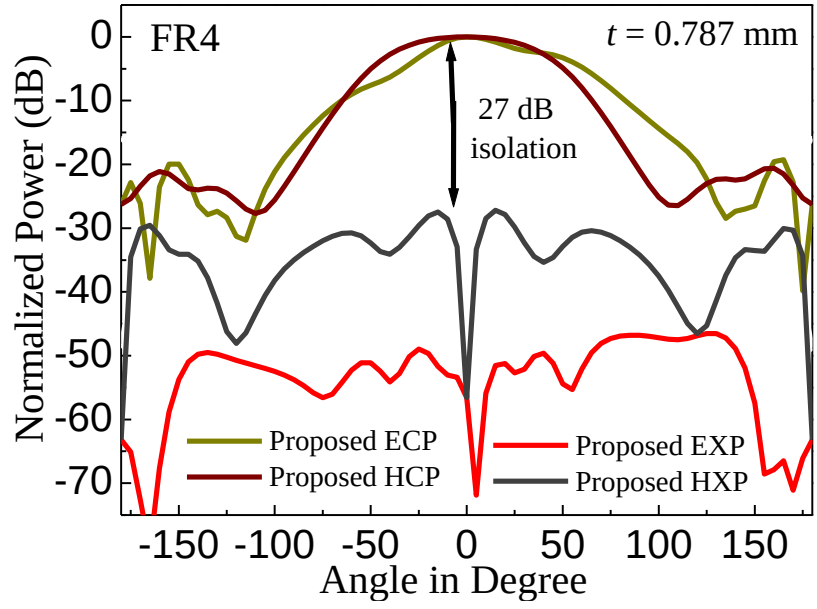

(a)

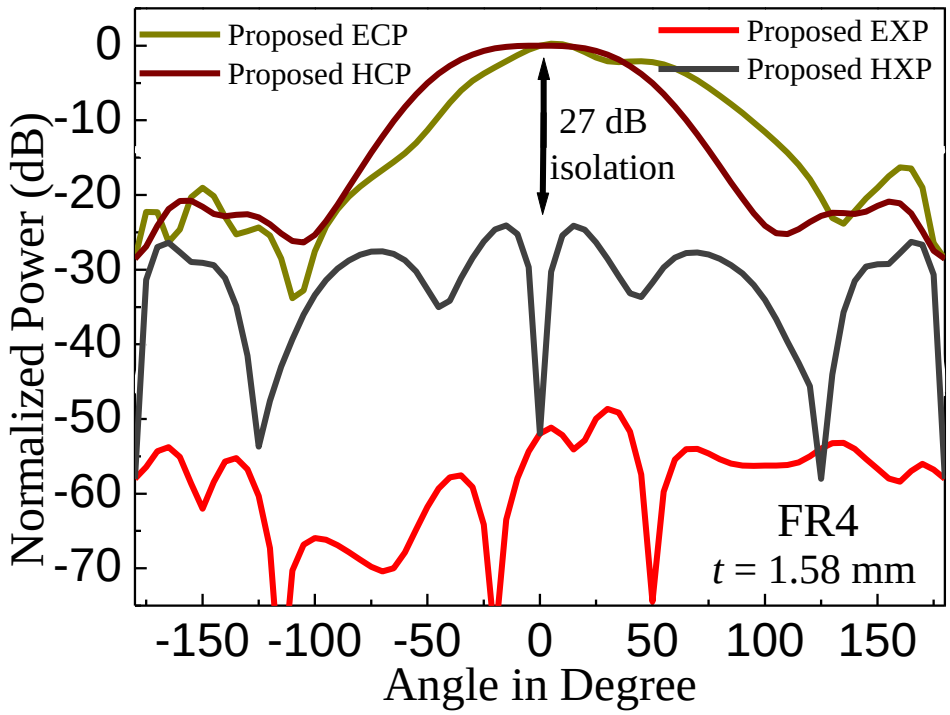
Proposed ECP
Proposed HCP
Proposed EXP
Proposed HXP
27 dB
isolation
FR4
t = 1.58 mm
Normalized Power (dB)
0
-10
-20
-30
-40
-50
-60
-70
-150 -100 -50 0 50 100 150
Angle in Degree

(b)

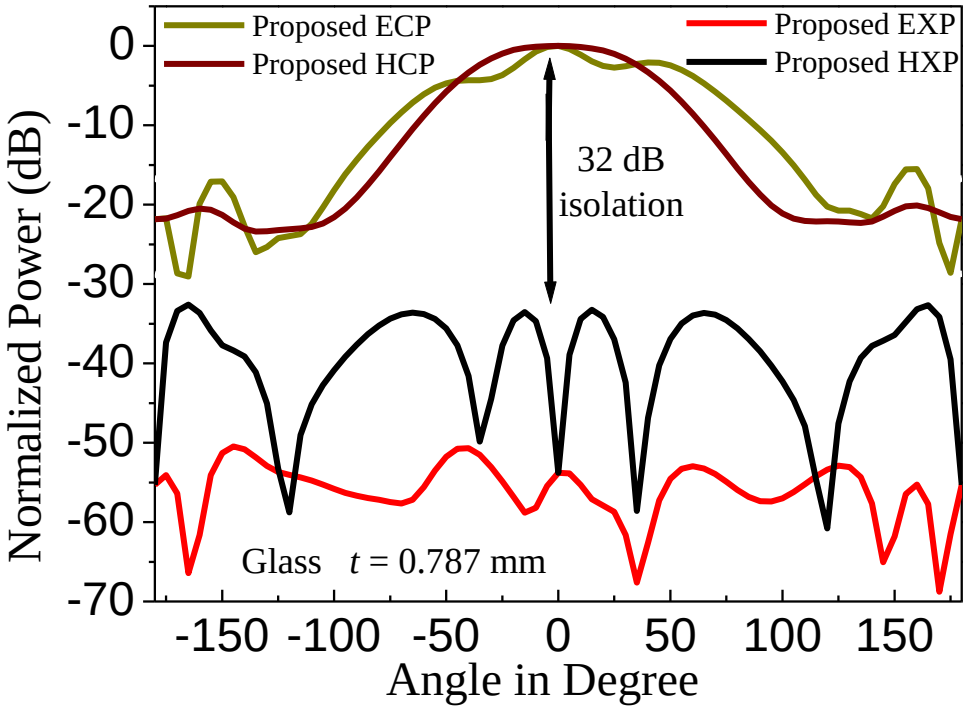
Proposed ECP
Proposed HCP
Proposed EXP
Proposed HXP
32 dB
isolation
Glass t = 0.787 mm
Normalized Power (dB)
0
-10
-20
-30
-40
-50
-60
-70
-150 -100 -50 0 50 100 150
Angle in Degree

(c)

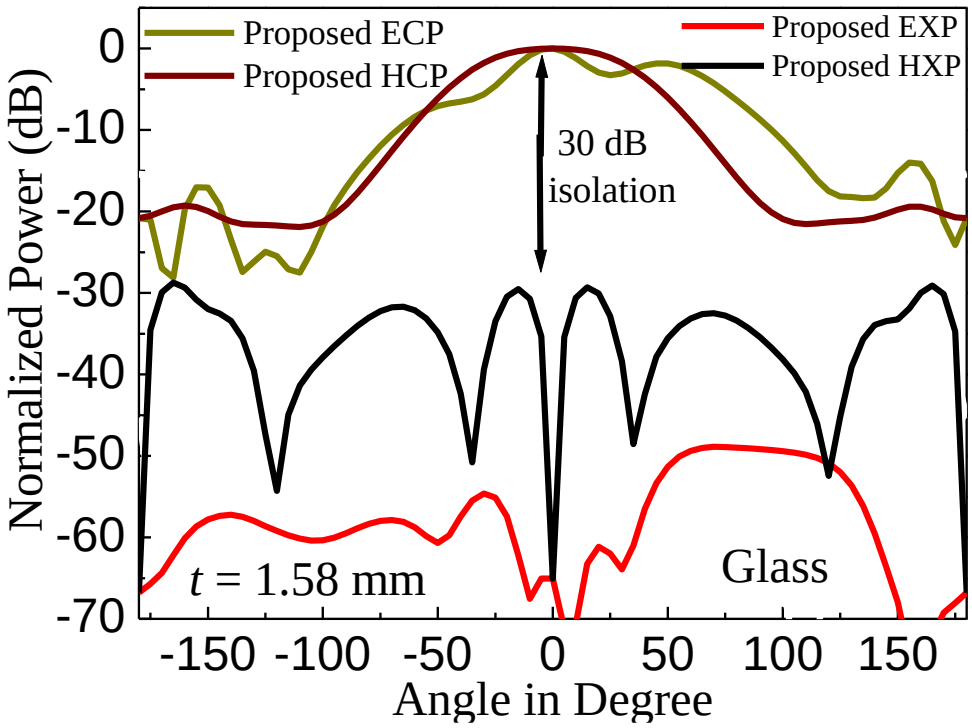

(d)

Fig. 2.6 Simulated radiation pattern of the proposed antenna (θ = 100°)(a) FR4 substrate with thickness 0.787 mm (b) FR4 substrate with thickness 1.58 mm (c) Glass substrate with thickness 0.787 mm (d) Glass substrate with thickness 1.58 mm.

For the proposed antenna with FR4 substrate with substrate thickness (t) 0.787 mm and 1.58 mm a polarization purity of 27 dB is achieved (Fig. 2.6(a) and 2.6(b)) whereas the proposed antenna with glass substrate provides a polarization purity over 30 dB for both t = 0.787 mm and t = 1.58 mm (Fig. 2.6(c) and 2.6(d)).

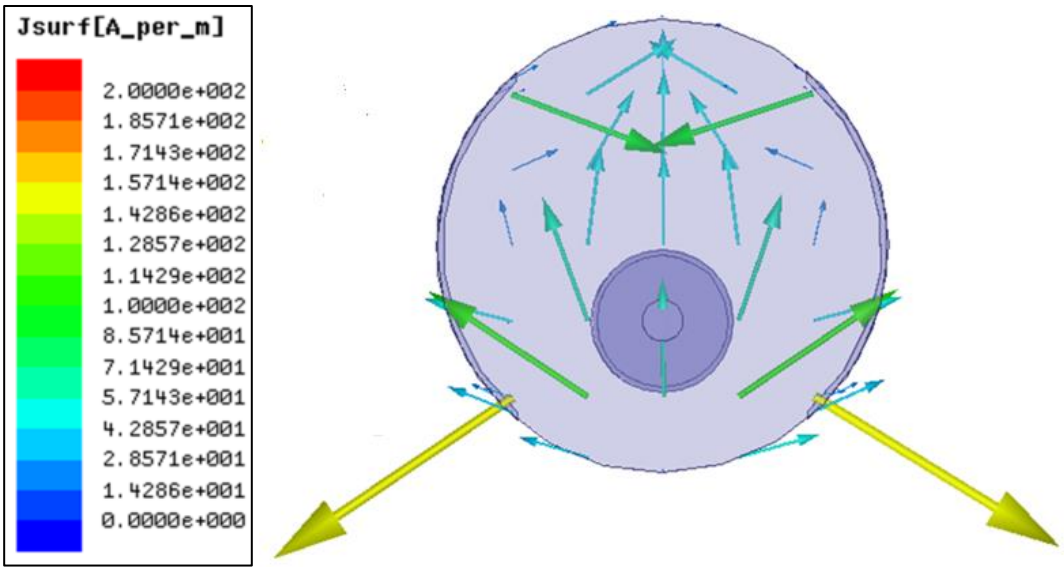

Fig. 2.7 Surface current distribution over patch for $\theta = 100^0$.

The surface current distribution of the proposed antenna is shown in Fig. 2.7. It confirms that the antenna is purely linear polarized with high PP. For all the cases the polarization purity is quite higher than the conventional circular microstrip structure.

2.3 Strip Loading Approach to Improve the Cross Polarization Performance of Circular Microstrip Antenna

A circular microstrip antenna (CMA) is designed by placing a copper strip at the top radiating side of a conventional CMA for better CP and XP separation (PP) in H plane as well as higher co-polarization gain as compared to the conventional CMA. The conventional CMA and the proposed CMA is shown in Fig. 2.8.

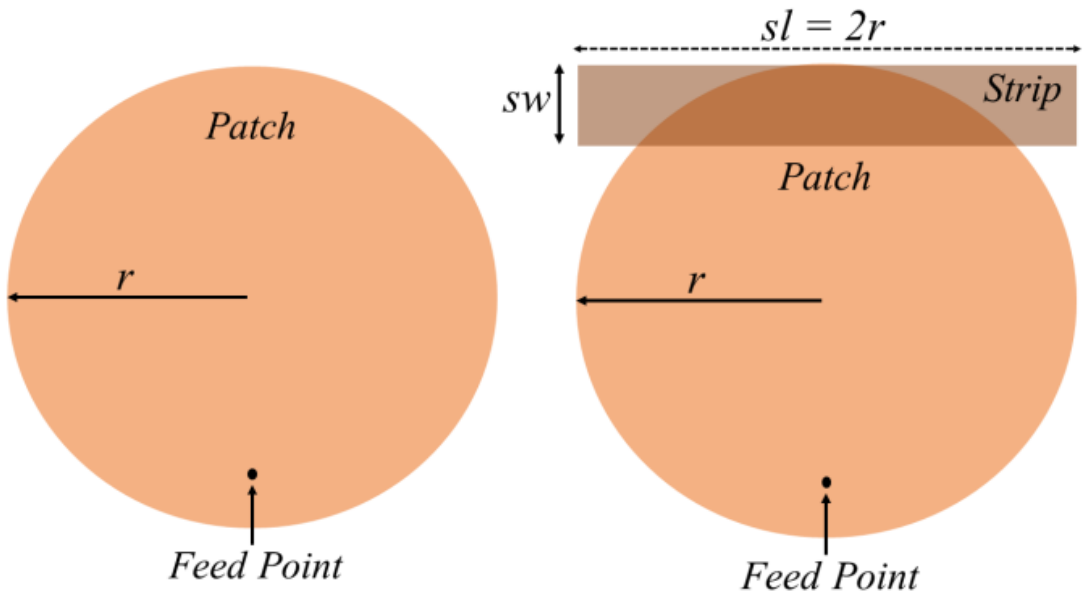

(a) (b)

Fig. 2.8 Schematic representation of (a) traditional CMA (b) proposed rectangular strip loaded CMA.

2.3.1. Evolution of Optimum Structure

Conventional CMA radiates electric fields from non-radiating sides in higher order (TM_{21}) mode that are mainly responsible for the XP radiation. To mitigates these fields and to achieve high gain conventional CMA has been modified by placing a rectangular strip at the top of the conventional CMA. To find out the structure that provides best possible outcome in terms antenna performance a robust parametric study has been performed with the support of [159].

Initially a conventional CMA of radius (*r*) 7 mm has been placed over the RT Duroid material of size 70 mm x 70 mm and thickness 1.575 mm. Then a rectangular strip is added at the top of the conventional CMA to enhance the PP as well as the co polarization gain. The length (*sl*) and width (*sw*) has been varied to get the optimum out puts. The rectangular strip is placed in such a way that the overall antenna dimension should not increase which is very much clear from Fig. 2.8 (b).

The CP-XP separation varies with respect to the variation of the length (*sl*) and width (*sw*) of the rectangular strip. This is shown in Fig. 2.9. The conventional CMA with radius (*r*) 7 mm provides a CP-XP separation of 17 dB in the H plane. As soon as the rectangular strip with *sl* = 8 mm and *sw* = 1 mm is attached at the top of the conventional CMA, CP-XP separation improves.

Then strip length (*sl*) has been increased up to a size same as the diameter of the conventional CMA i.e., 14 mm. It is done with a motto that the overall dimension of the antenna should not more than the conventional CMA with radius 7 mm. With *sl* = 1 mm the maximum CP-XP separation of 21 dB has been achieved as shown in the Fig. 2.9.

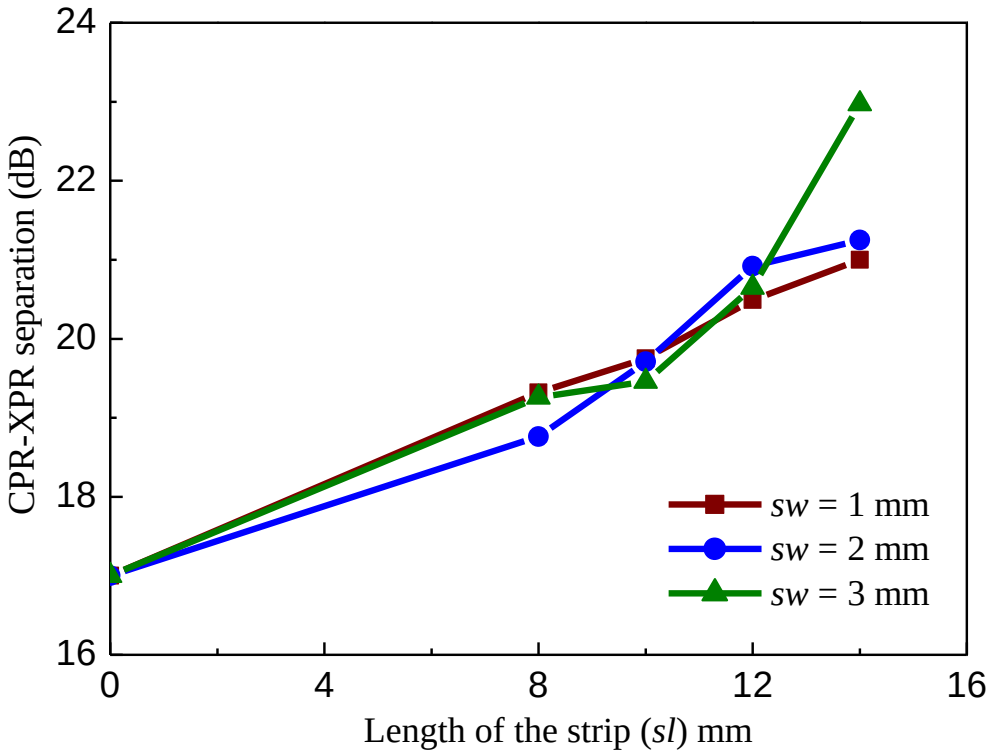

Fig. 2.9 Variation of CP-XP separation with respect to length of the rectangular strip with different values of rectangular strip width.

Next the width of the rectangular strip (*sw*) is increased to 2 mm and length (*sl*) of the strip is varied from 8 mm to 14 mm. Maximum CP-XP separation (PP) of 21.25 dB has been achieved with *sw* = 2 mm and *sl* = 14 mm. Next the width (*sw*) of the rectangular strip is increased to 3 mm and length (*sl*) of the strip is varied from 8 mm to 14 mm. Maximum CPR-XPR separation of 23 dB has been achieved with *sw* = 3 mm and *sl* = 14 mm. Further increment of width(*sw*) of the rectangular strip degrades the radiation performance of the proposed structure.

The co polarized gain varies with respect to the variation of the length (*sl*) and width (*sw*) of the rectangular strip. This is shown in Fig. 2.10. The conventional CMA with *r* = 7 mm provides a co polarization gain of 5 dBi. As soon as the rectangular strip with *sl* = 8 mm and *sw* = 1 mm is attached at the top of the conventional CMA, the co-polarized gain improves. With *sl* = 1 mm the maximum co polarization gain of 7 dBi has been achieved as shown in the Fig. 2.10.

Next the width (*sw*) of the rectangular strip is increased to 2 mm and length (*sl*) of the strip is varied from 8 mm to 14 mm. Maximum co polarization gain of 7 dBi has been achieved with *sw* = 2 mm and *sl* = 14 mm.

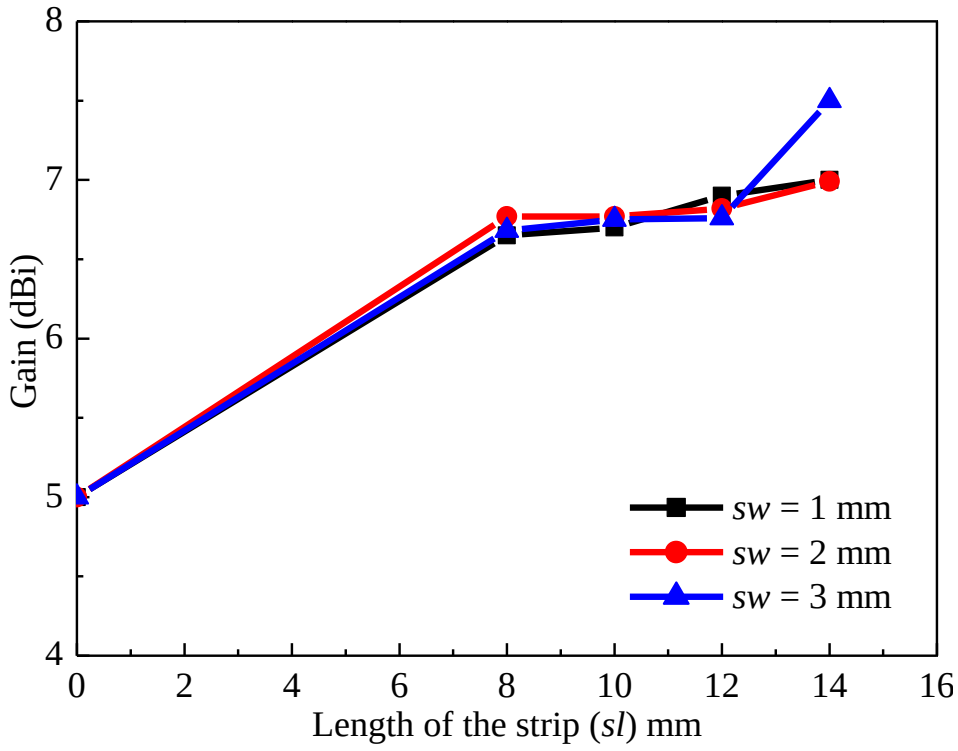

Fig. 2.10 Variation of co polarization gain with respect to length of the rectangular strip with different values of rectangular strip width.

Next the width (*sw*) of the rectangular strip is increased to 3 mm and length (*sl*) of the strip is varied from 8 mm to 14 mm. Maximum gain of 7.5 dBi is attained with *sw* = 3 mm and *sl* = 14 mm. As the optimum PP is also achieved with *sl* = 14 mm and *sw* = 3 mm so the co-polarized gain with these dimensions is considered as the optimum one. Table 2.1 shows the dimensions of the optimized structure.

TABLE 2.1 The detailed parameters of the proposed rectangular strip loaded CMA (Substrate thickness h = 1.575 mm)

Substrate	ε_r	***Ground plane*** **(mm^2)**	***r*** **(mm)**	***sl*** **(mm)**	***sw*** **(mm)**
RT-Duroid	2.33	70 x 70	7	14	3

2.3.2. Performance from Optimized Antenna Structure

The comparison of reflection co-efficient (S_{11}) profile of the optimum structure and the conventional structure has been shown in Fig. 2.11 with the help of [159]. Conventional CMA resonant at 7.21 GHz and the proposed rectangular strip loaded CMA with length (*sl*) 14 mm and width (*sw*) 3 mm resonates at 6.71 GHz. The proposed structure is working at X band frequency and provides very good impedance matching.

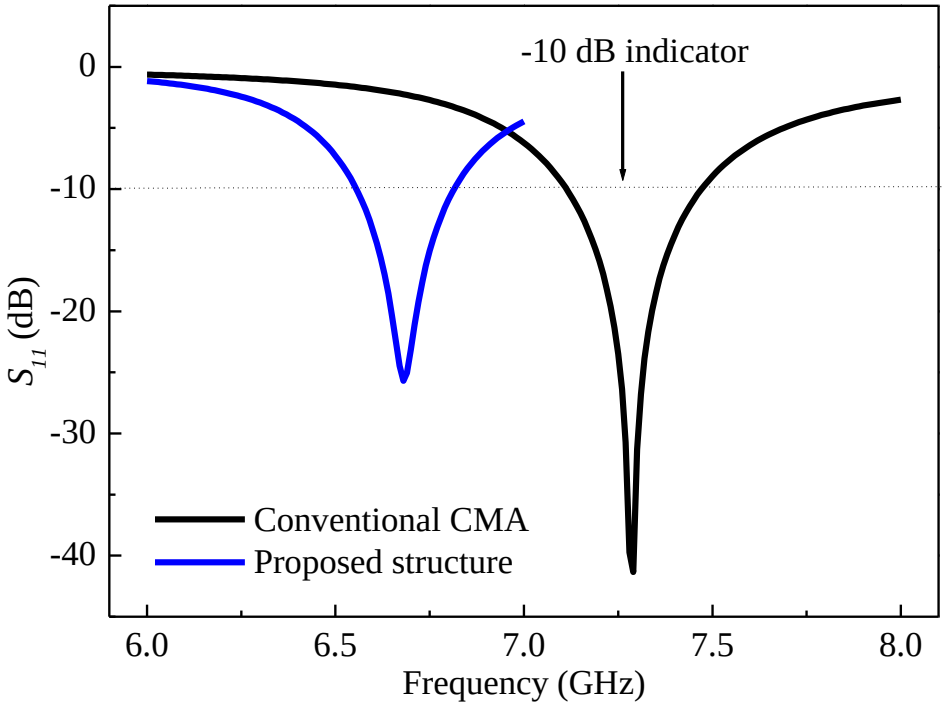

Fig. 2.11 Simulated S_{11} profile of conventional CMA and proposed rectangular strip loaded CMA.

Fig. 2.12 projects the normalized E plane gain profile of the traditional CMA and rectangular strip loaded CMA. From the figure it is very much clear that the co polarization radiation profile of the proposed CMA is quite comparable to that of the traditional CMA. The cross-polarization radiation profile of the proposed antenna is quite below -50 dB though it does not have that much significance.

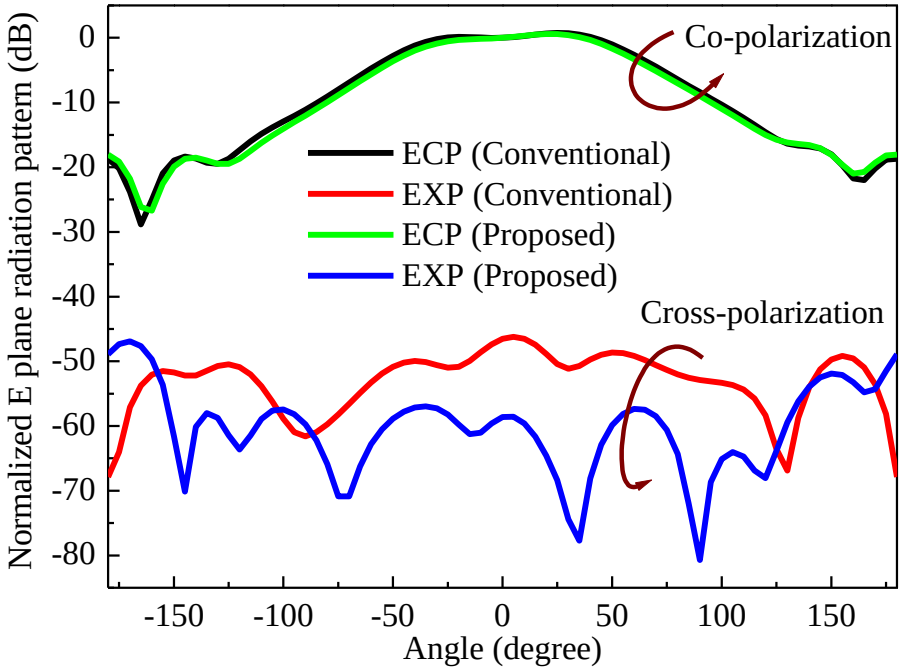

Fig. 2.12 E-plane gain profile of the conventional CMA and rectangular strip loaded CMA (optimum).

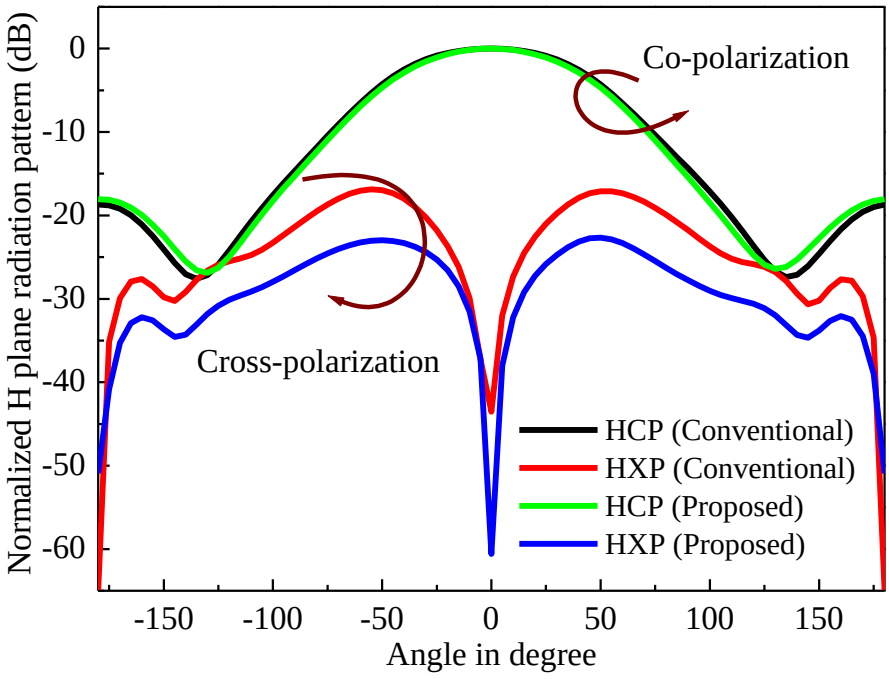

Fig. 2.13 H-plane gain profile of the conventional CMA and rectangular strip loaded CMA (optimum).

The complete H plane CP and XP profile of the proposed model and conventional CMA has been revealed in Fig. 2.13. From the figure it can be noticed that the XP is very high mainly around $\varphi = 45^0$ plane. The conventional CMA gives a PP of 17 dB while the proposed structure provides 23 dB of PP. The proposed structure improves the PP by 4 dB without affecting the co-polarization radiation profile. The copolarization radiation profile in magnetic plane of rectangular strip loaded CMA is similar to that of the traditional CMA.

The field distribution over the substrate has been investigated to validate the improvement in cross polarized radiation in the proposed patch and has been shown in Fig. 2.14. Uniform distribution of electric fields among both half section of the rectangular strip loaded CMA can be seen from the Fig.2.14 which is one of the reasons behind the high gain as discussed in [149].

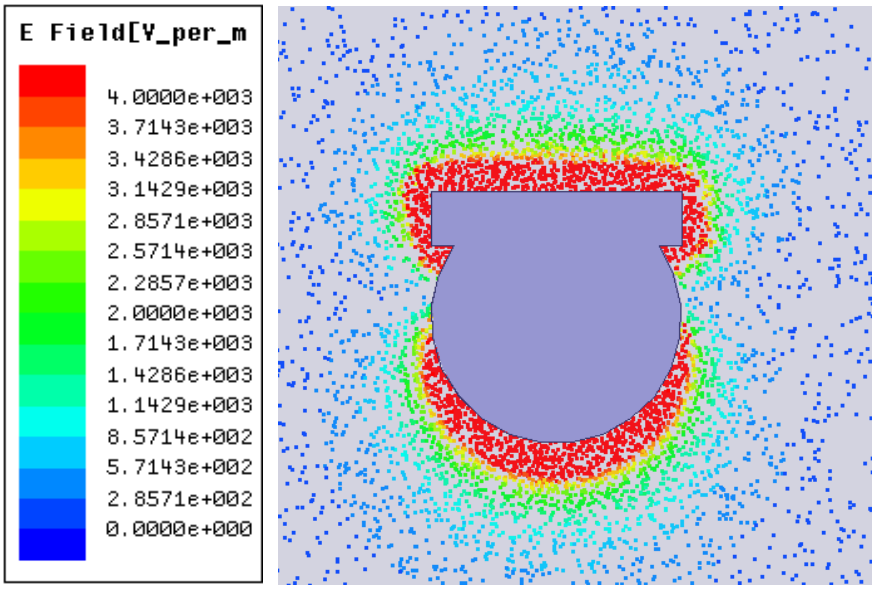

Fig. 2.14 Field distribution over the substrate of the proposed structure (optimum).

2.4. Conclusion

In this chapter two approach has been proposed to improve the co-polarization gain and polarization purity performance of a conventional circular microstrip antenna.

In the first approach four circular microstrip antennas (with shorted non-radiating sides) with different substrate (FR4 and glass) and different substrate thickness (0.787 mm and 1.575 mm) have been investigated to improve the PP without hampering basic

radiation pattern. In this design, the patch is slightly bigger than the conventional CMA. In fact, because of incorporation of shorting strips, dielectric constant of the substrate becomes modified and it eliminates surface wave. This improves overall performance of the present antenna. The parametric studies over all the structures show that the proposed structures with shorting angle (θ) 100^0 provides the best results in terms of co-polarization gain and polarization purity. The proposed structure (θ = 100^0) with FR4 substrate provides a PP of 27 dB while with glass substrate the polarization purity is more than 30 dB. The polarization purity obtained from all the structures are quite higher than the conventional CMA structures with FR4 and glass substrates.

In the second approach, a conventional circular microstrip antenna has been modified by placing a rectangular strip at the top of the patch to improve the copolarization gain as well as polarization purity mainly in H plane. The rectangular strip length and width has been varied to get a proper shape of the rectangular strip which will provide best performance of the proposed structure. The co polarization gain of 7.5 dBi with 23 dB polarization purity is observed from the proposed structure. The simultaneous improvement of copolarization gain and polarization purity without disturbing the conventional E plane radiation pattern is very much required in modern wireless communication.

CHAPTER

3

Wideband Circular Microstrip Antenna with Improved Polarization Purity using Defected Ground Structure Approach

3.1 Introduction

In the previous chapter, the introduction of continuous shorting strip and strip loading on circular microstrip antenna (CMA) has been investigated for improved polarization performance. However, along with the same the improvement in input characteristics such as input impedance bandwidth is also very important in the era of modern high speed wireless communication systems. In that context, the microstrip antenna is a very good candidate and finds potential applications in modern communication because of its integration with an active device and having an excellent features like low weight, dual-polarization, easy to fabricate [23, 26]. Apart from these excellent features it has some major demerits like narrow beamwidth, gain, low co-polarization gain, poor polarization purity (PP) issue, as is discussed in earlier chapter.

The co-polarized electric fields are generated from the radiating sides of the circular microstrip antenna (CMA) in its dominant TM_{11} mode and radiates in the broadside direction. Few extents of orthogonal polarized fields called cross-polarization (XP) radiation took place at first higher order mode i.e., TM_{21} mode which was theoretically investigated in [149].

Scientists and researchers have started working to address these issues and some handful investigations have been carried out to address the input and radiation performance of conventional CMA. These include different structures of defected patch surface (DPS), defected ground surface (DGS), and the incorporation of shorting post technique. CMA with circular shape [141], Arc-shape [143] DGS are reported

with polarization purity of 5-7 dB but some impedance bandwidth-related issues have been come across in those documentation. Arc shaped DPS model has been reported in [157 - 158] which obtained polarization purity around 20-23 dB. Different type of rectangular slots on circular patch surface has been documented in [160] where around 22% bandwidth and 3.24 dB copolarization gain has been reported without any betterment of PP. Around 18 dB of XP suppression has been documented in [161-163] by modulating the feed structure. However, all these investigations led to complexity in the manufacturing process and more investigation is required to find a simpler technique for suppression of the XP radiation. Different type of cavity enclosed CPA has been investigated in [164 -165] for bandwidth enhancement, where 7 – 8% impedance bandwidth is documented in [164] and around 20% impedance bandwidth is observed in [165] without much improvement in polarization purity. In all the above reports enhancement of either impedance bandwidth or polarization purity has been reported. The simultaneous improvement of these parameters has not been reported till now.

Therefore, to address the lacunae of previously investigated structures and for the simultaneous enhancement in impedance bandwidth, polarization purity with stable co-polarization gain, two defected ground structures (DGSs) namely curved dumbbell shape defected ground structure (CDDGS) and rectangular defected ground structure (RDGS) are discussed in this chapter. Both the defected structures are deployed on the ground plane at the non-radiating edge of the conventional CMA designed with RT-Duroid substrate with dielectric constant (ε_r = 2.33) and height (h = 1.58 mm).

The detail study on the enhancement of different input and radiation parameters of conventional CMA are discussed with CDDGS structure in section 3.2. This includes theoretical background and parametric study (section 3.2.1), optimum proposed structure (section 3.2.2), and results (section 3.2.3). Similar investigation with another proposed structure (RDGS integrated CMA) is presented in the subsequent section 3.3. The conclusion of the performance of both the proposed structures is documented in section 3.4.

3.2 Curved Shaped Defected Ground Structure: A way to achieve high Polarization Purity, Wide Bandwidth and Stable Gain

A pair of curved dumbbell shape defect (CDDGS) has been deployed on the ground plane at the non-radiating edge of the conventional CMA on RT-Duroid substrate with dielectric constant (ε_r = 2.33) and height (h = 1.58 mm) to address the limitation of the earlier investigation. The schematic representation o the proposed antenna is shown in Fig. 3.1.

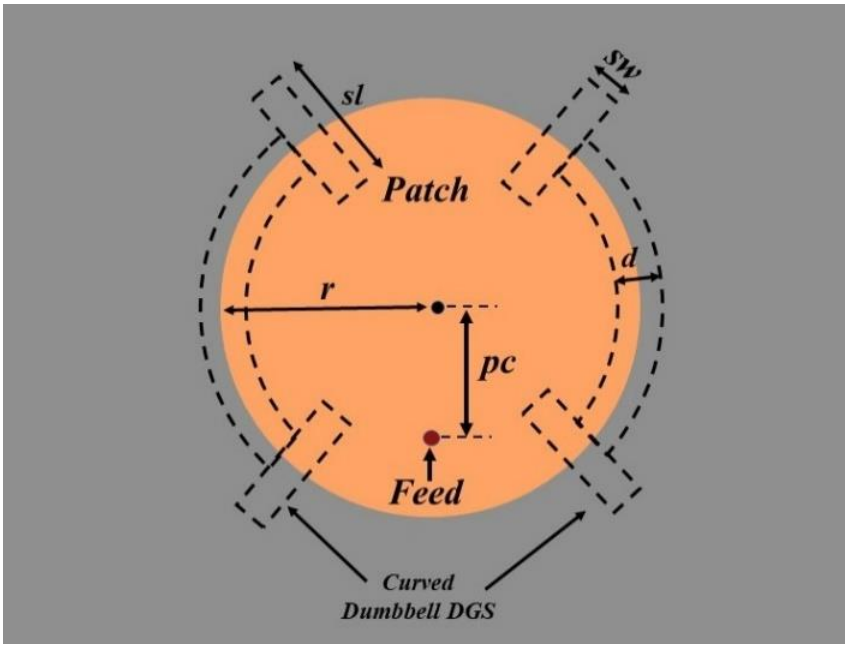

Fig. 3.1 Top view of the proposed structure with curved dumbbell shape DGSs at the non-radiating edges.

3.2.1 Theoretical Background and Parametric Studies

The conventional CMA radiated linearly polarized electric field along the broad side direction of the patch. It's generally occurred due to the fringing field that resides at the radiating edges of the patch which is the dominant mode TM_{11} [26],[157]. Nevertheless, a few handfuls amount fringing fields of the dominant mode are existing at the non-radiating edge of the conventional CMA as shown in Fig.3.2.

The orthogonal resonance field of week TM_{11} mode in CMA along with higher-order orthogonal excitation mode TM_{21} is the key factor in order to producing high XP radiation from the non-radiating edges of the CMA [161]. The field distribution of higher-order filed in TM_{21} mode is orthogonal to the fundamental dominant mode TM_{11}

as shown in Fig. 3.2(b). A closed inspection is that the radiation from non-radiating edges is mainly responsible for XP radiation. Therefore, a symmetrical pair of curved dumbbell shape DGS have been incorporated on the ground plane to eliminate such radiation without hindering its dominant mode TM_{11} mode radiation.

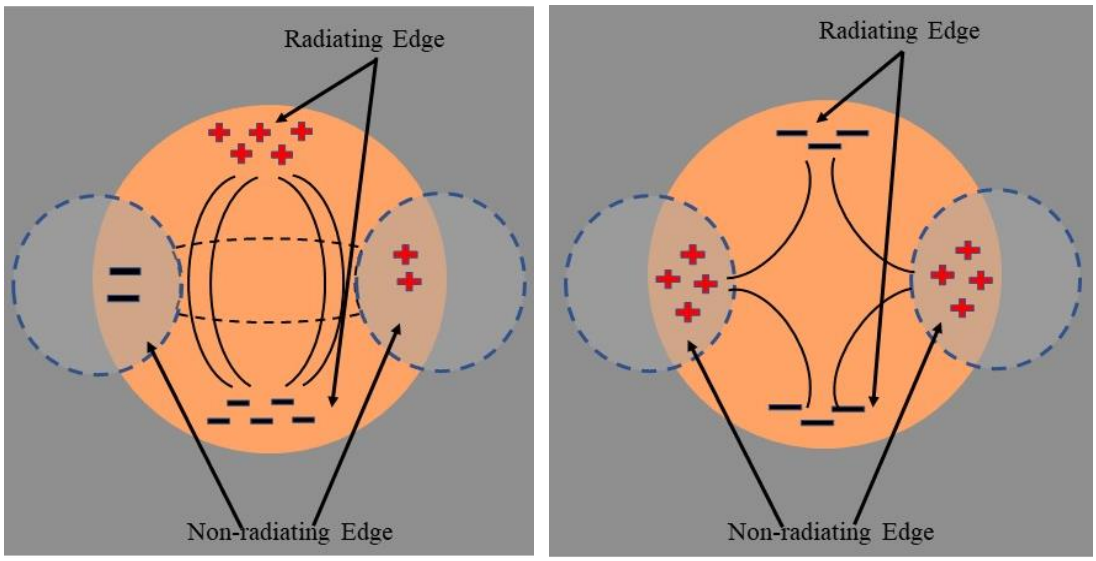

(a) (b)

Fig. 3.2 Electric field and current distribution over the patch surface (a) Fundamental dominant TM_{11} mode (b) Next higher-order TM_{21} mode.

The parametric studies have been done using a commercially available software package (high-frequency structure simulator; HFSS v.14) [159] to find out the best possible dimensions of the proposed structure. At first, a circular patch antenna with radius (r) 7 mm on RT-Duroid (ε_r = 2.33) substrate has been designed. After that a pair of symmetric curved dumbbell shape DGS have deployed on the ground plane at the non-radiating sides of the CMA. Then parametric studies have been carried out by varying different parameters of the CDDGS (as shown in Fig. 3.1) to obtain the best output from the proposed structure.

Fig. 3.3 shows the polarization purity plot when the width (sw) of the rectangular head of the CDDGS is varying keeping the length of the rectangular head (sl) and width (d) of the dumbbell arc fixed at 4 mm and 0.5 mm respectively. As sw varies from 0.5 mm to 2.5 mm, initially PP decrease then it increases to a maximum isolation of 23.9 dB at sw = 1 mm then again, the PP decreases gradually. So, the width (sw) of the rectangular head of the CD-DGS is considered as 1 mm for optimum results.

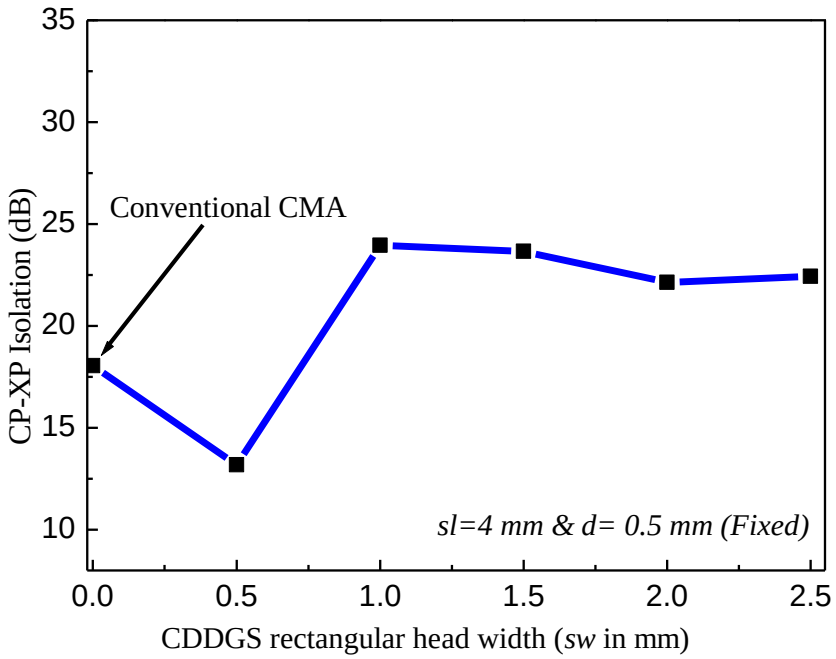

Fig. 3.3 Simulated plot of CP-XP isolation with respect to variation of CD-DGS rectangular head slot width (*sw*). (Keeping *d* = 0.5 mm, *sl* = 4 mm fixed).

Now, keeping *sw* = 1 mm (optimized) and *sl* = 4 mm (fixed), the width of the dumbbell arc (*d*) of CD-DGS is varying from 0.5 mm to 2.5 mm and it is observed that at *d* = 0.5 mm it provides best result in terms of CP-XP isolation (PP) as shown in Fig. 3.4. So, the optimum value of the width of the dumbbell arc (*d*) of CD-DGS is considered as 0.5 mm.

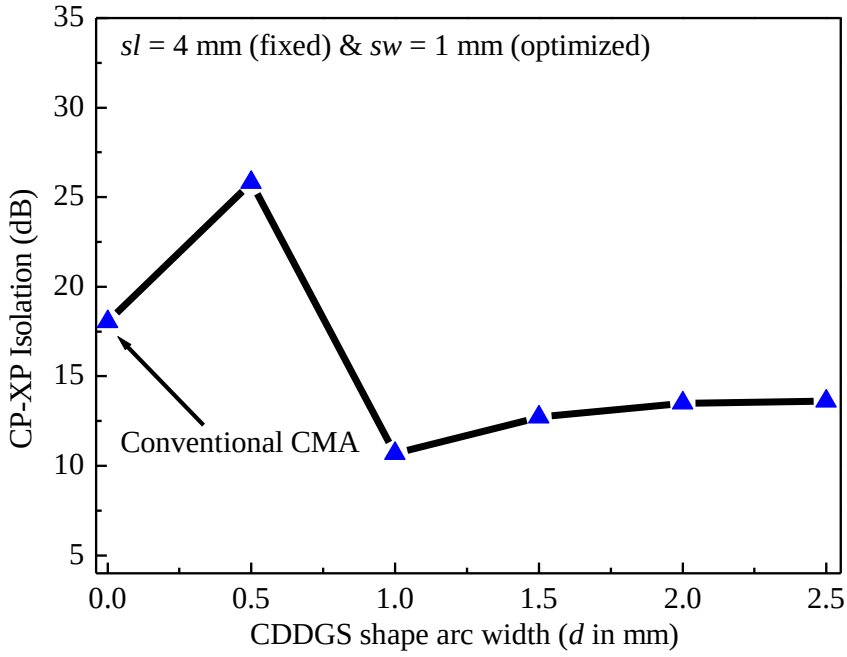

Fig. 3.4 Simulated plot of CP-XP isolation with respect to variation of dumbbell arc (*d*) of CD-DGS. (*sw* = 1 mm (optimized), *sl* = 4 mm (fixed)).

After finalizing the optimum value of the width (*sw*) of the rectangular head of the CDDGS and the width of the dumbbell arc (*d*) of CDDGS next the effect of the length (*sl*) of the rectangular head of the CDDGS structure has been studied by varying the *sl* from 2 mm to 5 mm and documented in Fig. 3.5. It has been seen that the polarization purity decreases while increasing *sl* up to 3.5 mm but after that polarization purity improves without hampering other radiation profile parameters. Conventional CMA (*sl* = *sw* = *d* = 0 mm) provide the CP-XP isolation around 18 dB whereas the proposed structure with *sl* = 4 mm, *sw* = 1 mm (optimized) and *d* = 0.5 mm (optimized) provides CP-XP isolation of 26 dB.

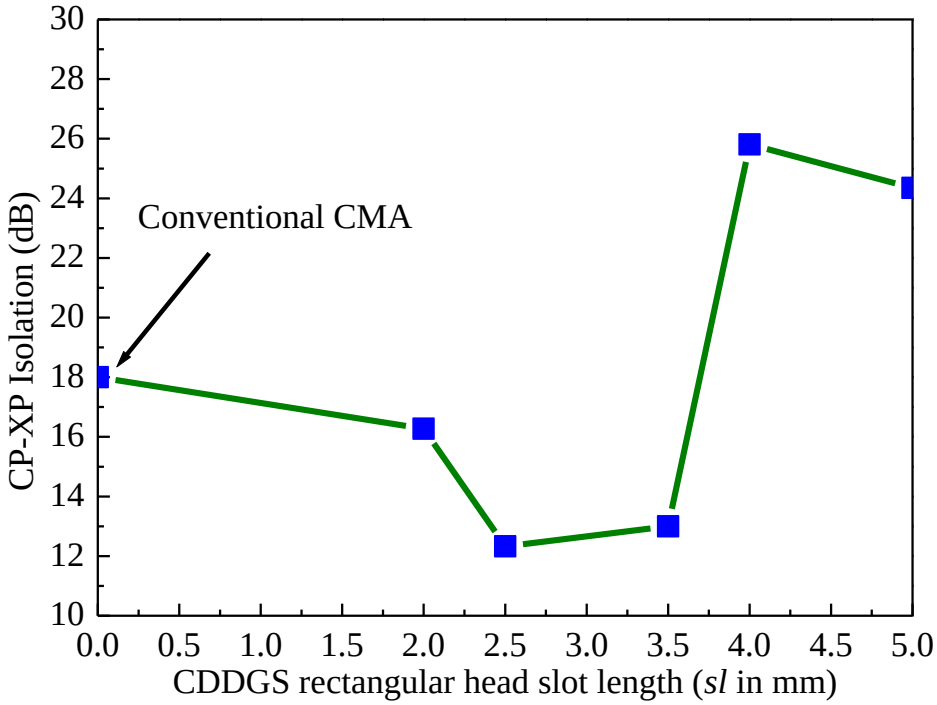

Fig. 3.5 Simulated plot of CP-XP isolation with respect to variation of CD-DGS rectangular head slot length (*sl*) (*sw* = 1 mm (optimized), *d* = 0.5 mm (optimized).

The H-plane XP level plot is shown in Fig. 3.6. This plot further confirms that as soon as the CDDGS is incorporated at the non-radiating edges of the conventional CMA the H-plane XP level reduces which in turn shows the improvement of polarization purity by the proposed curved dumbbell shape defected ground structure (CDDGS) incorporated CMA that is discussed earlier.

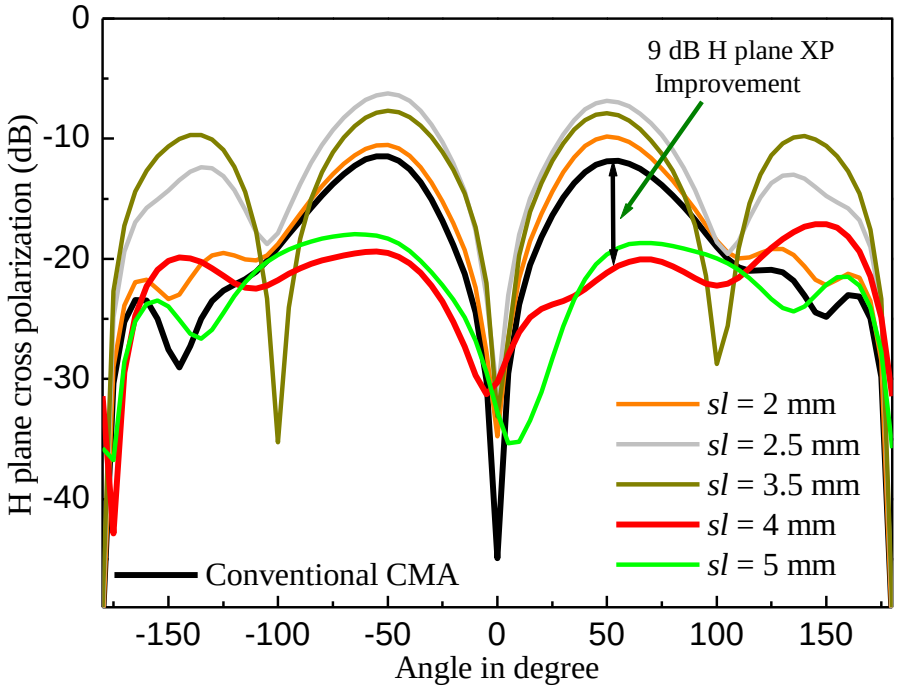

Fig. 3.6 H plane cross-polarization radiation with respect to CDDGS rectangular head slot length (*sl*).

Fig. 3.7 clearly shows the gain profile of the CDDGS incorporated CMA. It is clearly evident that the incorporation of curved dumbbell shape defected ground structure (CDDGS) at the non-radiating edge does not hamper the co-polarization gain performance. The gain profile is quite the same as conventional CMA and stable also.

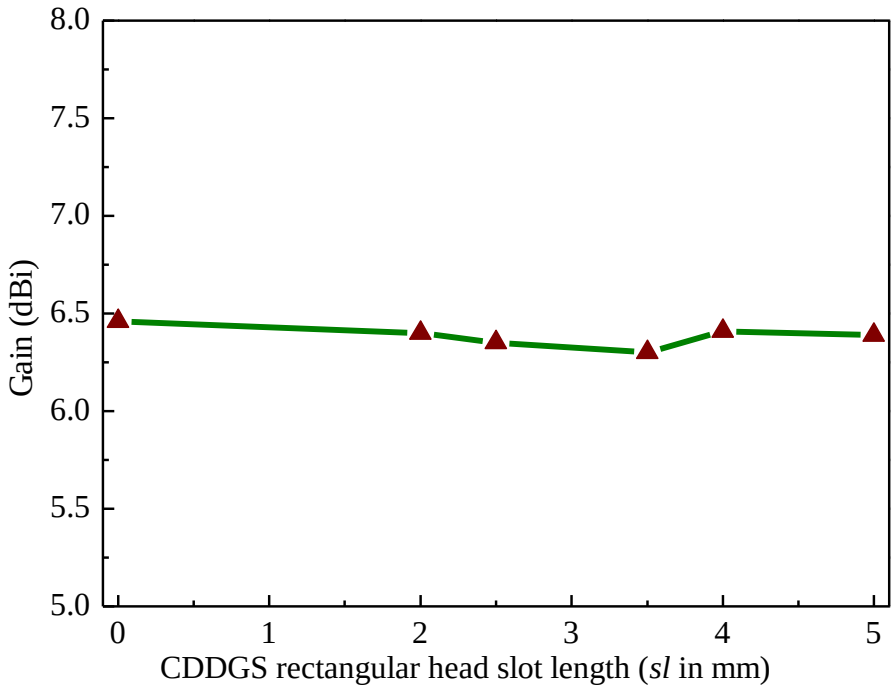

Fig. 3.7 Variation of gain of the proposed CD-DGS structure with respect to CD-DGS rectangular head slot length (*sl*).

3.2.2 Optimum Structure

At the beginning, a conventional CMA antenna has been designing which having radius (*r*) 7 mm on the top of RT-Duroid substrate (ε_r = 2.33) with height (*h*) 1.75 mm over the ground of 70*70 mm^2. After that a symmetrical pair of curved dumbbell shape DGS structure has been deployed on the ground plane at the non-radiating edges where the width of the arc of CDDGS (*d*) is 0.5 mm, the width (*sw*) of the rectangular head of the CDDGS is 1 mm and the length (*sw*) of the rectangular head of the CDDGS is 4 mm. The values of the different parameters of the optimum structure have been finalized through parametric studies that is already discussed carried out as shown in Fig. 3.1.

3.2.3 Simulated Result and Discussions from Optimized Structure

The reflection coefficient profile of any antenna structure shows how efficiently the matching is done. Proper matching is very much required to get the optimum performance from any antenna structure. The comparison of the reflection coefficient (S_{11}) profile of conventional and proposed structures has been reviled in Fig. 3.8 with the help of [159]. Reflection co-efficient profile is clearly evident that the convention CMA has narrow impedance bandwidth around 4% while the CMA with CDDGS provides an impedance bandwidth of 12% without effect of frequency spectrum which is quite good as compare than conventional CMA but both structures provide very good impedance matching.

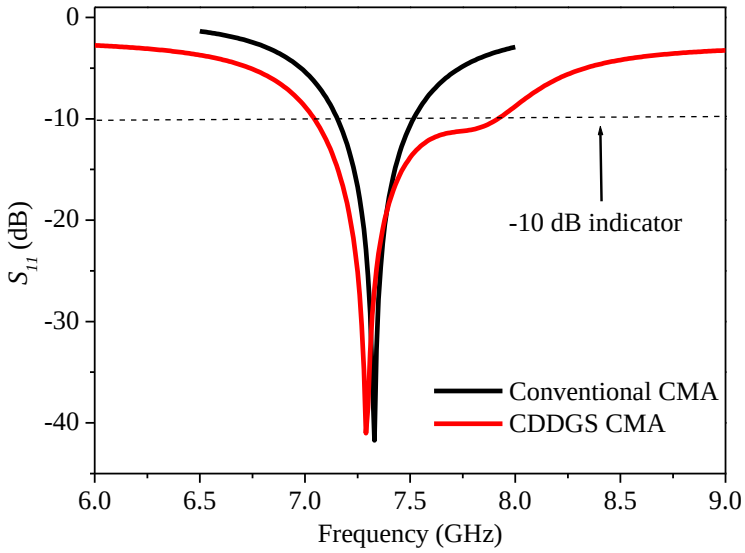

Fig. 3.8 Simulated S_{11} profile of conventional and proposed CDDGS integrated CMA.

The complete E plane CP and XP radiation profile of conventional and proposed structure have been revealed in Fig. 3.9. The E plane CP radiation of the proposed structure is quite same as conventional CMA, where both the structures attain 6.41 dBi gain and XP radiation is below -30 dB which is quite good and convincing. Fig. 3.9 also provides a clear evident that the incorporation of the CDDGS at the non-radiating edge does not affect the CP radiation of the E plane.

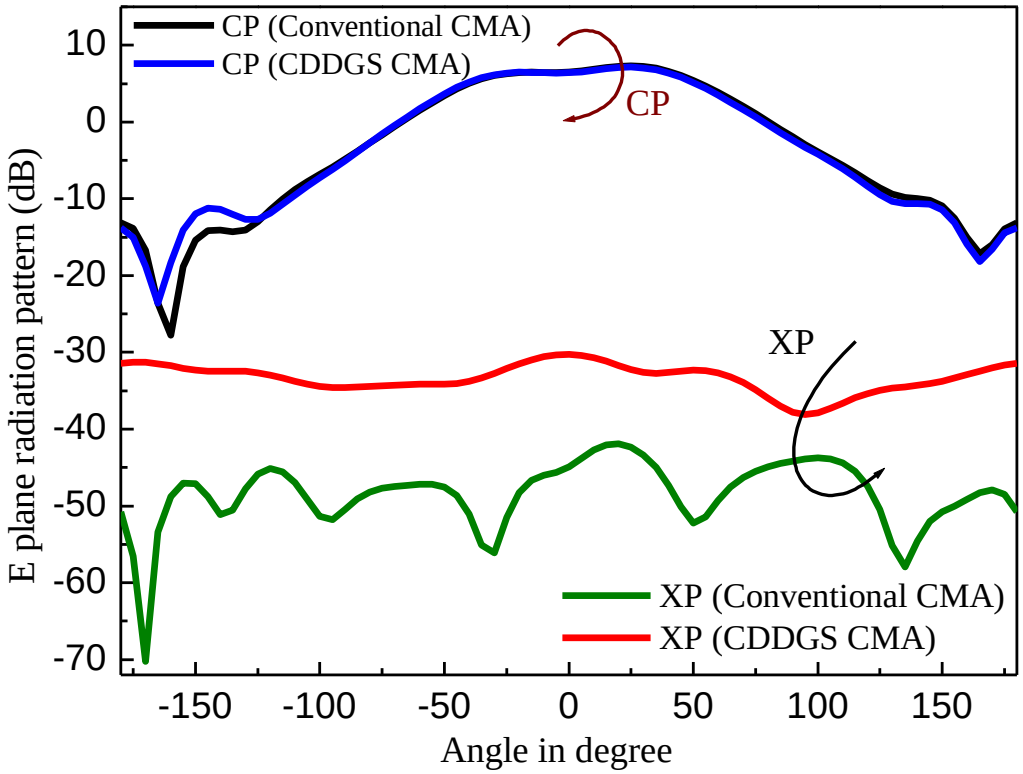

Fig. 3.9 E plane radiation pattern of the conventional and proposed structure.

The H plane radiation pattern of the proposed structure and conventional CMA has been shown in Fig. 3.10. In this present model, the H plane cross-polarization has been surprisingly improved as compared to the conventional CMA without hindering the broad side co-polarization radiation. Deployment of CDDGS in the H plane peak XP radiation decreased by almost 9 dB where the CP profile of conventional and proposed structures remain constant. The peak value of XP of the proposed structure and conventional CMA is -20.4 dB and -11.45 dB respectively.

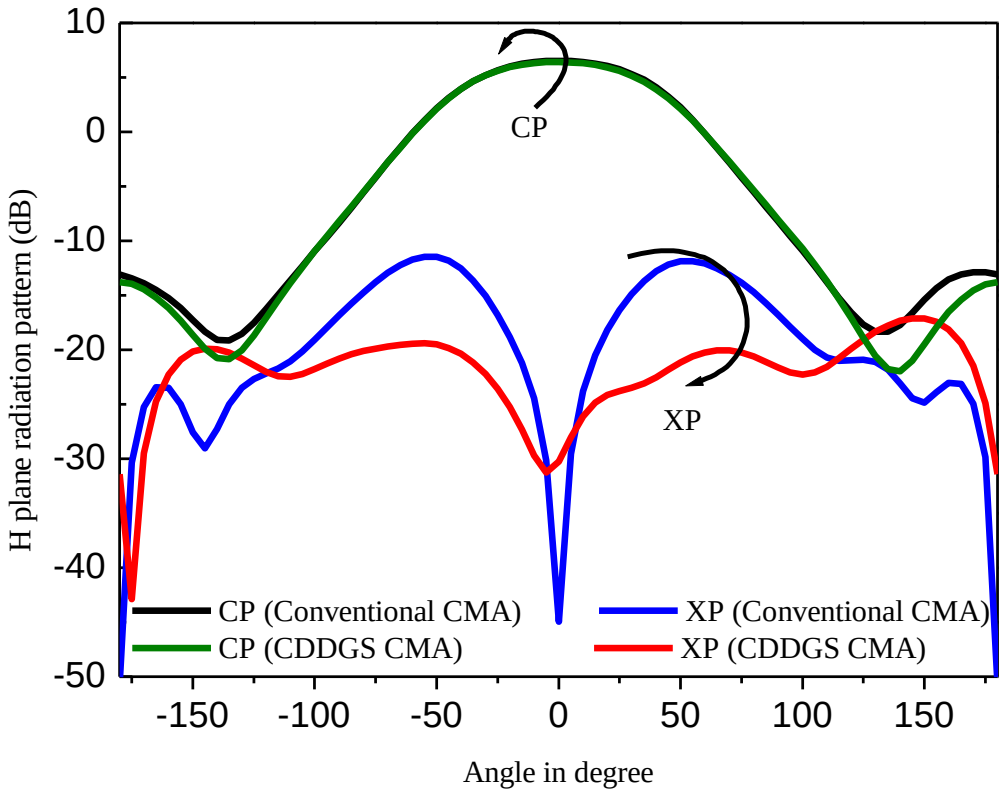

Fig. 3.10 Normalized H plane radiation pattern of the conventional and proposed structure.

3.3 Rectangular Shaped Defected Ground Structure Integrated CMA: A Way to Enhance Impedance Bandwidth and Polarization Purity

In the previous section impedance bandwidth and polarization purity of a conventional CMA is improved by placing curved shaped dumbbell DGS at the non-radiating edges of the patch. In high-speed wireless communication systems much wider impedance bandwidth is required. So, for high-speed wireless communication systems impedance bandwidth is further enhanced by placing a pair of rectangular DGS at the radiating edges of a conventional CMA on RT-Duroid substrate with dielectric constant (ε_r) 2.33 and height (h) 1.58 mm in order to counsel the limitation of the earlier structure and for the concurrent improvement in impedance bandwidth and polarization purity. The proposed rectangular DGS incorporated CMA is shown in Fig. 3.11.

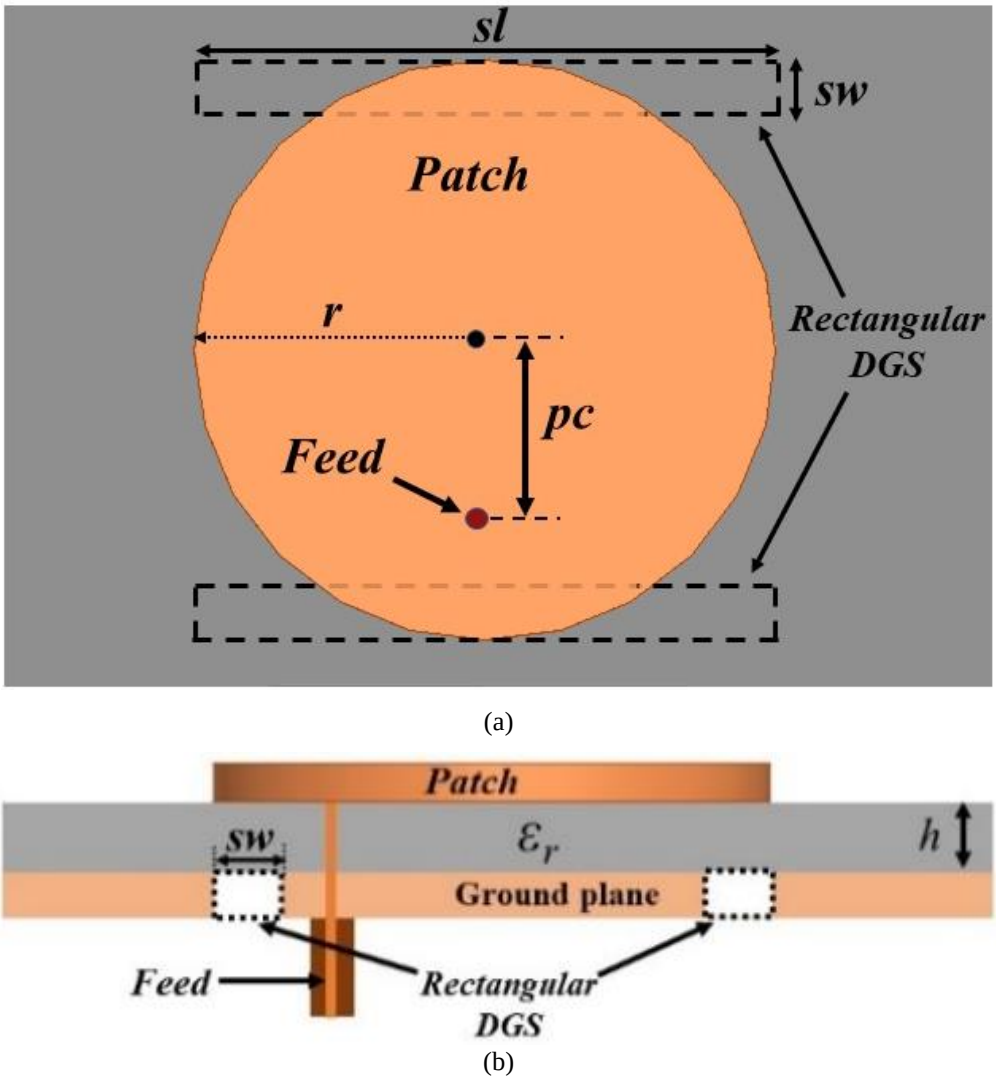

Fig. 3.11 Schematic representation of proposed Rectangular defective ground structure (RDGS) integrated CMPA (a) top view (b) side view.

3.3.1 Theoretical Background and Parametric Studies

The conventional CMA is basically an open resonator. Any type of modification by placing defects below the patch or on the ground plane definitely hampers the tradition cavity boundary conditions and changes the field between ground plane and patch. This changes in the filed distribution also influences the input as well as the radiation characteristics of the modified structure. The defect size and shape critically decide the behaviour of the cavity fields so the selection of the defect dimensions is very much important to get the best performance from the modified antenna structure.

The bandwidth of the antenna is inversely proportional to the quality factor and quality factor is inversely proportional to the different losses occurred in the antenna. So, the bandwidth increases with the increase in loss which increases as the defect size increases.

With the above theoretical concept, a pair of rectangular DGSs has been incorporated on the ground plane at the radiating sides of a conventional CMA with radius (*r*) 7 mm. The length (*sl*) of the rectangular DGS (RDGS) is kept as the same as the diameter of the CMA so that the overall dimension of the circular patch does not increase. Then the width (*sw*) of the rectangular DGS is varied to get the optimum dimension of the width of the RDGS.

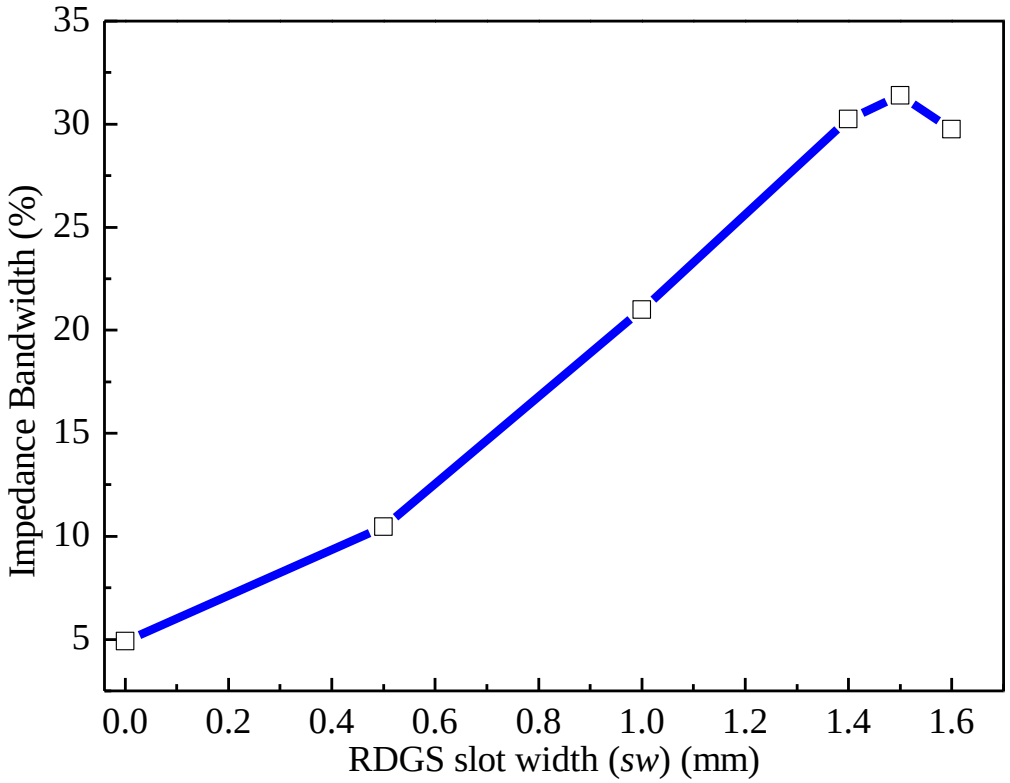

Fig. 3.12 Variation of impedance bandwidth (%) as a function of RDGS width with RDGS length (*sl*) fixed at 14 mm.

Initially, RDGS with width length 0.5 mm (*sw* = 0.5 mm) is placed. Improvement of the impedance bandwidth of proposed structure is observed as compared to the conventional CMA. The conventional CMA (*sl* = *sw* = 0 mm) provides a impedance bandwidth of 5% whereas the impedance bandwidth increases to 11% with RDGS

structure with length 14 mm and width 0.5 mm (*sl* = 14 mm and *sw* = 0.5 mm) as shown in Fig. 3.12.

Figure 3.13 also confirms the improvement of impedance bandwidth and shows that due to the RDGS deployment the resonant frequency corresponding to the lowest order mode moves towards the upper side in the frequency spectrum. The effective permittivity of the substrate changes due to the incorporation of the RDGS [166]. The width (*sw*) of the RDGS increases further up to 1.6 mm. As the width (*sw*) increases the impedance bandwidth increases up to *sw* = 1.5 mm then for *sw* = 1.6 mm it decreases. Both Fig. 3.12 and Fig. 3.13 confirms this. The impedance bandwidth with *sw* = 1.5 mm is 32% which is much higher than the conventional CMA.

Along with the impedance bandwidth, the studies on polarization purity are also performed. Fig. 3.14 shows the variation of XP in H plane as the width (*sw*) varies form 0.5 mm to 1.6 mm keeping the RDGS length (*sl*) fixed at 14 mm. Initially, the polarization purity decreases after placing the RDGS but later it improves and provides best polarization purity with *sw* = 1.5 mm. The polarization purity is only 15 dB in case of conventional CMA whereas with modified structure it is around 24 dB.

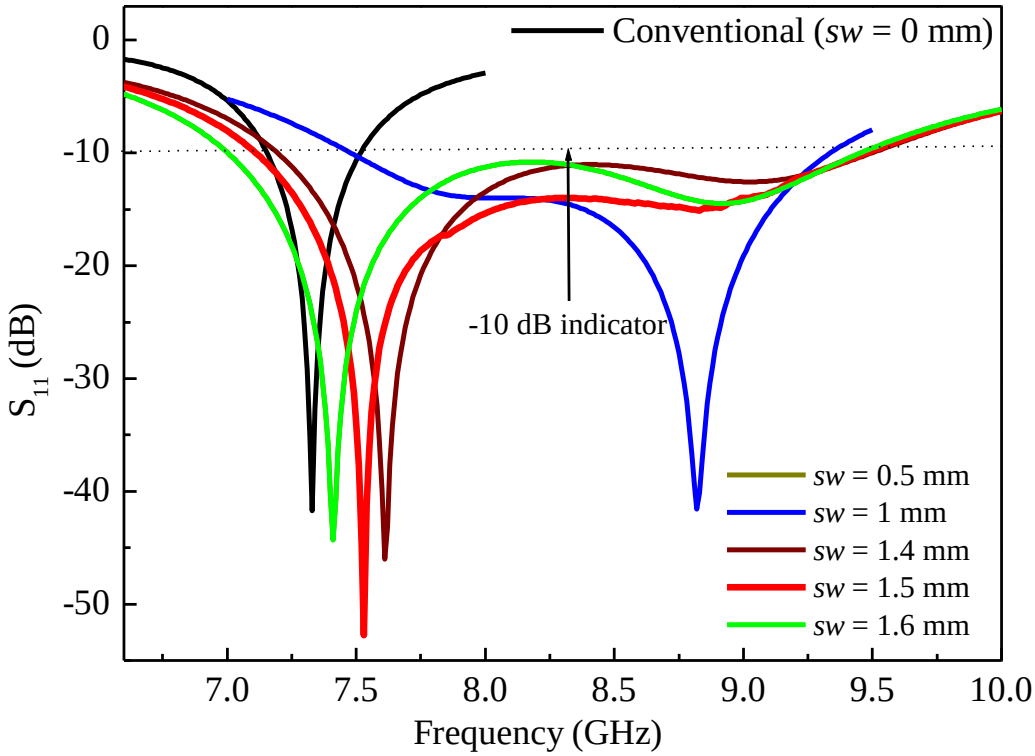

Fig. 3.13 Reflection coefficient profile for conventional CMA and RDGS incorporated CMA with RDGS length (*sl*) fixed at 14 mm.

With the above parametric studies on impedance bandwidth and polarization purity it is confirms that the RDGS integrated CMA structure provides optimum performance with *sl* = 14 mm and *sw* = 1.5 mm.

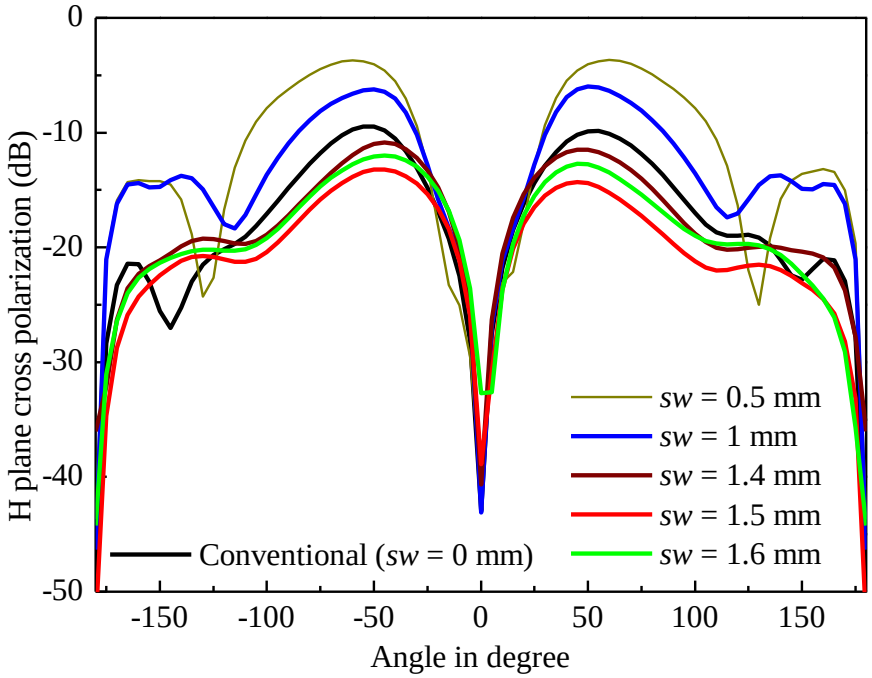

Fig. 3.14 Variation of H plane XP level as a function of RDGS width (*sw*) with RDGS length (*sl*) fixed at 14 mm.

3.3.2 Optimum Structure

At first conventional circular microstrip antenna has been designed which having radius (*r*) 7 mm on RT-Duroid material with dielectric constant (ε_r) 2.33 and height (*h*) 1.58 mm. After that a pair of rectangular DGS (RDGS) has been deployed at the radiating edge where the length (*sl*) of the rectangular DGSs is kept same as the diameter of the circular patch i.e., 14 mm. From the parametric studies it is seen that the rectangular DGSs with width (*sw*) 1.5 mm provides the best output in terms of impedance bandwidth and polarization purity. This is way the final proposed structure has been built as shown in obtained in Fig 3.11. The detailed parameters of the proposed RDGS integrated CMA are documented in Table 3.1.

TABLE 3.1 The detailed parameters of the proposed rectangular DGS loaded CMA (Substrate thickness *h* = 1.575 mm)

Substrate	ε_r	***Ground plane* (mm^2)**	***r* (mm)**	***sl* (mm)**	***sw* (mm)**
RT-Duroid	2.33	70 x 70	7	14	1.5

3.3.3. Results and Discussions

This section discusses the output obtained with the help of [159] from the optimized proposed structure. Fig. 3.15 depicted the reflection coefficient (S_{11}) profile of the conventional CMA and proposed CMA with RDGS structure. Conventional CMA resonates at 7.27 GHz whereas proposed antenna with RDGS resonates at 7.53 GHz so it clearly evident that due to the deployment of rectangular DGS structure at the radiating edge the resonance frequency has been shift towards higher frequency spectrum but it quite same as conventional patch and both structures provide very good impedance matching. It is very much clear that the conventional CMA has narrow impedance bandwidth in the order of 5% whereas the proposed modified structure provides an impedance bandwidth of 32% which is much higher as compared to the conventional CMA.

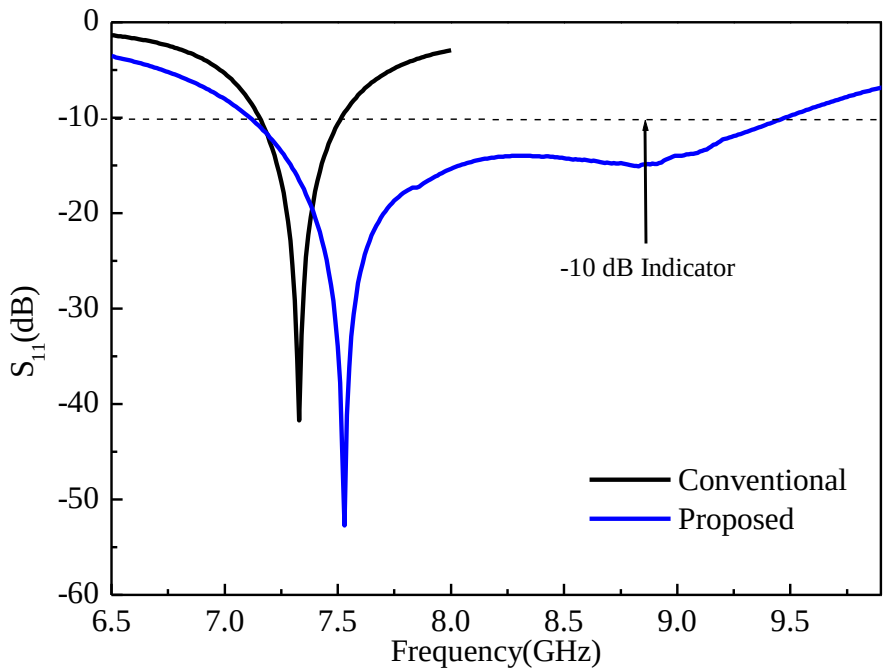

Fig. 3.15 Simulated reflection coefficient profile of conventional and proposed rectangular DGS integrated CMA.

The E plane normalize radiation profile has been revealed in Fig. 3.16. The figure clearly evident that E plane XP is below -37 dB for both conventional CMA as well as the proposed antenna, which is quit convincing. The co-polarization radiation in E plane has not been affected much due to the incorporation of rectangular DGSs at the radiating edges.

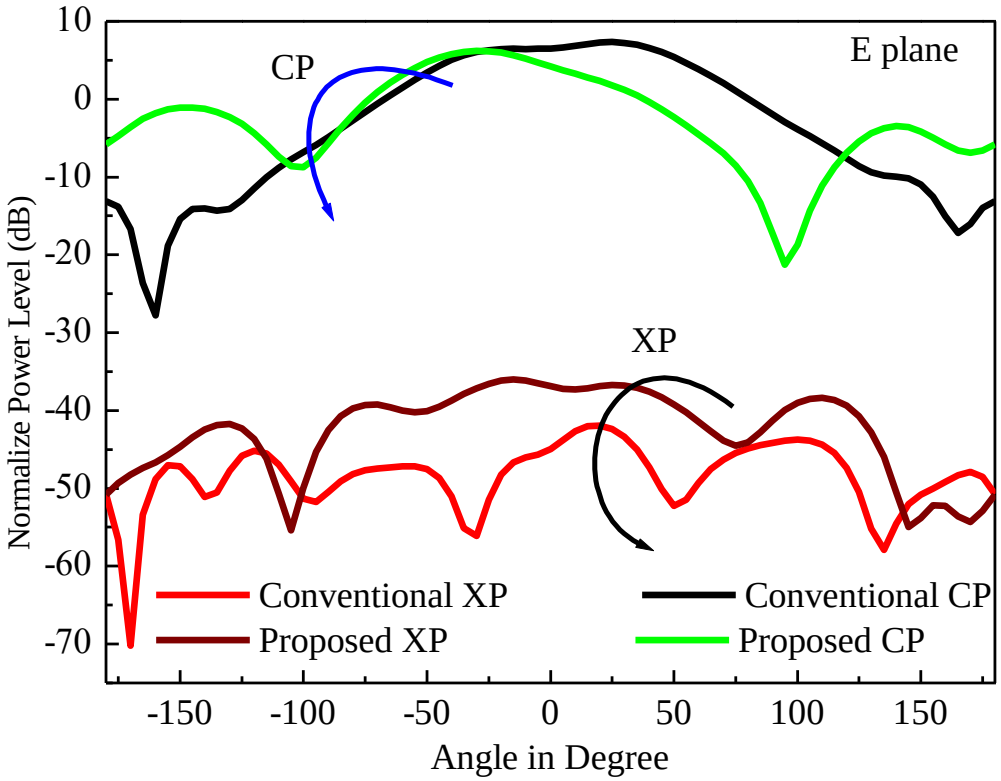

Fig. 3.16 Normalized E plane radiation pattern of conventional and proposed rectangular DGS integrated CMA.

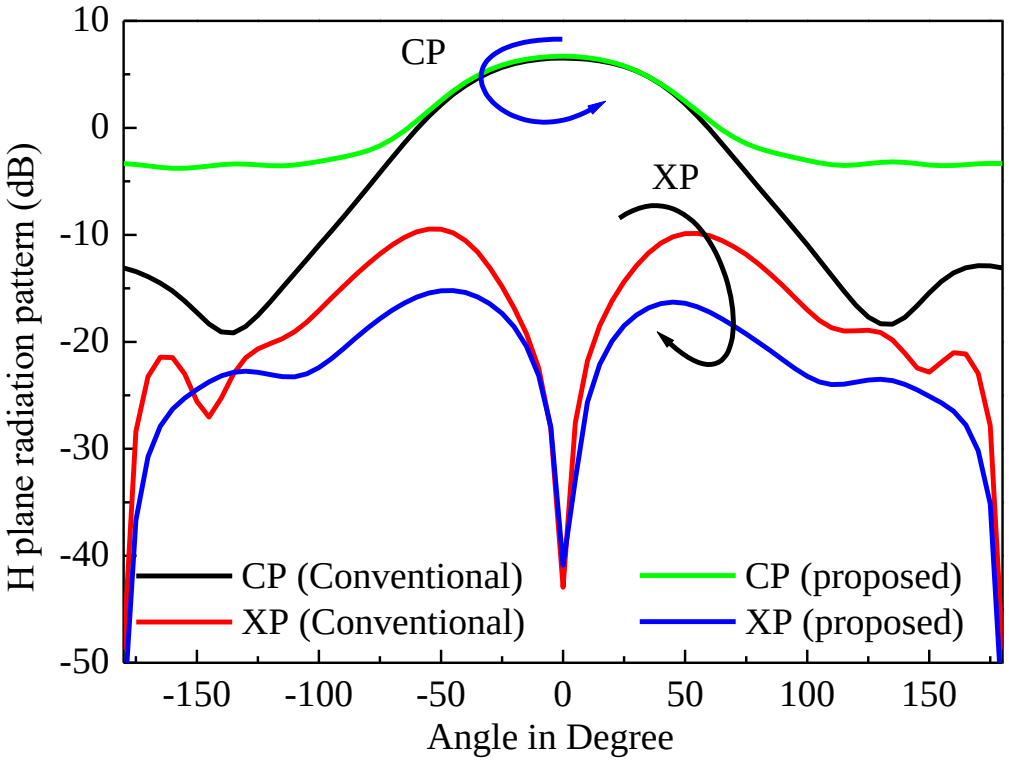

Fig. 3.17 Simulated conventional and proposed structure radiation pattern in H plane.

Comparison of proposed model and conventional CMA H plane radiation pattern has been revealed in the Fig. 3.17. The peak H plane co-polarization gain is 6.52 dBi and 6.69 dBi in case of conventional CMA and proposed antenna respectively. The peak XP level in H plane is -9.45 dB and -18.2 dB in case of conventional CMA and proposed antenna respectively. The deployment of rectangular DGSs at the radiating edge do not affect the co polarization radiation in H plane whereas the peak XP radiation decreases by almost 9 dB. This clearly improves the PP by a factor of 9 dB in case of RDGS integrated CMA.

3.4. Conclusion

In this chapter two defected ground structure integrated CMA has been discussed to improve the impedance band width, polarization purity with stable co-polarization gain. In the first structure a pair of curved dumbbell shape DGS (CDDGS) structures have been deployed at the non-radiating edge of conventional CMA which provides around 26 dB polarization purity with 12% impedance bandwidth with a stable co-polarization gain of 6.41 dBi. Next for further improvement of the impedance bandwidth a pair of rectangular defects has been placed on the ground plane just beneath the radiating edges of the conventional CMA. With this rectangular DGS integrated CMA 32% impedance bandwidth and around 25 dB CP-XP isolation (polarization purity) have been achieved. For both the DGS structures a detailed parametric study has been carried out to find the optimum dimensions of the defect structures. The simultaneous improvement of impedance bandwidth, polarization purity has been achieved without disturbing the conventional E plane radiation pattern which is very much required in modern wireless communication.

CHAPTER

4

Reduced Surface Wave Approach with Modulation of Fringing Field to Yield Concurrent Improvement in Radiation Properties of Circular Microstrip Antenna

4.1 Introduction

The classical circular microstrip antenna (CMA) with defected ground surface (DGS) and strip loading approach for the improvement in radiation characteristics specially the polarization purity (PP) has been vividly discussed in chapter 2 and chapter 3. Notably, gain and efficiency enhancement of CMA was not seen in those approaches. Nevertheless, the concurrent improvement in overall radiation characteristics is very much crucial and challenging for antenna researchers which has been dealt in the present chapter.

The CMA based on reduced surface wave (RSW) theorem is a typical category of microstrip antennas that extremely reduces the surface wave fields than conventional microstrip antennas. Therefore, such RSW inspired CMA is immensely preferable as they have reduced horizontal radiation and less edge diffraction for a finite-sized ground plane. Moreover, the fundamental TM_0 surface wave causes increased mutual coupling between distant antenna elements which is undesirable for any array or MIMO configuration in modern 5G communications. However, such TM_0 surface wave elimination is impossible in conventional design (as it has zero cut off frequency) until a special surface wave mitigation technique has been employed. As the surface wave propagates laterally along the substrate, the lateral radiation occurs and will usually interact with other associated circuitry or the supporting structure of hand-held communication equipment. Therefore, the RSW inspired CMA is presently a state-of-the-art research topic for scientific and antenna research community.

In the last several years, many works have been reported to enhance the gain of microstrip antennas (MA) [26, 148, 167 - 169] by employing composite microstrip-monopole topology or modifying the dielectric material as air substrate or air dielectric composite substrate. However, all these efforts are given in rectangular patch geometry rather than circular. The gain and efficiency enhancement in circular patches have been investigated in [137, 150 - 155, 170]. Amid them, the technique such as slot-loading with aperture coupling [150] and the use of 3 stacked ground plane with slot and shorting vias [170] have been adopted to achieve around 7.8 dBi gain with no improvement in polarization purity (PP). However, around 90% efficiency that has been achieved in [170] is at the cost of its high-profile nature. To further achieve maximum gain from 7.2 dBi to 9 dBi with PP of 18-19 dB only, the annular ring antenna in [152] was loaded with shorting vias (with branch line couplers), while numerous shorting vias beneath the circular patch have been reported in [153]. Even though the structures reported in [152 – 153, 170] can achieve an efficiency of 69% to 73%; its corresponding investigations have failed to address the typical antenna performances such as gain, efficiency, and polarization purity. Notably, a structure similar to [152 – 153, 170] has been reported in [137], and it can achieve high gain and efficiency of 11 dBi and 89%, respectively. Although desirable gain and efficiency are exhibited in [137], it suffers from poor PP of 17 dB and a much-distorted radiation pattern with a high side-lobe level. To attain high gain of around 6.8 dB to 8 dBi for patch antenna, various techniques have been investigated, such as the adaptation of circular dual-stacked dense dielectric patch [154], replacement of circular patch geometry hexadecagon circular patch [155], and the use of graphene-based patch [156]. However, these techniques have shown no improvement in either efficiency or polarization purity.

The improvement in PP is very important for modern wireless applications. Numerous efforts have been given by modifying the patch geometry [157, 171], use of shorting metal strip [172], multiple shorting vias [173], slotted patch with shorting vias [174] or using of DGS [141], to improve PP of microstrip antenna, in which maximum PP of approximately 22 dB to 23 dB is achieved but with no improvement in gain and efficiency. Notably, other applications such as the base station terminal for

a microcellular system, its corresponding antenna is mounted on the same substrate used for the active microwave components [175]. In these cases, horizontal radiation (lateral) arises from the surface wave is the key factor to mutilate the antenna performances. Therefore, the isolation between bore-sight gain (BG) to horizontal direction gain (HG), which is referred to as BG-HG isolation is a crucial factor to determine in those cases. This is in fact, a very important parameter for the applications in GPS receiving antenna that trim down low elevation angle interfering signals [176].

In order to address the lacunae of the earlier studies and for the improvement in gain, efficiency, and the polarization purity, a CMA with a pair of shorting strips (shown in Fig. 4.1) has been proposed and fabricated based on RSW theorem in the present chapter.

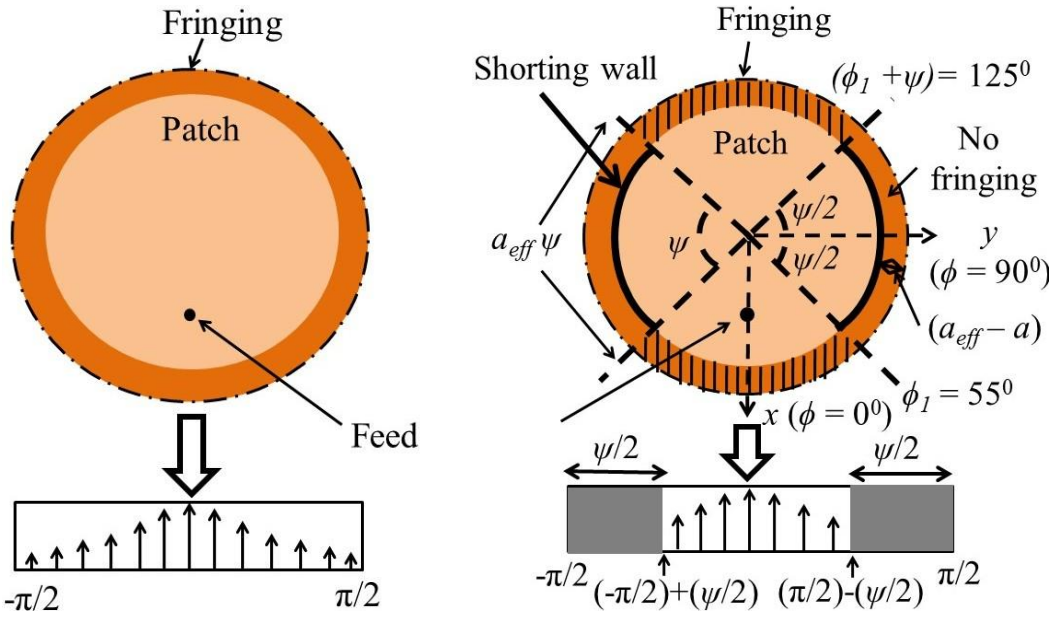

Fig. 4.1 The schematic representation of patch (a) conventional CMA and (b) the proposed antenna with field distribution at lower radiating slots for conventional and proposed antenna.

The chapter has been arranged in the following way. A thorough quantitative analysis is presented for clear visualization-based understanding in section 4.2 which includes the concept of excited mode (section 4.2.1), effective permittivity and resonant frequency (section 4.2.2), gain and efficiency (section 4.2.3), and cross polarized radiation (section 4.2.4). The parametric studies and optimization of the structure to obtain the best output from the proposed structure is presented in section 4.3. Section 4.4 discuss the details of the proposed structure and the experimental

setup. The proposed structure has been validated through the experimental measurements in section 4.5. The conclusion of the proposed work is documented in section 4.6.

4.2 Theoretical Insight

4.2.1 Excited Mode

The circular patch antenna can be modelled as cylindrical cavity resonator with its dominant mode as TM_{11}. At this dominant mode, there is one circumferential field variation and it produces maxima (anti-nodal points) at $\phi = 0^0$ and 180^0 while it has minima (nodal points) at $\phi = 90^0$ and 270^0. Certainly, shorting strip or shorting vias at nodal points ($\phi = 90^0$ and 270^0) does not hamper the dominant TM_{11} mode field configuration. Contrarily, shorting strip or shorting vias at such position definitely hampers other higher order modes like TM_{21} and TM_{31} as they have anti-nodal points there. Therefore, to keep the mode unperturbed, the shorting element must be given at the minima (nodes) of the standing wave distribution. Following this concept, cored patch with air or concentric shorting ring designs have been reported in [152], [177 - 179] where, the dominant mode is not perturbed. However, when the substrate material is removed or replaced by other material, wave number changes [178], [180 - 181]. This effectively modifies the effective dielectric constant of the substrate [178, 180 - 182].

Similar to them, the present antenna also exhibits the dominant TM_{11} mode with modified substrate permittivity. Therefore, the frequency shifts, as is explained in the next section. Here, the shorting strip is incorporated judiciously in the specific position (along non-radiating periphery near $\phi = 90^0$ and 270^0) of circular patch to suppress other possible TM_{21} and TM_{31} higher order modes while keeping the dominant TM_{11} mode unperturbed.

Simulated electric surface current on the patch and electric field magnitude within the substrate for conventional CMA and proposed antenna are depicted in Fig. 4.2 confirms the explained mode of the proposed patch and it is definitely dominant TM_{11} mode.

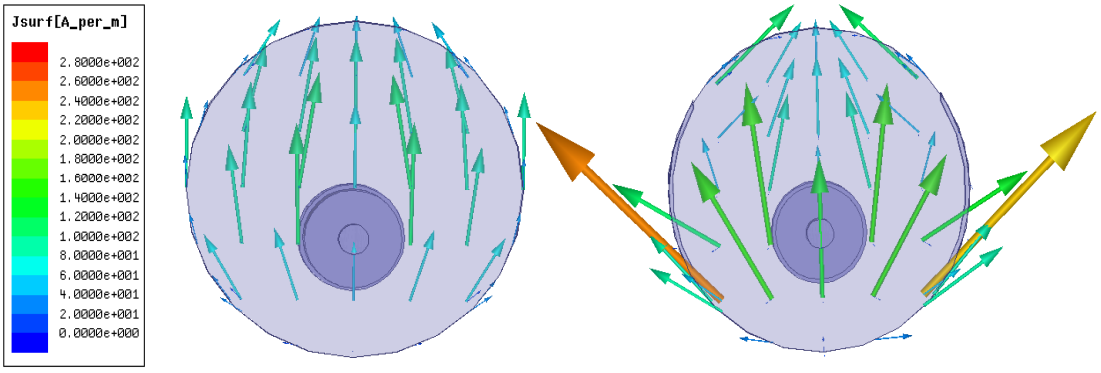

(a) (b)

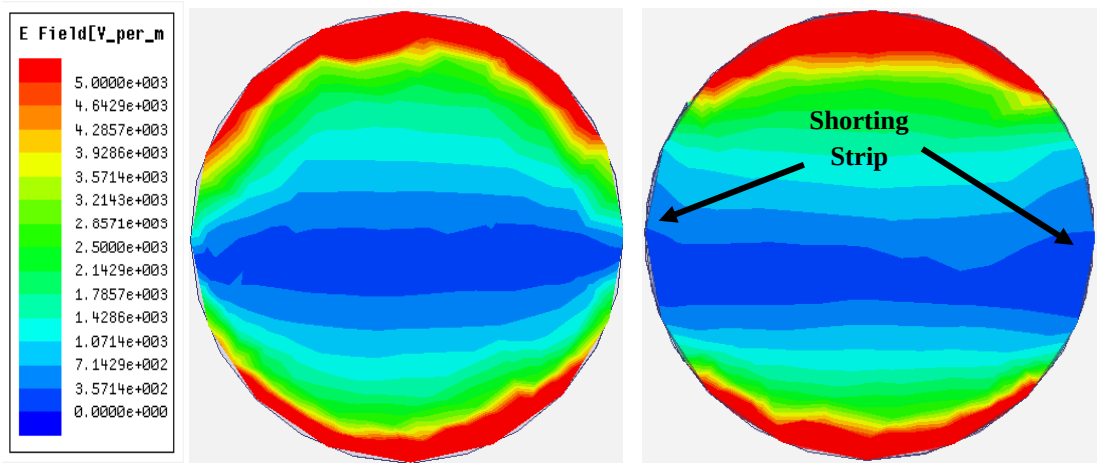

(c) (d)

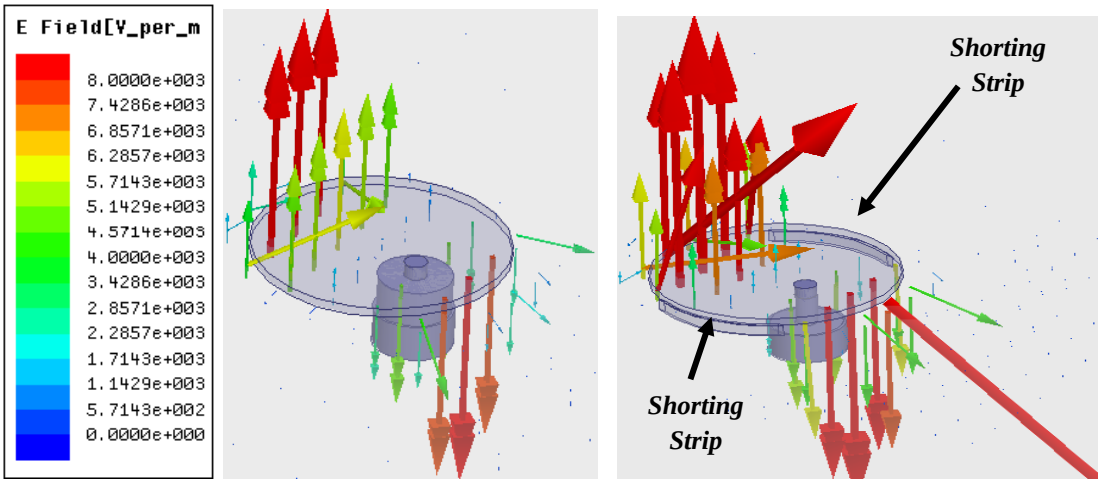

(e) (f)

Fig. 4.2 Electric surface current vector on patch surface (a) conventional circular patch, (b) Proposed patch, Electric field magnitude over patch surface (c) conventional circular patch, (d) Proposed patch, Electric field vector within substrate (e) conventional circular patch, (f) Proposed patch, [All figures are in same scale which is provided at left of each row]

In the present structure, the shorting strip is placed in such a way, the dominant mode is kept unaltered while it suppresses higher order orthogonal modes. Therefore, the excited mode is still TM_{11} mode but with a frequency shift towards the higher side of the spectrum as explained later in section 4.2.2.

When the substrate material is removed or replaced by other material, wave number changes [178 - 181]. This effectively modifies the effective dielectric constant of the substrate [178 - 182]. For cored patch with air or concentric shorting ring designs [177], it is found that the first solution exhibits still TM_{11} mode. It has been shown in open literature [177] that, the second solution may exist and that is TM_{12} and is only possible for high dielectric constant. The critical value of that high dielectric constant is 8.3846. Therefore, substrate with dielectric constant more than 8 may excite other mode like TM_{12} rather than dominant TM_{11} mode. Therefore, it is confirmed that in the present antenna, the mode does not change in all the cases with shorting strips or posts. It may also be noted that, there is a critical dependence of shorting element position to perturb the mode.

However, it is agreed that, sometimes the mode changes due to shorting strip [172, 183]. Nevertheless, it is not the case for all shorted structures. It is observed that in [177], [152 – 153, 184 - 185], mode is still dominant TM_{11} mode. However, in some cases frequency shifts are observed. That is mainly due to change of substrate permittivity. Similar to them, the present antenna also exhibits the dominant TM_{11} mode with modified substrate permittivity. Here, the shorting strip is incorporated judiciously in the specific position (lateral side of patch; along non-radiating sides from 55^0 to 125^0 i.e., $\psi = 70^0$ as shown in Fig. 4.3) of circular patch to suppress other possible TM_{21} and TM_{31} higher order modes. It is done with a view to perturb the anti-nodal points of such TM_{21} and TM_{31} higher order modes while it does not hamper the dominant TM_{11} mode. In fact, the nodal point exists for TM_{11} mode at the position of shorting strip and hence the mode TM_{11} becomes unperturbed. Therefore, though boundary condition differs in present case, it doesn't hamper the dominant mode much. This is explained in the Fig. 4.3 where, the circumferential electric field variation along patch circumference ($\varphi = 0^0$ to 180^0) is shown for possible modes.

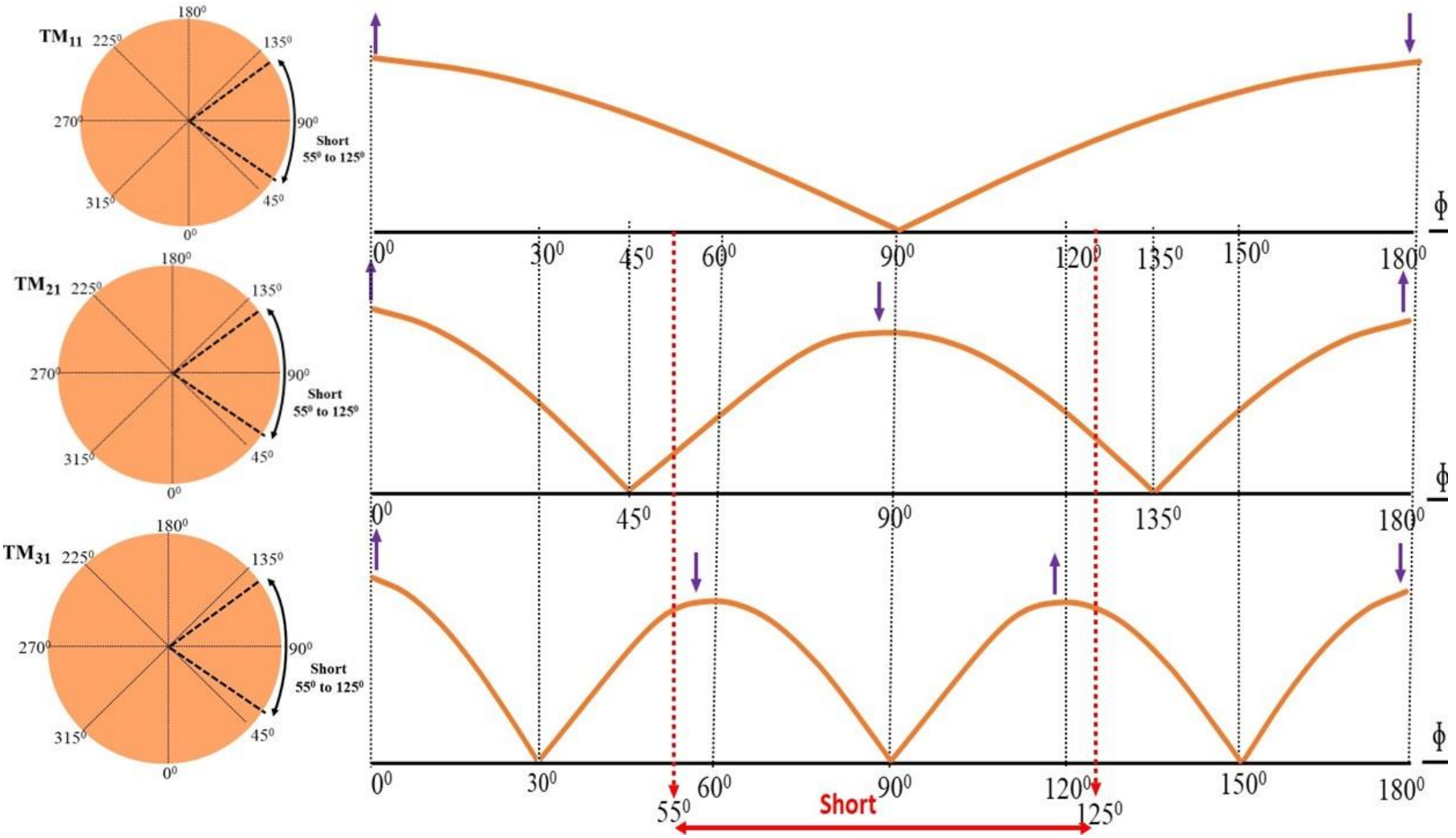

Fig. 4.3 The effect of shorting strip on mode

The cavity field distribution for few possible modes which has a tendancy of automatic excitation can be written as [26],

$$\left.\begin{array}{rll} & E_z = E_0 J_m(K_\rho \rho) Cos(m\phi) & \\ TM_{11} \rightarrow & E_z = E_0 J_1\left(1.84\frac{\rho}{a}\right) Cos\phi & \\ TM_{21} \rightarrow & E_z = E_0 J_2\left(3.05\frac{\rho}{a}\right) Cos(2\phi) & \\ TM_{31} \rightarrow & E_z = E_0 J_3\left(4.20\frac{\rho}{a}\right) Cos(3\phi) & \end{array}\right\} \quad (4.1)$$

Close inspection of (4.1) and Fig. 4.3 reveals that, antinodes of *TM21* and *TM31* will be suppressed due to short. To perturb any mode, the best way is to put a shorting element at the antinodal point of that specific mode. Notably, *TM11* mode is unaffected as null point or mainly nodal point exists in the specific 55^0 to 125^0 region.

The Fig. 4.3 clearly corroborates that, the higher order *TM21*, *TM31* modes are definitely suppressed due to shorting strip (as the shorting element is at anti-nodal points of such modes) while it trivially affects the dominant *TM11* mode. Although, some of the dominant *TM11* mode field is also suppressed but it is up to small extent. Rather, such minimal suppression of dominant *TM11* mode field near non-radiating edges causes spill out of fields through radiating edges and this helps to improve the radiation performance. Therefore, few insignificant electric field (near the nodal point of *TM11* mode) is suppressed due to shorting strip which certainly do not perturb the dominant mode much. Rather, it reduces cross polar radiation as well as increases aperture efficiency as is described in the following section.

Again, *TM12* mode will not be excited as there are no short inside the patch area as explained in Fig. 4.3.

4.2.2 Effective Permittivity and Resonant Frequency

As the quasi-static approach to developing the effective permittivity of the substrate in MA is the most simple and lucid technique [180 - 182], it is adopted in the present investigation. There, the dense array of a metallic [180] or air posts [181] to synthesize the substrate permittivity has been employed to yield lower or even negative value [180]. Therefore, in the present study, a pair of shorting strips has been adopted, and it can be considered as an ultra-closed array of shorting vias. Notably, it is done

with a view to obtaining a good estimation of synthesized dielectric constant using a quasi-static technique, as is indicated in [181].

Initially, the antenna has been designed for 12 GHz frequency based on the RSW theorem [177] but the patch size is a little larger than the conventional CMA [178]. Considering the patch radius (a = 7 mm) on PTFE substrate (with thickness h and substrate permittivity ε_r), its effective radius with fringing becomes a_{eff}. As the shorting strips (of angular range ψ) are located at around ϕ = 90˚ and 180˚, the fringing field will not be affected by the dominant TM_{11} mode.

The effective permittivity of CMA is mainly dependent on the effective disc capacitance with fringing. Referring to Fig. 4.1(b), the shorted region is not effectively contributing to disc capacitance, and hence the effective disc capacitance of the proposed antenna may be written as,

$$C_P = \frac{a_{eff}^2(\pi-\psi)}{h}\varepsilon_r \tag{4.2}$$

This capacitance of the proposed antenna may be considered to be equivalent to a similar conventional CMA (of the same effective radius a_{eff}) with new effective permittivity $(\varepsilon_r)_N$. Therefore, equating the disc capacitances,

$$\frac{\pi a_{eff}^2}{h}(\varepsilon_r)_N = \frac{a_{eff}^2(\pi-\psi)}{h}\varepsilon_r \tag{4.3}$$

the following can be derived,

$$(\varepsilon_r)_N = \varepsilon_r\sqrt{(1-\frac{\psi}{\pi})} \tag{4.4}$$

and the resonant frequency of the proposed antenna can be written as,

$$(f_r)_P = \frac{1.84c}{2\pi a_{eff}\sqrt{(\varepsilon_r)_N}} = (f_r)_c\frac{1}{\sqrt{(1-\frac{\psi}{\pi})}} \tag{4.5}$$

In equation (4.5), it can be seen that the effective permittivity $(\varepsilon_r)_N$ decreases with ψ, and subsequently, the resonant frequency will increase.

To design the proposed RSW based on CMA, the effective permittivity must be in the form of [177], i.e.

$$(\varepsilon_r)_N = \left(\frac{\beta_{TM0}}{k_0}\right)^2 \tag{4.6}$$

And the ratio on the right-hand side is a normalized phase constant (NPC) [26] that can be written for PTFE substrate with $\varepsilon_r = 2.33$ as,

$$\left(\frac{\beta_{TM0}}{k_0}\right)^2 = [1 + 0.16(k_0 h)^2]^2 \quad (4.7)$$

Here, β_{TM0} is the propagation constant of the fundamental surface wave mode and k_0 is the normal propagation constant in free space. Therefore, equation (4.4) in conjunction with equations (4.6) and (4.7) has been utilized for the design of proposed RSW inspired CMA as shown in Fig. 4.4. It shows that the true RSW CMA (where the surface wave is not generated) can be designed with such shorting strips with an angular range of $\psi = 100^\circ$ (solution of equations (4.4), (4.6) and (4.7)). However, if $\psi < 100^\circ$, the surface wave can still be minimized those results in a new CMA that has high efficiency and gain along with low XP radiation. Based on the above theory, a comparison of calculated and simulated resonant frequencies of the new antenna as a function of ψ for two different substrate thicknesses ($h = 0.787$ mm and $h = 1.575$ mm) is presented in Fig. 4.5. Here, despite the differences in h, as ψ increases, the effective permittivity will decrease, and the gain and efficiency of the antenna are improved, which consequently leads to a higher resonant frequency. Excellent agreement is also revealed between the calculated results and simulations.

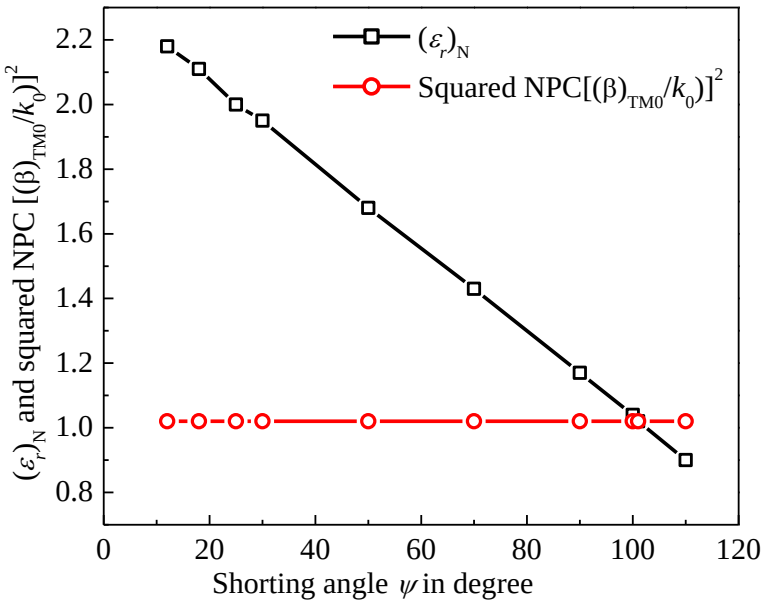

Fig. 4.4 Plot for solution of equations (4.4) and (4.7): Variation of $(\varepsilon_r)_N$ and NPC as a function of shorting angle ψ.

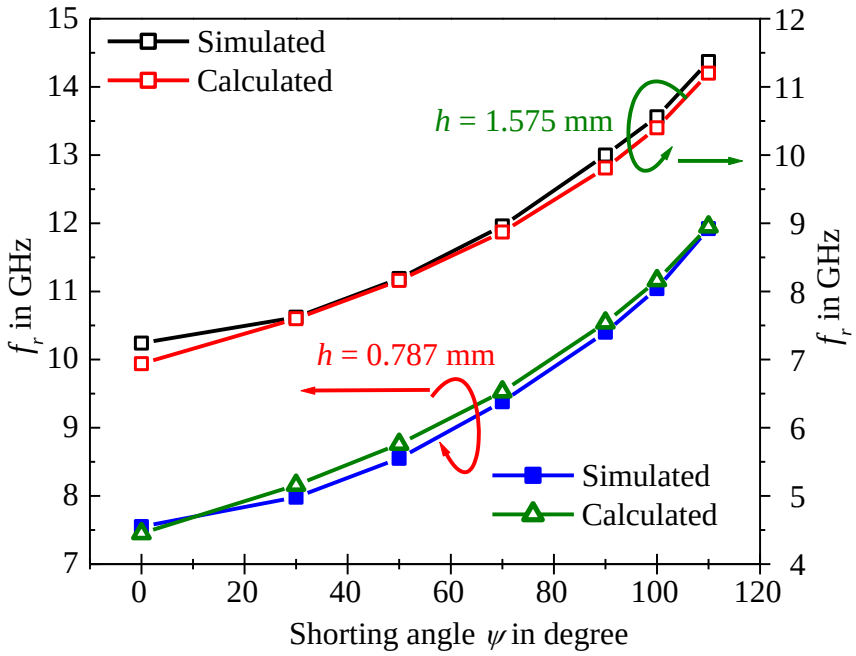

Fig. 4.5 Computed and simulated variations of resonant frequency as a function of shorting angle ψ for two different substrate thickness.

4.2.3 Gain and Efficiency

The suppression of surface waves in the proposed antenna can yield much better efficiency and peak CP gain [186]. Furthermore, it also reduces the radiation along the horizon, which is a parameter of significant importance for finite-sized ground plane [179]. The relation between peak gain of conventional CMA and the proposed antenna may be written as,

$$\frac{G_P}{G_o} = \frac{\eta_P}{\eta_o}\frac{\lambda_0^2}{\lambda_1^2}\frac{(A_{eff})_P}{(A_{eff})_c} \tag{4.8}$$

where, G_P, η_P, λ_1 and $(A_{eff})_P$ are the gain, efficiency, resonant wavelength and effective aperture of the proposed antenna, respectively, while the same for conventional CMA is G_0, η_0, λ_0, and $(A_{eff})_c$. Now, the relation between effective apertures of the same is

$$\frac{(A_{eff})_P}{(A_{eff})_c} = \frac{(\varepsilon_{ap})_P}{(\varepsilon_{ap})_C}\left(1 - \frac{\psi}{\pi}\right) \tag{4.9}$$

in which the radiations take place from the slots at the radiating aperture, as explained in Fig. 4.1 (lower radiating edge slot is shown). The average electric field for dominant TM_{11} mode at the slot aperture for conventional CMA and proposed antenna can be computed as,

$$(E_{av})_C = \frac{1}{\pi}\int_{-\pi/2}^{\pi/2} J_1(1.84)Cos\phi d\phi \tag{4.10}$$

$$(E_{av})_P = \frac{1}{(\pi-\psi)}\int_{-\pi/2+\frac{\psi}{2}}^{\pi/2+\frac{\psi}{2}} J_1(1.84)Cos\phi d\phi \tag{4.11}$$

Using [187], the aperture efficiency may be calculated as,

$$\left.\begin{aligned}(\varepsilon_{ap})_C &= \left[\frac{[(E_z)_{av}]^2}{[(E_z^2)_{av}]}\right]_C \\ (\varepsilon_{ap})_P &= \left[\frac{[(E_z)_{av}]^2}{[(E_z^2)_{av}]}\right]_P\end{aligned}\right\} \tag{4.12}$$

Once again, to compute surface wave efficiencies [28] for conventional CMA and proposed antenna

$$\left.\begin{aligned}\eta_C &= \left(\frac{P_r}{P_r+P_{surf}}\right)_C \\ \eta_P &= \left(\frac{P_r}{P_r+P_{surf}}\right)_P\end{aligned}\right\} \tag{4.13}$$

and the radiation power and surface wave power may be computed [26] as

$$P_r = 40k_0^2(k_0h)^2[1-\frac{1}{\varepsilon_r}+\frac{2}{5\varepsilon_r}]$$

$$P_{surf} = 30\pi k_0^2 \frac{\frac{\varepsilon_r(x_0^2-1)}{(x_0^2-1)^{3/2}}}{\varepsilon_r\left[\frac{1}{\sqrt{(x_0^2-1)}}+\frac{\sqrt{(x_0^2-1)}}{(\varepsilon_r-x_0^2)}\right]+k_0h\left[1+\frac{\varepsilon_r{}^2(x_0^2-1)}{(\varepsilon_r-x_0^2)}\right]} \tag{4.14}$$

where, $x_0 = \frac{\beta_{TM0}}{k_0}$.

For conventional CMA, $k_0 = \frac{2\pi}{\lambda_0}$ and ε_r $(= 2.33)$ is the relative permittivity of substrate while, to compute for proposed structure one need to use $k_1 = \frac{2\pi}{\lambda_1}$ and $(\varepsilon_r)_N = \varepsilon_r(1-\frac{\psi}{\pi})$ in place of k_0 and ε_r .

Therefore, using equations (4.9) - (4.14), equation (4.7) may be written as,

$$\frac{G_P}{G_o} = \frac{\chi_P}{\chi_C}\frac{\lambda_0^2}{\lambda_1^2}(1-\frac{\psi}{\pi}) \tag{4.15}$$

where,

$$\frac{\chi_P}{\chi_C} = \frac{\eta_P}{\eta_o}\frac{(\varepsilon_{ap})_P}{(\varepsilon_{ap})_C} \tag{4.16}$$

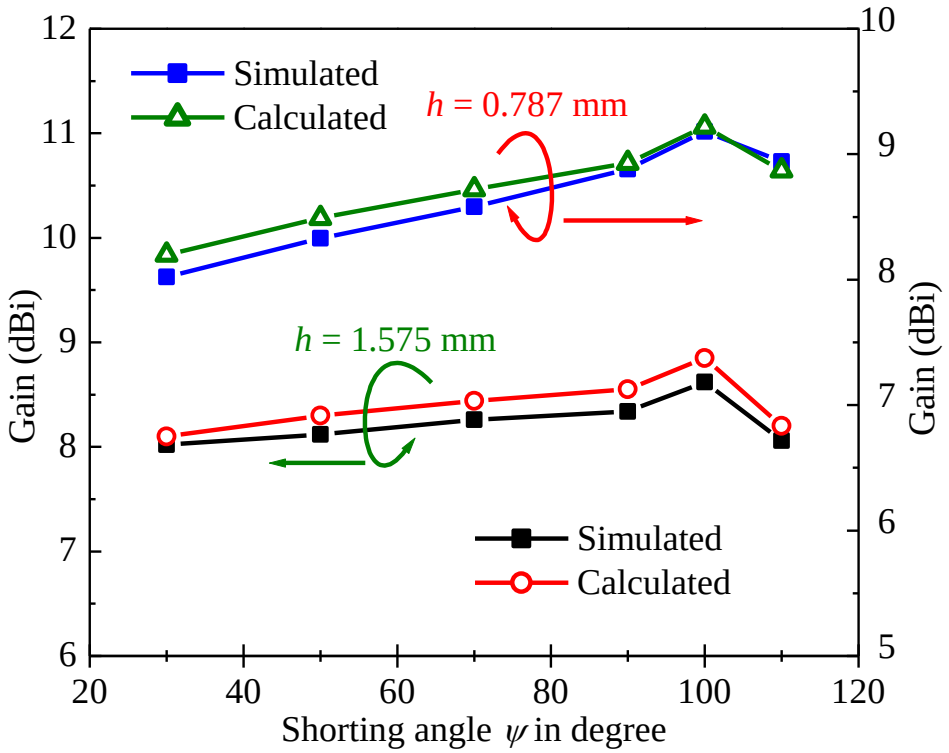

(a)

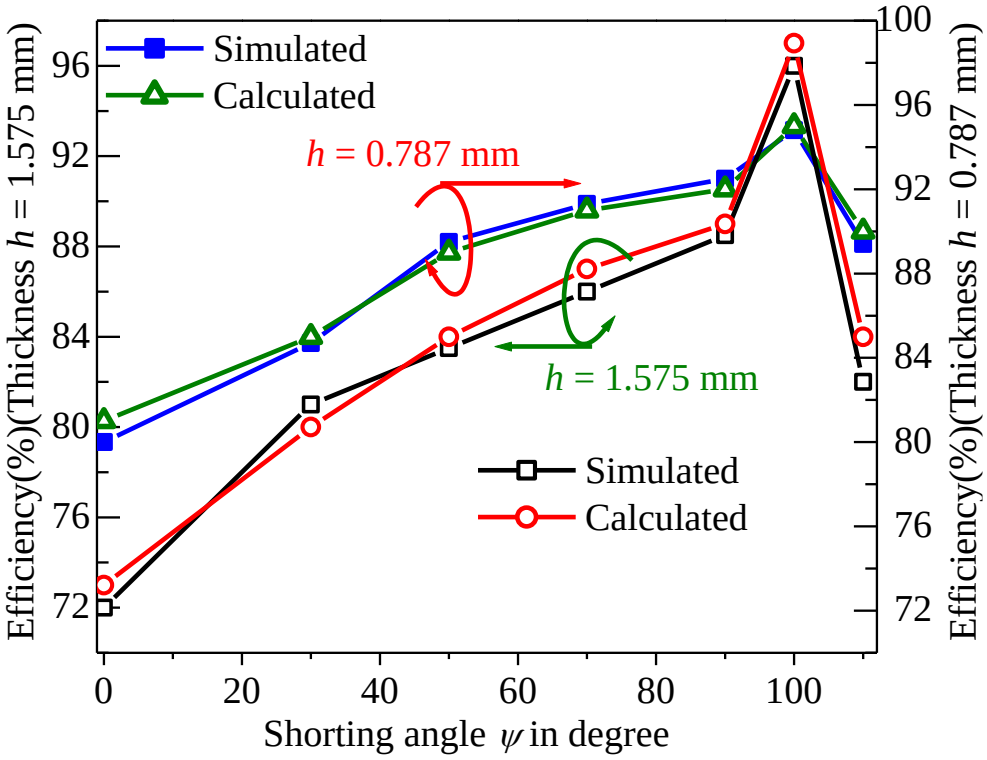

(b)

Fig. 4.6 Variation of (a) peak gain and (b) efficiency of the proposed antenna as a function of shorting angle ψ for two substrate thicknesses.

Here, χ_P and χ_C are the efficiencies of the proposed and conventional CMA. Therefore, the gain and efficiency of the proposed antenna can be written as,

$$\left.\begin{aligned} G_P &= 10Log_{10}\left(\frac{G_P}{G_o}\right) + G_o \\ \chi_P &= \eta_P\left(\varepsilon_{ap}\right)_P \end{aligned}\right\} \tag{4.17}$$

Using equation (4.17), the gain and efficiencies of the proposed antenna as a function of ψ for two different substrate thicknesses (h = 0.787 mm and h = 1.575 mm) are presented in Fig. 4.6. Here, good validation is revealed between the calculated results and simulations. It is also observed that when ψ =100˚, the gain and efficiency will be at their peak values. Notably, these phenomena are expected because at ψ = 100˚, the surface wave is completely eliminated, and as a result, the radiation along the horizon reduces. The isolation between bore-sight gain and horizontal gain (BG-HG isolation) is depicted in Fig. 4.7, and it confirms that the horizontal radiation is reduced. Hence, such an antenna is also useful for GPS receiving antenna that reduces low angle interfering signals [188].

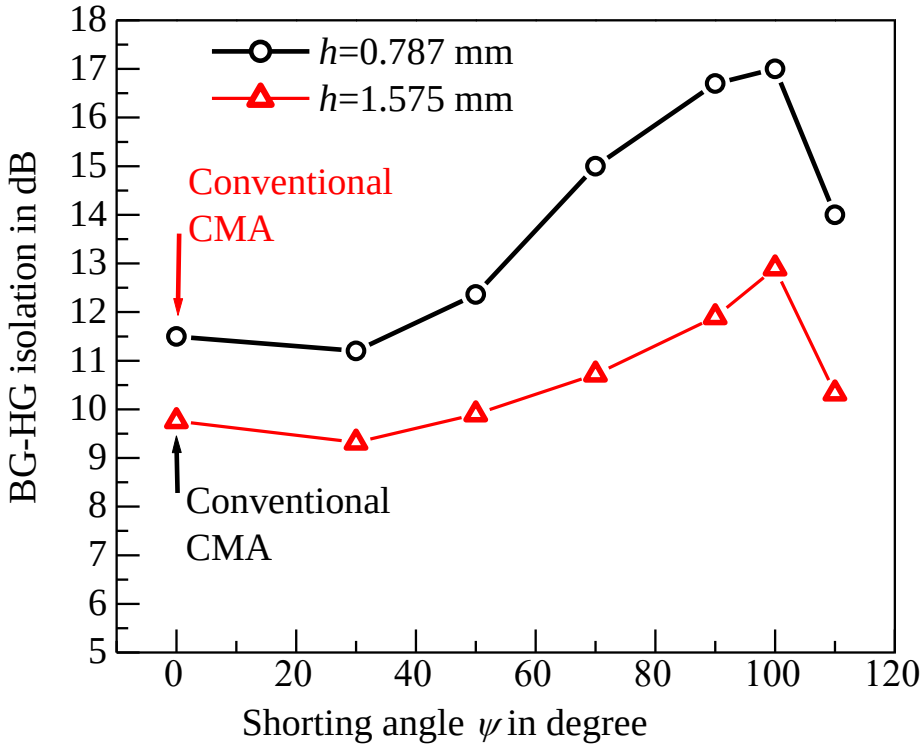

Fig. 4.7 Variation of BG-HG isolation of the proposed antenna as a function of shorting angle ψ for two substrate thickness.

4.2.4 Cross Polarized Radiation in Principal Planes

The cross polarized (XP) radiation of a CMA is mainly due to radiation from non-radiating sides of the CMA. The orthogonal fields contributing to XP radiation arise mainly due to the first higher-order TM_{21} mode [14],[19], which has the antinodal point along the ϕ = 90˚ beneath the patch. Furthermore, the orthogonal component of the dominant TM_{11} mode in the range from ϕ = 40˚ to 110˚ (beneath the patch) is also responsible for the XP radiation of CMA [14],[19]. Therefore, the shorting strip is incorporated in the said angular region, so as to suppress the orthogonal radiation from both the TM_{21} and TM_{11} modes, and consequently, the XP radiation is reduced which leads to higher CP-XP isolation. Notably, the proposed RSW inspired antenna reduces the radiation in the horizontal direction at its E-plane, and hence it brings symmetry in the E- and H-plane CP profiles. This in turn reduces the XP radiation from the proposed antenna as well. The XP radiation performance in comparison to CP is depicted in Fig. 4.8. It reveals 22 dB polarization purity in the principal planes.

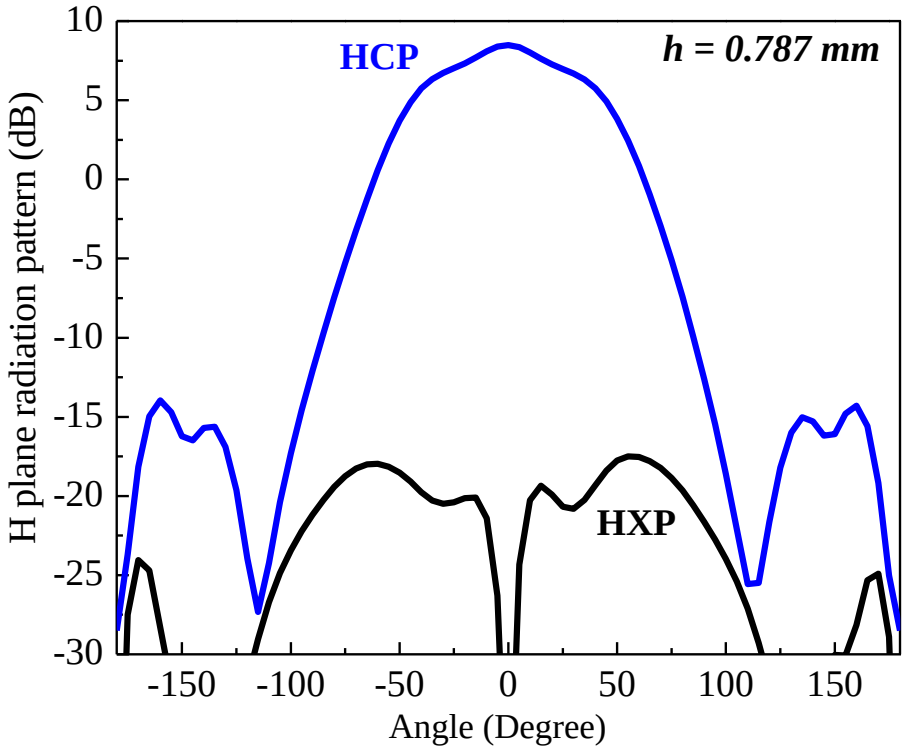

Fig. 4.8 Simulated H plane radiation patterns of the proposed antenna for shorting angle $\psi = 70^0$.

4.2.5 Cross Polarized Radiation in Diagonal Planes

The XP radiation is low at E plane (i.e., at $\varphi = 0^0$) for linearly polarized patch antenna. However, it is significantly high at H plane (i.e., at $\varphi = 90^0$). However, this XP radiation worsen more at diagonal planes i.e., along $\varphi = 45^0$ and $\varphi = 135^0$.

In this section, simulated radiation pattern at $\varphi = 45^0$ diagonal plane of proposed antenna and the conventional CMA (excited at same frequency) has been compared and presented in Fig. 4.9.

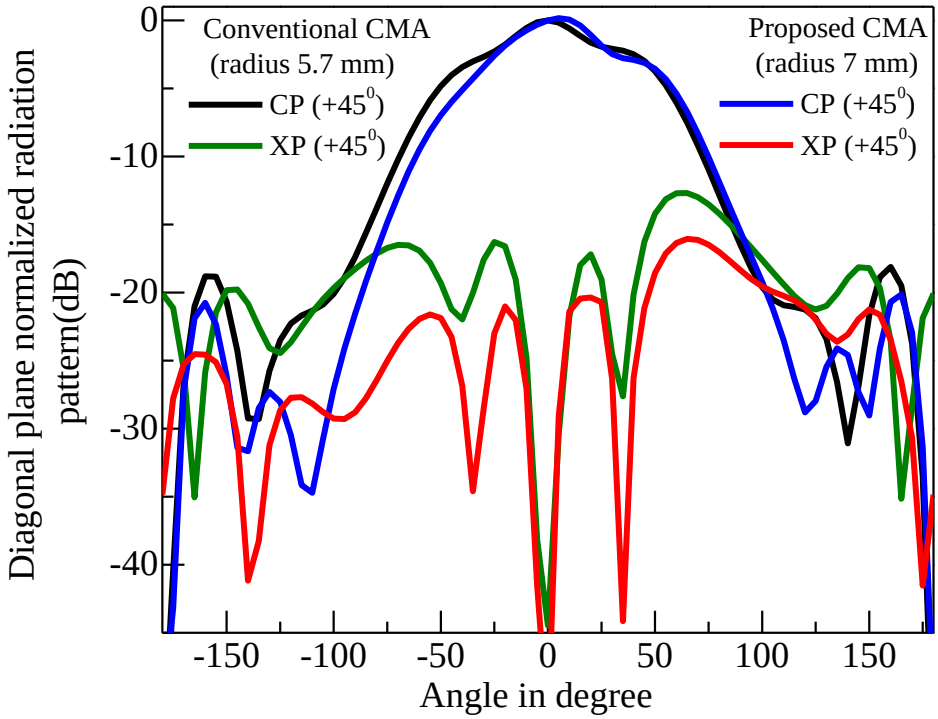

Fig. 4.9 Comparison of diagonal plane radiation pattern of conventional CMA and proposed shorted circular patch at same frequency.

In fact, the investigations [189] on diagonal plane XP radiation shows that, the issue can be undertaken by modulating both the radiating and non-radiating edge fields. Contrarily, both E and H plane XP radiations can be reduced by reducing non-radiating edge fields only.

Based on Ludwig's third definition, the cross-polarization field (E_{xp}) of microstrip antenna can be written as [R1],

$$\left.\begin{aligned} E_{xp} &\propto 2E_y(cos\theta cos^2\phi - sin^2\phi) + 2E_x sin\phi cos\phi(1 + cos\theta) \\ &\propto 2E_x[\frac{E_y}{E_x}(cos\theta cos^2\phi - sin^2\phi) + sin\phi cos\phi(1 + cos\theta) \end{aligned}\right\} \quad (4.18)$$

From (4.8), it is clear that, for $\varphi = 0^0$ and $\varphi = 90^0$, $E_{xp} \propto E_y$ while it is $E_{xp} \propto \frac{E_y}{E_x}$ for $\varphi = 45^0$ diagonal plane.

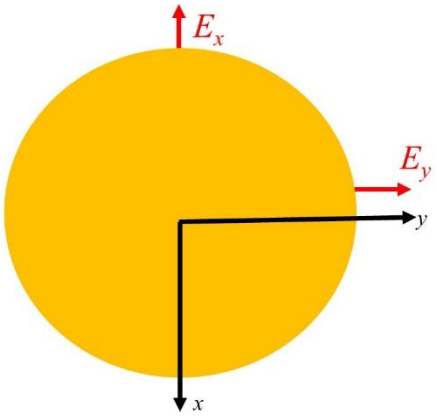

Fig. 4.10 Co-polar field vector Ex and cross polar field vector (Ey) for CMA.

Therefore, to minimize 45^0 diagonal plane XP radiation, cross field E_y of non-radiating edge is to be reduced and radiating edge field E_x to be increased (Fig. 4.10). Contrarily, to minimize E and H plane XP radiation, the suppression of E_y field of non-radiating edge is sufficient. Therefore, it is definitely challenging to address the issue of $\varphi = 45^0$ diagonal plane XP.

In this scenario, the present antenna can successfully address the issue of diagonal plane XP. In fact, the shorting strip not only eliminates non-radiating edge field (E_y), but also increases radiating edge field (E_x). Essentially, the shorting strip suppresses the fields at non-radiating edges (E_y component decreases) and hence the fields are spilled out through radiating edges (E_x component increases). The simulated electric field magnitude of conventional CMA and the proposed antenna is presented in Fig. 4.11 confirms the conjecture.

Consequently, polarization purity is improved in diagonal $\varphi = 45^0$ plane is case of present antenna. The simulated radiation pattern of the present antenna at $\varphi = 45^0$ diagonal planes has been compared with conventional CMA excited at same frequency in Fig. 4.10. It reveals that, the PP of the present antenna is 17 dB while the same for conventional CMA is only 12 dB at $\varphi = 45^0$ diagonal plane. Therefore, 5 dB more XP suppression is evident from the present design at diagonal plane in comparison to conventional CMA. Therefore, the present antenna can successfully improve PP not only in principal planes, but also at diagonal planes.

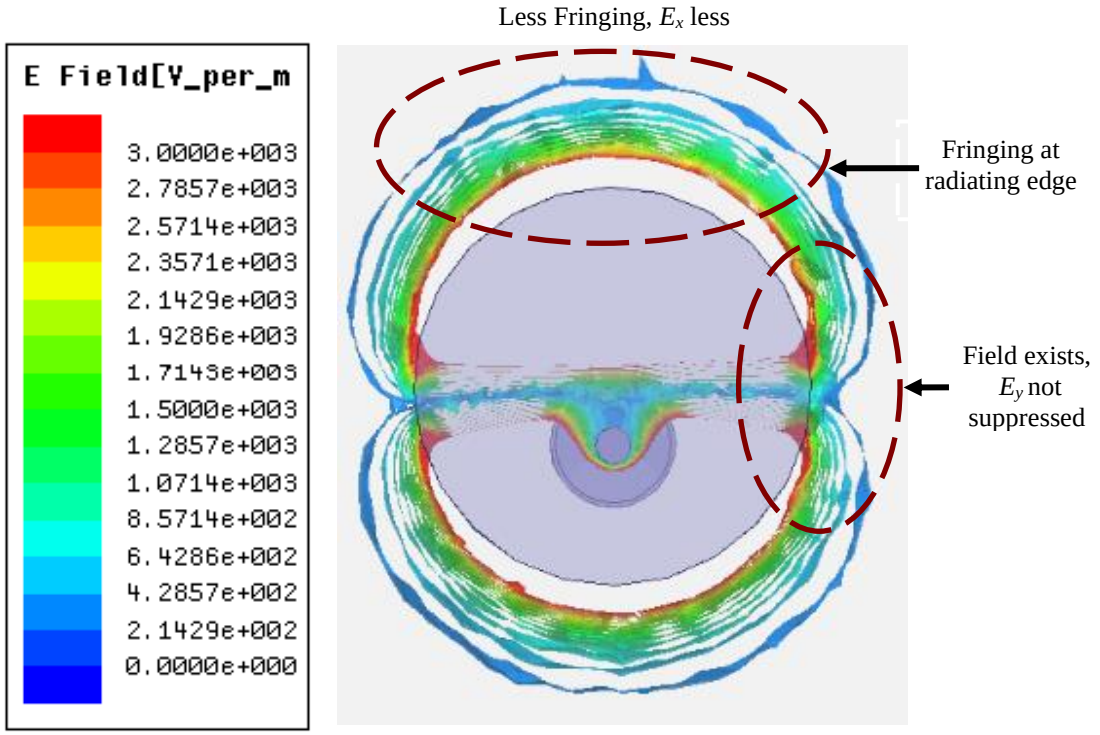

(a)

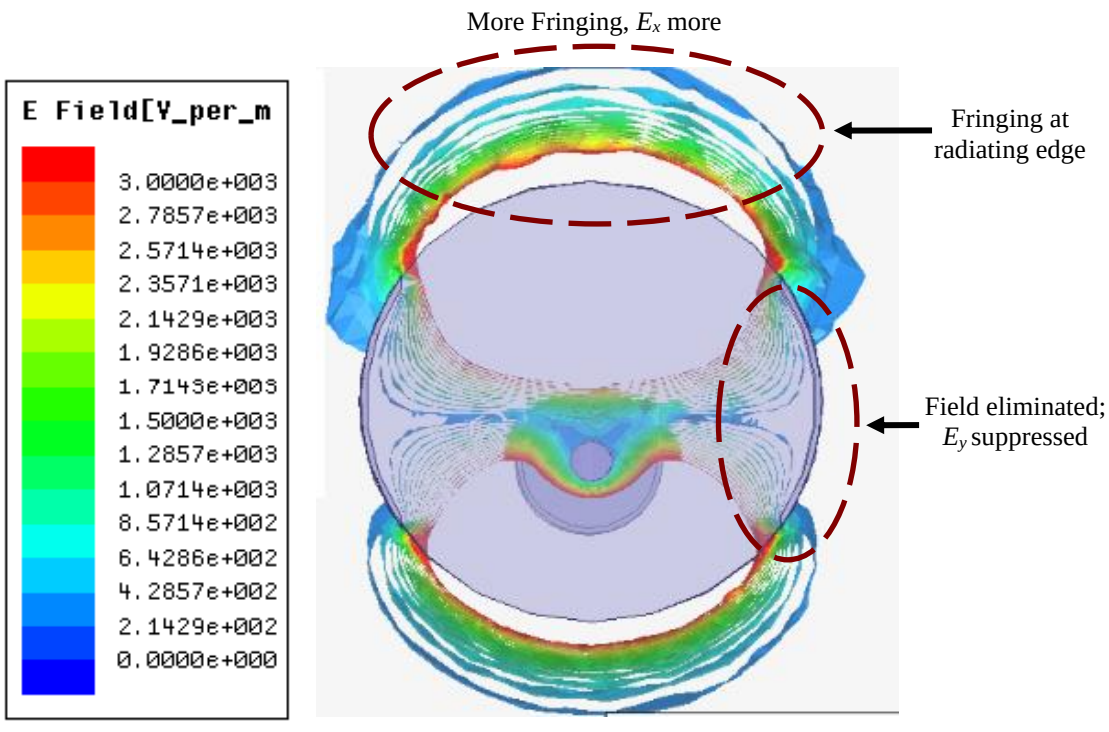

(b)

Fig. 4.11 Simulated electric field magnitude distribution within substrate at excited mode (a) conventional CMA (b) proposed CMA.

4.3 Parametric Studies and Optimization

A detailed parametric study for various shorting angles (ψ) has been carried out to find the optimum ψ, so that optimum performance in terms of gain, efficiency, polarization purity, and improved BG-HG isolation can be yielded without hampering the basic CP radiation characteristics of the circular patch. Initially, a conventional CMA with radius a = 7 mm has been designed for X band frequency, and its corresponding feed position has also been optimized to achieving the best results using [159].

The simulated radiation patterns of the proposed antenna in both the principal planes are shown in Fig. 4.12 for two different substrate heights (h = 1.575 mm and h = 0.787 mm). It is observed that, as the shorting angle (ψ) increases the peak CP gain also increases for both the antennas (with different h). Furthermore, the CP gain attains its maximum value at $\psi = 100^{\circ}$, as is predicted in section 4.2.3. Even though the gain is maximum at $\psi = 100^{\circ}$, the E-plane radiation pattern contains a deep null at around (-50˚) in the two substrate thicknesses, which may be due to the oblique radiation incurred by the shorting strips in CMA. Notably, no apparent degradation is noticed at the H-plane radiation profile for $\psi = 100^{\circ}$.

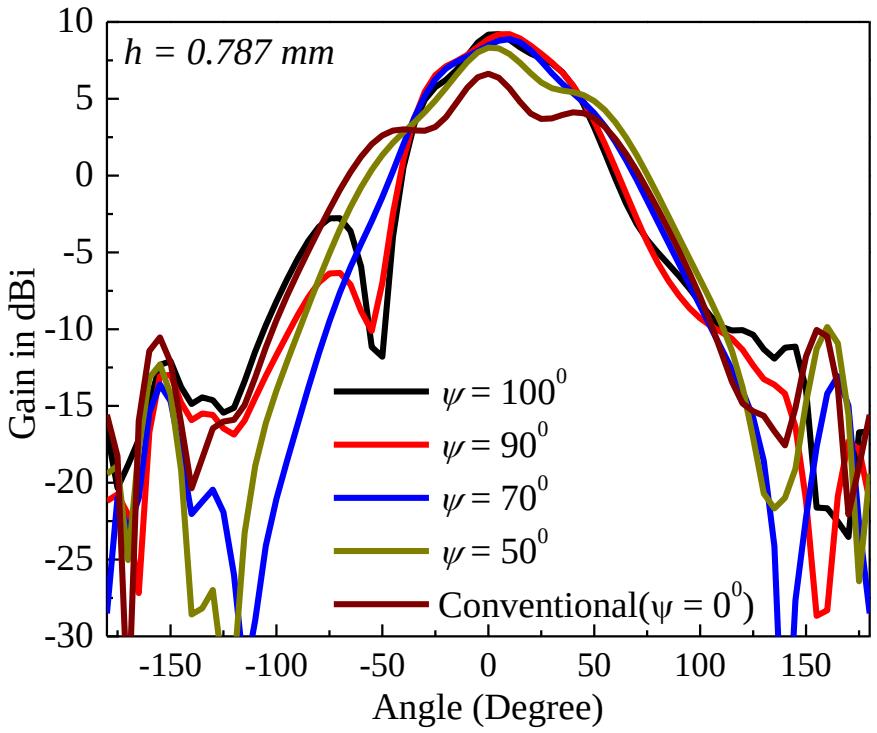

(a)

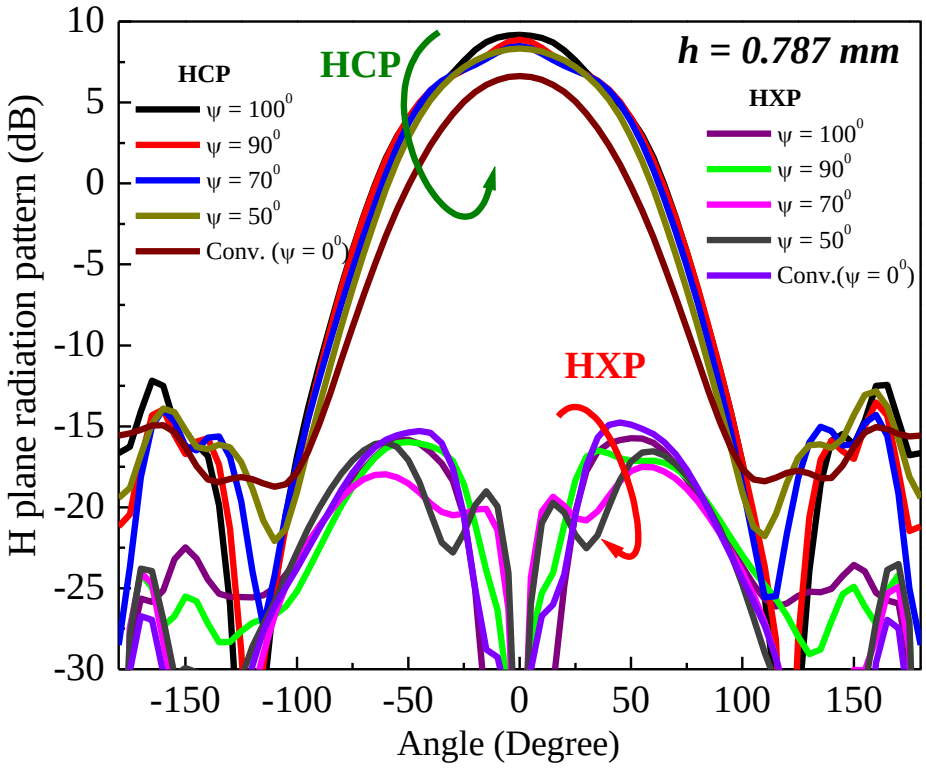

(b)

Fig. 4.12 Simulated radiation patterns (a) E plane and (b) H plane for the conventional CMA and the proposed antenna for different shorting angle ψ.

The simulated electric current distribution of proposed patches with ψ = 70˚ and 100˚ is shown in Fig. 4.13. It reveals strong oblique current lines from both the upper and lower shorting strip edges which create a deep null in E plane at off bore sight. Contrarily, very weak oblique current line is noticed at lower shorting strip edge for ψ = 70˚ and causes no distortion at E plane off bore sight radiation.

Therefore, ψ = 70˚ has been considered by the proposed antenna that yields the best performance with a stable radiation pattern in both the principal planes. The XP radiation in the E-plane is always below -35 dB, which is insignificant and hence are not shown for brevity. It may also be noted from Fig. 4.12 that the polarization purity improves with the increase in shorting angle (ψ). The proposed antenna with h = 1.575 mm and ψ = 70˚ provides a polarization purity of 22 dB as compared to the polarization purity of 16 dB in the case of conventional CMA (with the same substrate thickness). On the contrary, the proposed antenna with h = 0.787 mm and ψ = 70˚provides excellent polarization purity of 27 dB as compared to the polarization purity of 20 dB in the case of conventional CMA.

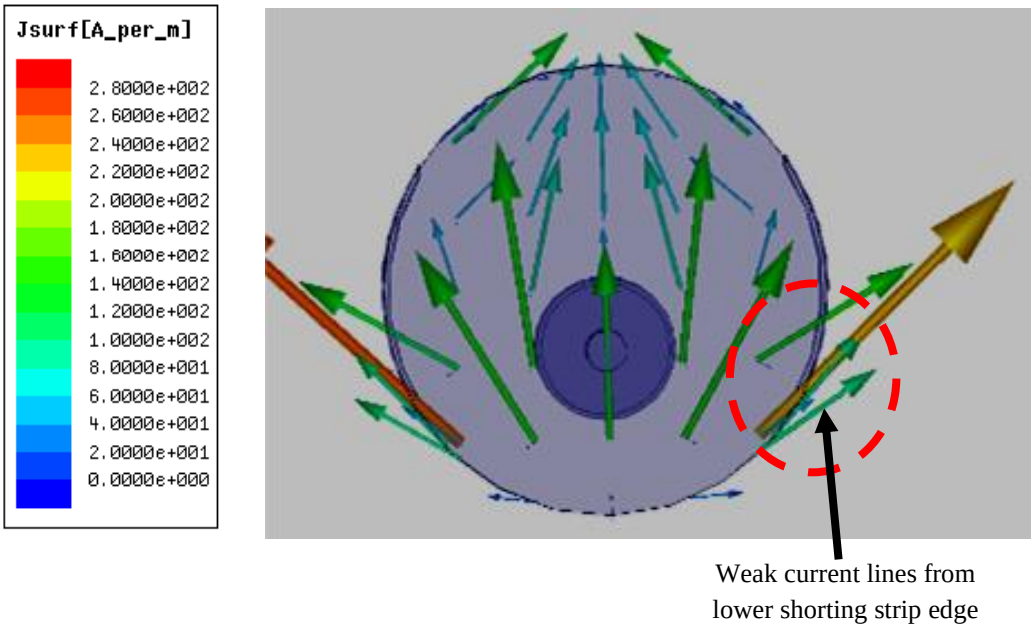

(a)

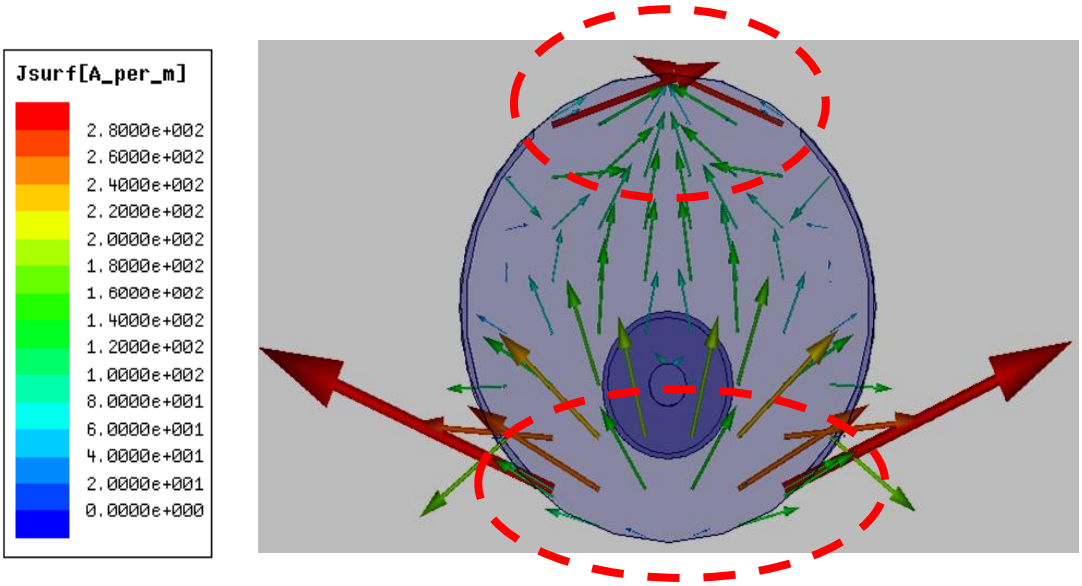

(b)

Fig. 4.13 Surface current distribution over patch for (a) $\psi = 70^{\circ}$ and (b) $\psi = 100^{\circ}$.

4.4 Proposed Structure

The proposed configuration of the CMA with a pair of shorting strips loaded at the non-radiating sides of the CMA is shown in Fig. 4.1. A prototype (Fig. 4.14) is designed by placing a circular patch of radius a = 7 mm on an RT–Duroid substrate (dielectric constant ε_r= 2.33) with thickness h = 0.787 mm and ground plane size of 60 × 60 mm^2. Based on the theoretical insight and parametric studies discussed in the previous sections, a pair of shorting strips of thickness 0.5 mm are loaded on the non-radiating sides of the CMA (with a wide shorting angle ψ = 70˚) between the patch and the ground plane. It may be noted that, the shorting is done at the periphery of circular patch at both the non-radiating sides with a sector angle of ψ = 70^0 (along lateral) as shown in Fig. 4.1(b).

(a) (b)

Fig. 4.14 Photo of fabricated prototype (a)Top view, (b) bottom view.

Actually, the shorting strip is incorporated at the perimeter of the above-mentioned sectors with the ground plane for which the dielectric is removed or engraved out by CNC and milling machine for PCBs model no CK-02R. Thereafter 0.5 mm thick copper sheet is used to short between the sector and the ground by soldering. The proposed antenna is fed by a typical 50 Ω SMA connector at a distance of 2 mm from the centre of the patch, so as to obtain good impedance matching. The top view and bottom view of the prototype is shown in Fig. 4.14. The conventional CMA of radius 5.7 mm is also fabricated on the same substrate to excite similar frequency and is fed optimally at 1.8 mm from the centre. The detail of the different parameters of the proposed and conventional antenna is presented in Table 4.1.

TABLE 4.1 The detailed parameters of the proposed and conventional antenna (Substrate permittivity $\varepsilon_r = 2.33$, thickness $h = 0.787$ mm)

Antenna type	Ground plane (mm^2)	a (mm)	Feed location (mm)	Shorting wall thickness (mm)	Ψ (˚)	Shorting strip range in terms of ϕ (˚)
Conventional CMA	60 x 60	5.7	1.8	-	-	-
Proposed CMA	60 x 60	7	2	0.5	70	±55˚ to ±125˚

4.5 Experimental Results and Discussions

The simulated [159] and measured results obtained from the proposed antennas are presented in this section. The reflection coefficient profile of the proposed antenna (both measured and simulated) is shown in Fig. 4.15, which reveals good agreement between the simulated and measured results. The simulated antenna resonates at 9.16 GHz, while the measured one was slightly lower at 9.13 GHz. Here, the simulated reflection coefficient has exhibited 10 dB impedance bandwidth of 2.18 % (9.1 – 9.3 GHz), and the measured one was 2.19% (9.04 – 9.24 GHz). The slight discrepancies between the measured and simulated results are mainly contributed by the minor fabrication error.

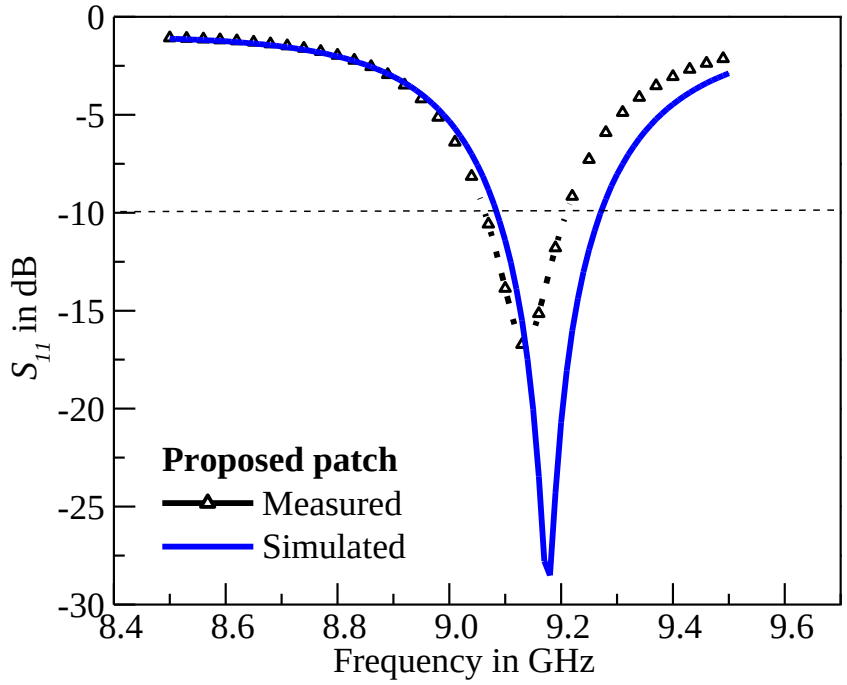

Fig. 4.15 Simulated and measured reflection coefficient profile of the proposed antenna.

The complete measured E-plane radiation pattern of the proposed antenna and the same for conventional CMA (at the same excitation frequency of 9.13 GHz) is depicted in Fig. 4.16(a). Here, the incorporation of the shorting strips at the non-radiating sides of the radiating patch does not hamper the co-polarization radiation; instead, the co-polarization gain is improved by almost 2.5 dB and attains a CP gain of 8.5 dBi. The XP radiation of the proposed antenna in the E-plane is also suppressed in comparison with the conventional CMA.

The measured E-plane polarization purity of the proposed antenna is around 45 dB, while in comparison with the conventional CMA is 35 dB. Notably, the radiation along the horizon (i.e., $\theta = 90^{\circ}$) of the proposed antenna is approximately 20 dB less than the peak CP gain, which is due to the suppression of surface wave in the proposed antenna. As for the conventional CMA case, it is 10 dB less than the peak CP gain.

The measured H-plane radiation patterns of the proposed antenna as compared with the conventional CMA are shown in Fig. 4.16(b). The CP radiation pattern of both the conventional CMA and the proposed antenna is similar to the ones shown in Fig. 4.16(a), showing peak CP gain enhancement of 2.5 dB in the proposed antenna as compared with the conventional CMA. As the H-plane polarization purity is a vital factor that determines the performance of a patch antenna at higher frequencies, in the case of conventional CMA, its corresponding H-plane polarization purity is quite low (polarization purity of around 17 dB at 9.13 GHz), whereas the proposed antenna has shown desirable polarization purity of approximately 25 dB.

Therefore, a 50% improvement in polarization purity is yielded by the proposed antenna in comparison with the conventional CMA. The radiation patterns are also quite stable in both principal planes. The measured gain and efficiency of the proposed antenna are compared with its simulated and calculated ones, and the results are depicted in Table 4.2. Here, excellent agreements are shown between all the efficiency of the proposed antenna.

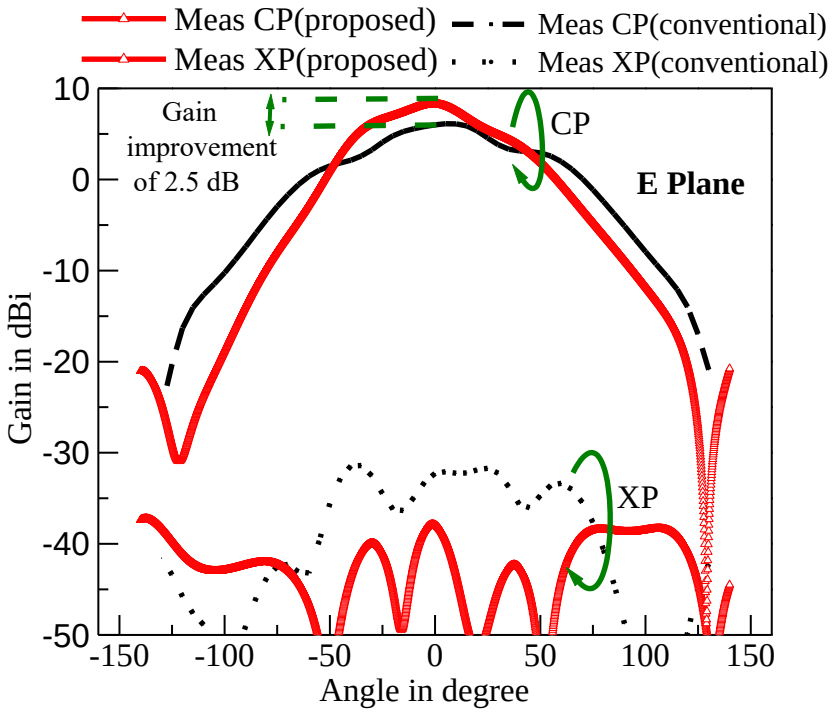

(a)

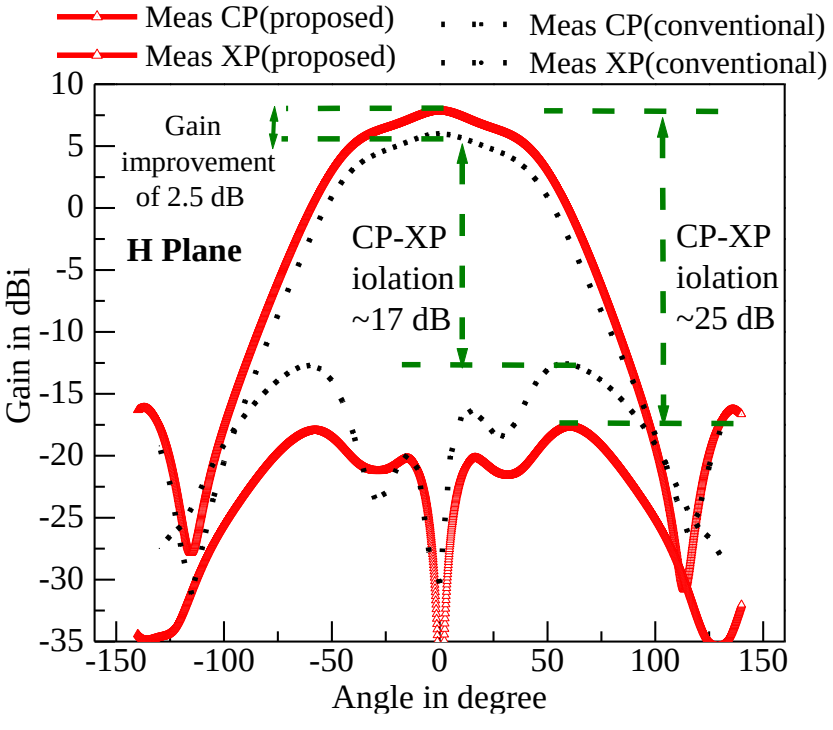

(b)

Fig. 4.16 Comparison of measured radiation patterns for conventional CMA and proposed antenna (a) E plane, (b) H plane (f = 9.13 GHz).

Table 4.2 Radiation properties of the proposed Antenna

Antenna	Radiation properties	Simulated	Measured	Calculated
Proposed structure with $\psi = 70^0$	Gain (dBi)	8.6	8.5	8.7
	Efficiency (%)	92	93	91

Table 4.3 Comparison of the proposed work with recently published works.

Reference	Antenna dimension (Patch area × profile [height])	Gain (dBi)	Minimum CP-XP Isolation (dB)	Efficiency (%)	Remarks
[137]	$0.59\lambda_0^2 \times 0.02\lambda_0$	11	19	89	RSW inspired antenna with much distortion in radiation pattern and very high side lobes.
[150]	$0.13\lambda_0^2 \times 0.02\lambda_0$	7.8	20	---	Four stacked planes with complex feeding.
[152]	$0.15\lambda_0^2 \times 0.02\lambda_0$	7.25	18	73.5	Complex structure integrated with branch line coupler. Dual feed RSW inspired antenna
[153]	$0.23\lambda_0^2 \times 0.03\lambda_0$	9	13	69	RSW inspired simple circular patch with shorting four vias.
[154]	$0.11\lambda_0^2 \times 0.16\lambda_0$	9.0	20	92	Use of multiple stacking with dual stacked dense dielectric circular patch make the structure too complex for manufacturing
[155]	$1.47\lambda_0^2 \times 0.07\lambda_0$	6.8	0	----	Hexadecagon circular patch with DGS makes significantly distorted radiation pattern)
[156]	$0.05\lambda_0^2 \times 0.04\lambda_0$	7.8	----	63	Asymmetric E and H plane radiation beam makes the radiation property poor.
[170]	$0.15\lambda_0^2 \times 0.14\lambda_0$	8	---	91	Use of slots, numerous vias with 3 stack ground plane makes the structure too bulky
Proposed	$\mathbf{0.13\lambda_0^2 \times 0.02\lambda_0}$	**8.5**	**25**	**93**	**Simple RSW inspired circular patch with pair of shorting strips makes concurrent improvements in gain, efficiency and polarization purity.**

Table 4.3 shows the performance comparison of the proposed antenna with other recently reported papers that have exhibited similar investigations. Besides having a simple overall structure, this table also shows that the proposed antenna performances in terms of CP gain, polarization purity, and efficiency are better than the other reported ones. One point to take note is the proposed antenna has demonstrated a very high CP-XP isolation (polarization purity) level of 25 dB as compared to the references.

4.6 Conclusion

A simple circular microstrip antenna with a pair of shorting strips loaded at the non-radiating sides has been successfully investigated analytically based on the RSW theorem to improve CP gain, efficiency, and polarization purity simultaneously. This analytical approach was further validated using the measurements. Besides improving the gain, efficiency, and polarization purity, the proposed antenna can also successfully suppress the radiation along the horizontal direction, which is worthy of modern array and MIMO wireless applications.

CHAPTER

5

Modulation of Cavity Field Under Circular Microstrip Antenna for Reduced Horizontal Radiation with Omni-Present Improvement of Radiation Properties

5.1 Introduction

Different configuration of classical circular microstrip antenna (CMA) along with reduced surface wave (RSW) inspired CMA have been thoroughly investigated in previous chapters. Concurrent improvement in all radiation properties is revealed from RSW inspired CMA. However, a true RSW CMA is slightly larger in size than classical CMA. Therefore, due care must be taken to yield concurrent improvement in radiation characteristics with slightly smaller sized antenna and that has been proposed and investigated in present chapter. Another major but less investigated shortcoming of CMA is a strong radiation fields along horizontal direction i.e., along ground plane. This radiation is undeniably undesirable for many applications like 5G MIMO, array [190 - 193] configuration or in vector sensors [194 - 195]. The far field coupling of antenna elements in an array is mainly due to the strong patch radiation along horizontal direction. Therefore, this can be only minimized by judicious design of antenna structure with reduced horizontal radiation.

The gain enhancement in circular patches has been investigated in [137, 150 – 156, 170]. The technique such as slot-loading with aperture coupling [150] and the use of 3 stacked ground plane with slot and shorting vias [170] have been adopted to achieve around 7.8 dBi gain with no improvement in co-polar to cross-polar radiation isolation i.e., polarization purity (PP). To further increase the gain from 7.2 dBi to 9 dBi with PP of 18-19 dB only, the annular ring antenna in [152] was loaded with shorting vias (with branch line couplers), while numerous shorting vias beneath

the circular patch have been reported in [153]. Notably, a structure similar to [152 – 153, 170] has been reported in [137], and it can achieve high gain of 11 dBi but suffers from poor PP of 17 dB and a much-distorted radiation pattern with a high side-lobe level. To attain high gain of around 6.8 dBi to 8 dBi for patch antenna, various techniques have been investigated, such as the adaptation of circular dual-stacked dense dielectric patch [154], replacement of circular patch geometry by hexa-decagon circular patch [155], and the use of graphene-based patch [156]. However, improvement in PP is not apparent from these.

The improvement in PP is very important for modern wireless applications. Efforts to achieve high polarization purity have been reported by modifying the patch geometry [157, 171], use of shorting metal patch [172] or using of DGS [141] in which maximum PP of approximately 22 dB to 23 dB is achieved but with no improvement in gain profile.

However, all these reported works do not deal with the said significant issue like suppression of horizontal radiation of patch antenna at its E plane which is usually only 8-10 dB down than peak co-polar gain. This, indeed a key challenge to the antenna scientists and developers in the epoch of 5G MIMO or array antennas. Employment of micromachined cavity below the patch [191], circular patch with shorting plates [193], the use of superstrate [196] or making the substrate dielectric as band gap structure by printing various patterns on it [197 - 198] have been found effective to reduce the horizontal gain of the antenna. Out of them except [191, 196], all the techniques are basically the surface wave elimination technique. However, it may be noted that, the surface wave eliminated antennas are much larger in dimension compared to conventional antenna which is detrimental to use in the era of miniaturization. On the contrary, micromachined patch is complex to design and manufacture and therefore not cost effective. Again, the use of radome (cover) absorbs and reflects radiation wave from antenna and cause transmission losses. Further, radome causes distortion of antenna main lobe in some cases. A plentiful works has been reported on planar antennas with employment of substrate integrated waveguide (SIW) [199] or different kind of meta surface [200] for reduction in RCS or mutual coupling or polarization conversion. However, there is lack of investigations where, efforts are given to make

conventional CMA more efficient for omni-present improvement in radiation characteristics.

In order to address the lacunae of the earlier studies, a circular geometry of the patch has been symmetrically modified with a pair of thin rectangular strip in this chapter. Further, 12 numbers of shorting pins are symmetrically placed at the corners of the patch as shown in Fig. 5.1(c). This is done with a view to partially eliminate the surface wave along with the gain reduction in horizonal direction.

The chapter has been arranged in the following way. The details of antenna evolution and analysis is presented for clear visualization-based understanding in section 5.2 which includes the concept of structural evolution (section 5.2.1), analysis of resonant frequency (section 5.2.2), perception of cavity field modulation with modifying patch geometry (section 5.2.3), concept of radiation characteristics (section 5.2.4) and circuit model approach (section 5.2.5). The optimized structure to obtain the best output is presented in section 5.3. Section 5.4 discusses the results obtained from the optimized antenna structure and also validates the simulated outputs through the experimental measurements. Section 5.5 concludes the proposed work that is presented in this chapter.

5.2 Antenna Evolution and Analysis

5.2.1 Structural Evolution

A simple CMA of radial dimension a = 7 mm has been designed on Rodger's RT Duroid 5880 dielectric substrate (permittivity ε_r = 2.2, thickness h = 0.787 mm) and is denoted as Antenna 1 (Ant#1) as shown in Fig. 5.1(a). Next, two thin rectangular strips of dimension ($2a \times w_1$) are loaded at the upper and lower sections of patch in such a way that the whole patch geometry will not be extended than the CMA of radial dimension a = 7 mm. It is named as Antenna 2 (Ant#2) and is shown in Fig. 5.1(b). As a last step, 12 shorting pins of diameter d (= 1.2 mm) with center-to-center spacing d_1 (= 1.5 mm) has been incorporated as shown in Fig. 5.1(c). That is the proposed antenna structure and it is named as Antenna3 (Ant#3).

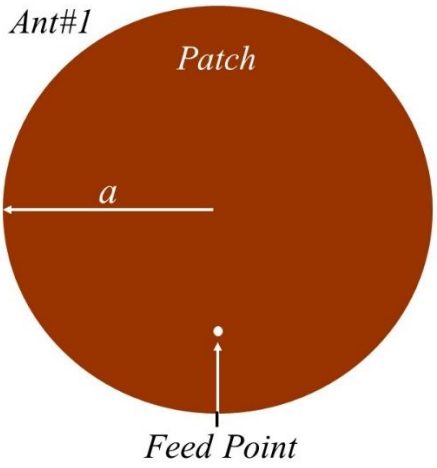

(a)

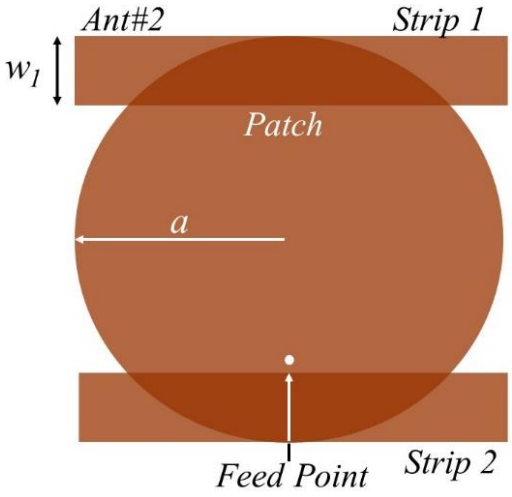

(b)

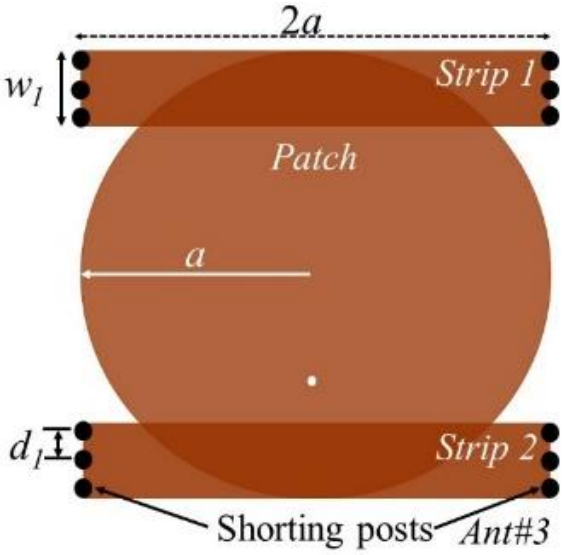

(c)

Fig. 5.1 Antenna Evolution (a) Ant#1, (b) Ant#2 (c) Ant#3.

5.2.2 Evolution Analysis: Resonant Frequency

A conventional circular patch of radial dimension a fabricated on a dielectric substrate (permittivity ε_r) resonates at fundamental TM_{11} mode with a resonant frequency f_r as,

$$f_r = \frac{1.84c}{2\pi a\sqrt{\varepsilon_r}} \Rightarrow {}^{\lambda_g}/_{2} = 1.7a \tag{5.1}$$

Now, this TM_{11} mode has one circumferential field variation and hence the semi-circular arc length of patch (S') should be $\lambda_g/2$ (Fig. 5.2(a)). Now,

$$S' = \pi a = 3.14a \neq {}^{\lambda_g}/_{2} \text{ rather } S' \rhd {}^{\lambda_g}/_{2} \tag{5.2}$$

Therefore, $\lambda_g/2$ is corresponding to circumferential length somewhat lesser than S'. Let us consider a new radius a' for which

$$\pi a' = {}^{\lambda_g}/_{2} = 1.7a \implies a' = 0.54a \tag{5.3}$$

Therefore, resonant frequency of conventional circular patch may be calculated as,

$$f_r = {}^{c}/_{\lambda_g} = \frac{c}{2\pi a'\sqrt{\varepsilon_r}} = \frac{c}{2\pi\times 0.54a\sqrt{\varepsilon_r}} \tag{5.4}$$

In the present investigation a CMA of radius a = 7 mm is considered and, in that case, a' = 3.8 mm. Therefore, considering the smaller radial circle of radius a' = 4 mm, a rectangular strip of width w_1= 3 mm and length ($2a$) = 14 mm has been placed at lower and upper section of the main patch (a = 7 mm) as shown in Fig. 5.2(a). Therefore**,** the current path will be modified (Fig. 5.3(a)) and hence it can be written as,

$$\pi a' + 2w_1 = {}^{\lambda_g}/_{2} \Longrightarrow f_r = {}^{c}/_{\lambda_0} = \frac{c}{2\sqrt{\varepsilon_r}[\pi a' + 2w_1]} \tag{5.5}$$

and the resonant frequency of the particular structure becomes 5.65 GHz. As per simulation through Ansoft's High Frequency Structure Simulator HFSS v.14 [159], the frequency is 6.13 GHz. Original patch with a = 7 mm resonates at 8.4 GHz. Therefore around 32% reduction of resonant frequency can be achieved with such new structure (Antenna#2).

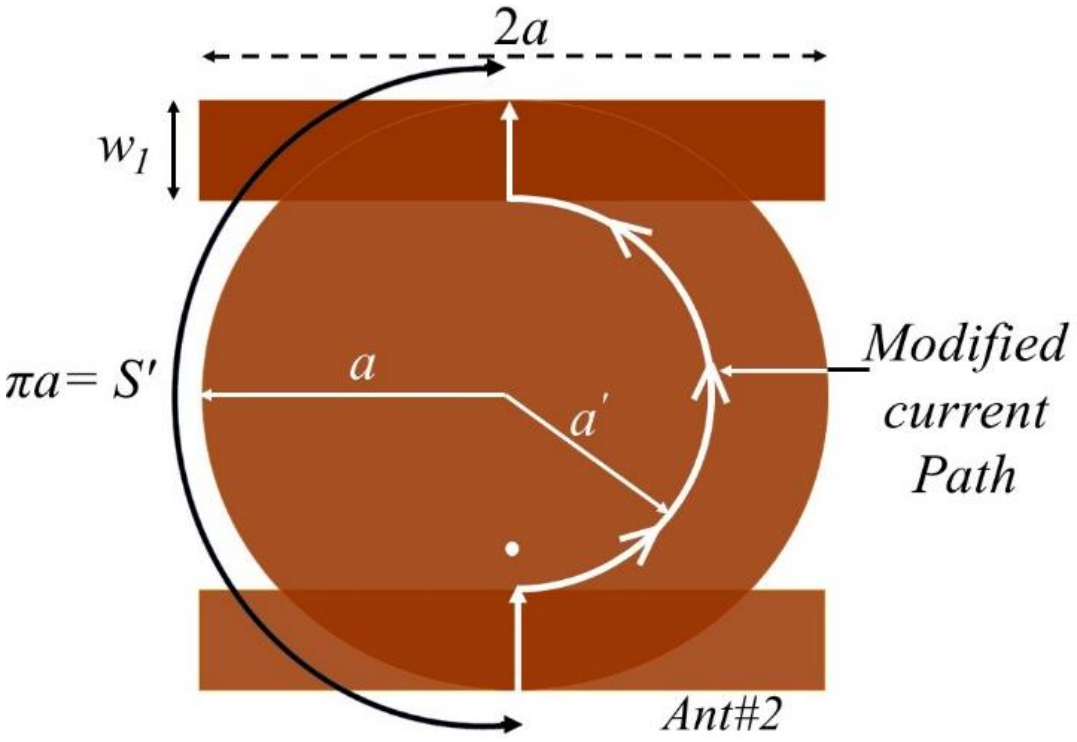

(a)

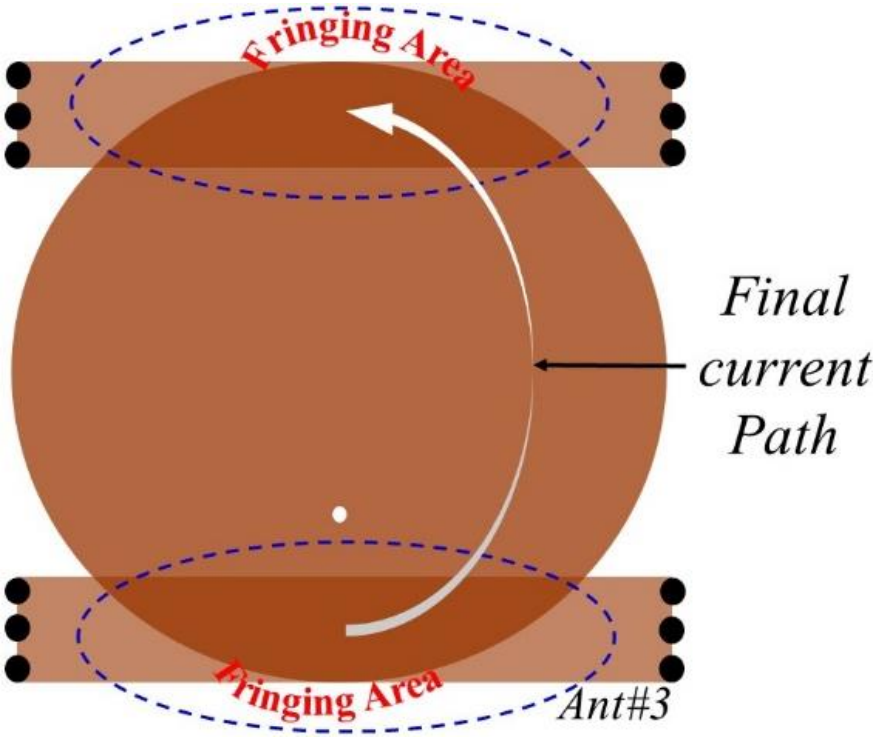

(b)

Fig. 5.2 Schematic representation of electric surface current path on patch (a) Antenna#2, (b) Antenna#3

Now, shorting pins of diameter 1.2 mm with center-to-center spacing d_1 = 1.5 mm has been incorporated as shown in section 5.2.1 (Fig. 5.1(c)) as discussed. As soon as the shorting pins are placed, current lines in Antenna#3 are again modified as is shown in Fig. 5.2(b) (schematic) and Fig. 5.3(b) (simulated). Fig. 5.2(b) and Fig. 5.3(b) reveal that the surface current on patch is similar to conventional CMA.

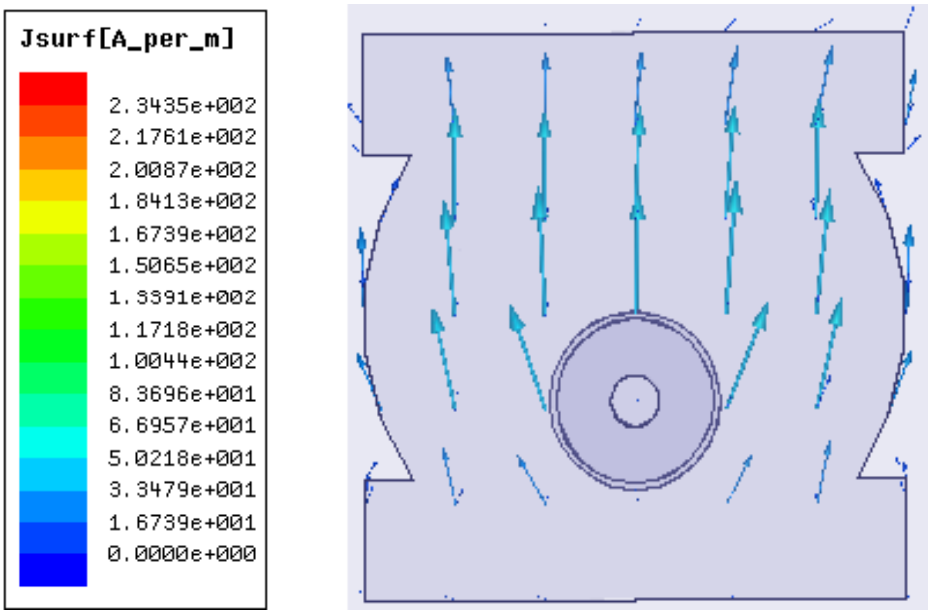

(a)

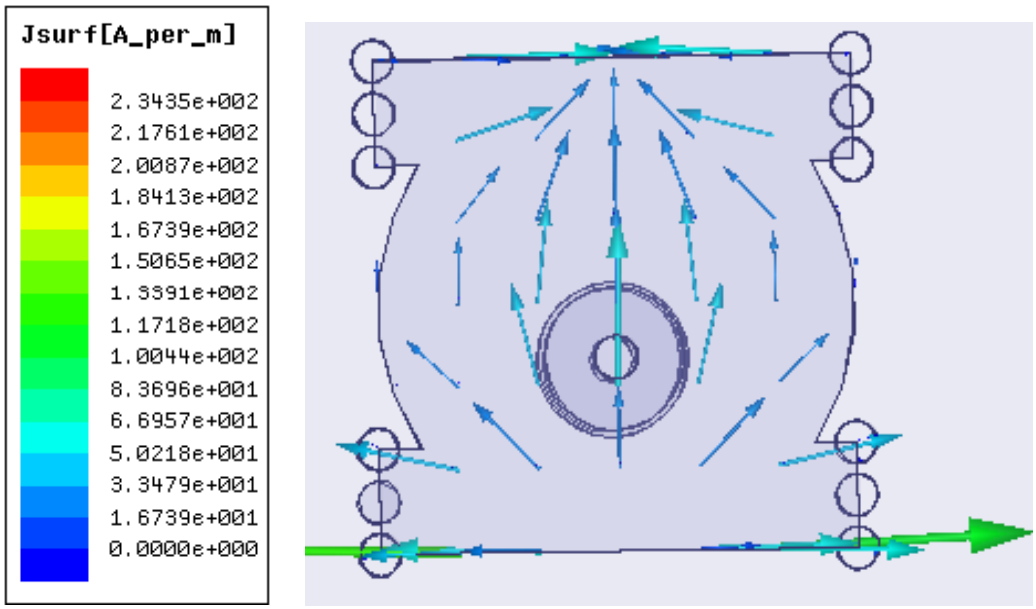

(b)

Fig. 5.3 Simulated electric surface current path on patch (a) Antenna#2, (b) Antenna#3

5.2.3 Evolution Analysis: Cavity Field Modulation with Modulating Patch Surface Geometry

The patch surface and ground plane as PECs and peripheral regions as PMCs develop the cavity beneath the patch and the resonant field inside the cavity critically depends on the patch surface geometry. As such, this cavity fields may be judiciously modulated to yield optimized performance from patch antenna. Here, along with patch surface geometry, the shorting posts also play a vital role to modulate the cavity fields.

In fact, the magnetic fields around the shorting pins in Antenna#3 force the electric fields to concentrate at central region of radiating edges and hence fringing increases at radiating edges. Therefore, close inspection of Fig. 5.4 and Fig. 5.5 reveal that, the incorporation of shorting pins (Antenna#3) modulates the cavity fields in such a way that the electric fields reside beneath the main circular disc plate (a = 7 mm) rather than distributed beneath the whole antenna patch plate as is the case for Antenna#2. Fig. 5.4 and Fig. 5.5 clearly depicts the fact. Although, structurally, Antenna#1 and Antenna#3 are different still, the cavity fields and consequently the fringing between Antenna#1 and Antenna#3 has a close resemblance as is clear from Fig. 5.4 (a) and Fig. 5.4(c). Fig. 5.5(a) and Fig. 5.5(c) confirms the observation in terms of electric vector**.**

Therefore, the capacitance of the structure changes which is manifested on the change in dielectric constant due to the incorporation of shorting pins.

Now, the patch plate area (A_P) of the structure in case of Antenna#2 may be written as,

$$A_p = \pi a^2 + 2\left[2aw_1 - \left\{\frac{a^2}{2}\theta_0 - (a - w_1)\sqrt{a^2 - (a - w_1)^2}\right\}\right] \qquad (5.6)$$

Again, the patch plate area of Antenna#3 is similar to Antenna#2. Therefore, the calculated area from (5.6) may be used to find the static capacitance of Antenna#3 with new dielectric constant (due to inner portion of the shorting pins).

Following the (5.6), the area of the structure becomes 190 mm^2 and the capacitance of this patch plate in Antenna#2 becomes

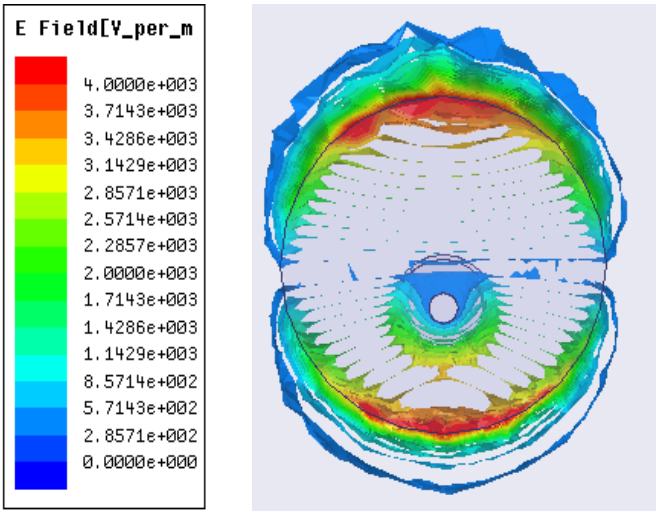

(a)

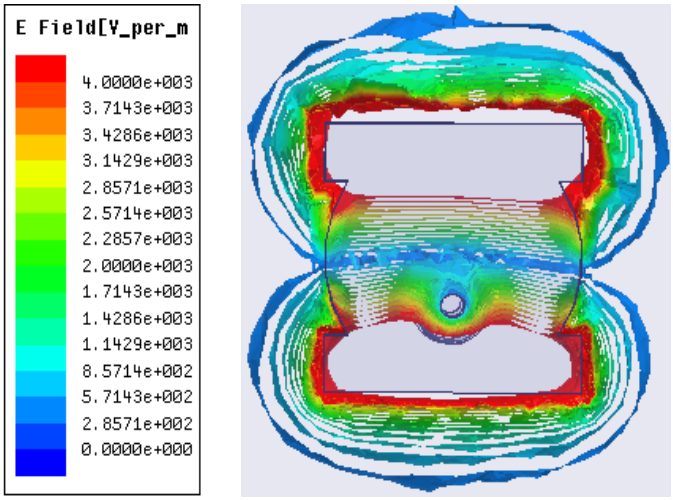

(b)

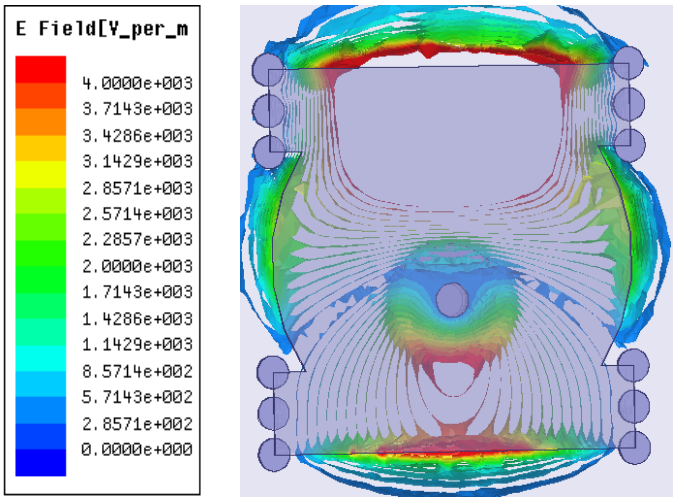

(c)

Fig. 5.4 Simulated electric field magnitude over substrate (a) Antenna#1, (b) Antenna#2, (c) Antenna#3

$$C_p = \frac{190}{h}(\varepsilon_r)_N \tag{5.7}$$

where, $(\varepsilon_r)_N$ becomes new dielectric constant due to the incorporation of shorting pins. Based on the discussions above, this C_P with new dielectric constant is equivalent to the capacitance (C_O) of original circular disc patch (a = 7 mm).

Now,

$$C_0 = \frac{\pi a^2}{h}\varepsilon_r = \frac{153}{h}\varepsilon_r \tag{5.8}$$

As the cavity fields beneath the patch in case of Antenna#1 and Antenna#3 has close resemblance, equating these two capacitances,

$$(\varepsilon_r)_N = 0.8\varepsilon_r = 1.7 \tag{5.9}$$

Now, due to incorporation of shorting pins at far end side of patch structure, major part of the current producing radiation follows the locus of conventional circular patch as is depicted in Fig. 5.2(b) and Fig. 5.3(b). Therefore, resonance frequency may be calculated by (5.4).

Therefore, the new resonant frequency becomes,

$$f_r = \frac{c}{2\pi \times 0.54 a\sqrt{(\varepsilon_r)_N}} = 9.7\ GHz \tag{5.10}$$

The simulated resonance frequency for Antenna#3 is 10.01 GHz. Simulated and computed resonance frequencies are documented in Table 5.1.

TABLE 5.1
Comparison of simulated and computed resonance frequency using proposed theory

Patch configuration	Simulated f_r (GHz)	Computed f_r (GHz)
Antenna#1	7.9	8.4
Antenna#2	6.13	5.7
Antenna#3	10.01	9.7

It may be noted that, to excite such 10 GHz frequency, the surface wave eliminated antenna has larger radius than present a = 7 mm patch. The surface wave eliminated antenna radius a_2 may be calculated as [26],

$$a_2 = 1.84/\beta_{TM0} \tag{5.11}$$

where, β_{TM0} is the propagation constant of first surface wave mode that is TM_0 surface wave and k_0 is the wave number of structure.

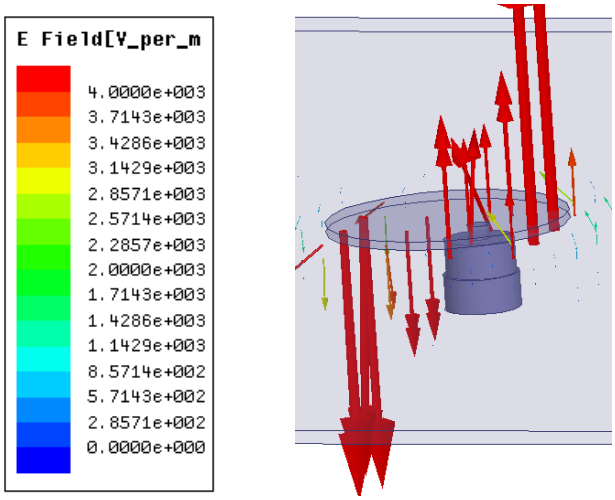

(a)

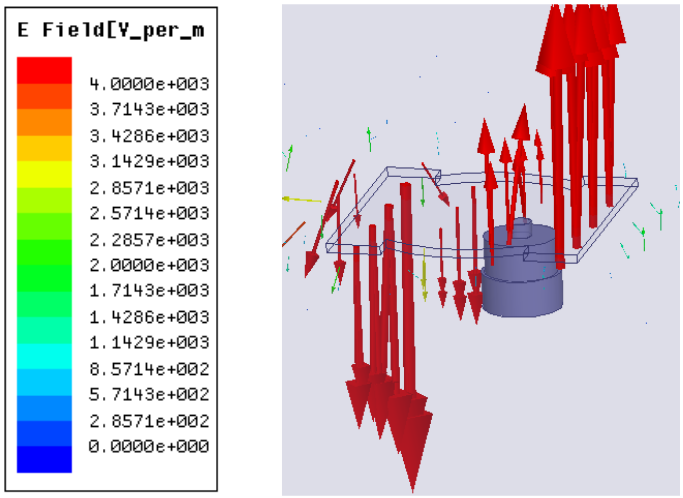

(b)

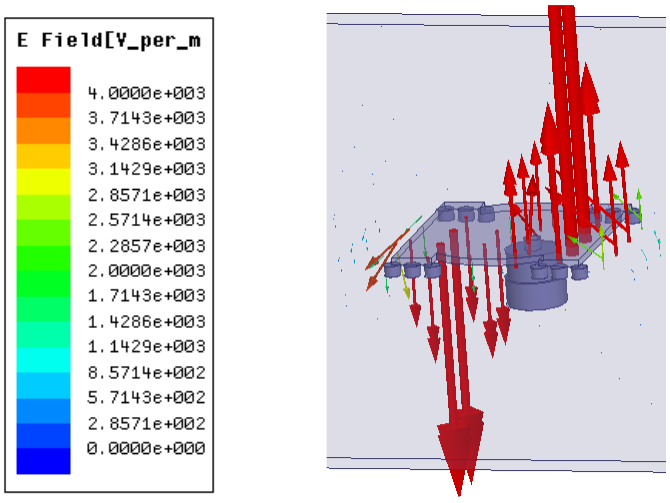

(c)

Fig. 5.5 Simulated electric field vector over substrate (a) Antenna#1, (b) Antenna#2, (c) Antenna#3

The relation between them may be written as [26],

$$\beta_{TM0}/_{k_0} = [1 + (k_0 h)^2] \quad (5.12)$$

Therefore, it yields that, for designing surface wave eliminated antenna or RSW antenna, the required patch radius is a_2 = 8.8 mm with patch area of 243.28 mm^2. Contrarily, the present patch area is 190 mm^2. Therefore, 21.9% reduction in patch area has been achieved with the present design in comparison to complete surface wave eliminated patch.

5.2.4 Evolution Analysis: Radiation Characteristics

The simulated gain and cross polarization of Antenna#1 and Antenna#2 at their H plane are depicted in Fig. 5.6 (a). The gain of the Antenna#2 at f = 6.13 GHz is 6.25 dBi while PP is 10 dB. Contrarily, Antenna#1 has peak gain of 7.64 dBi and the PP is 18 dB at f = 7.9 GHz. It may be noted that, Antenna#2 has somewhat flat-topped radiation beam which is good for certain applications. However, PP is poor with broadside profile of cross polar radiation which may affect the main co-polar beam.

The simulated gain and cross polarization of Antenna#1 and Antenna#3 at their H plane are depicted in Fig. 5.6(b). The gain of the Antenna#3 at f = 10.01 GHz is 10 dBi while PP is 30 dB. It may be noted that, Antenna#3 has somewhat wider radiation beam at it's H plane with high gain in comparison to Antenna#1.

The E plane radiation characteristics of Antenna#1, Antenna#2 and Antenna#3 is depicted in Fig. 5.6(c). The comparison of E plane radiation performance amongst all three antennas reveals that, Antenna#3 has best performance in terms of gain and PP. Notably, radiation along horizontal direction in Antenna#3 has significant improvement in comparison to Antenna#1 and Antenna#2.

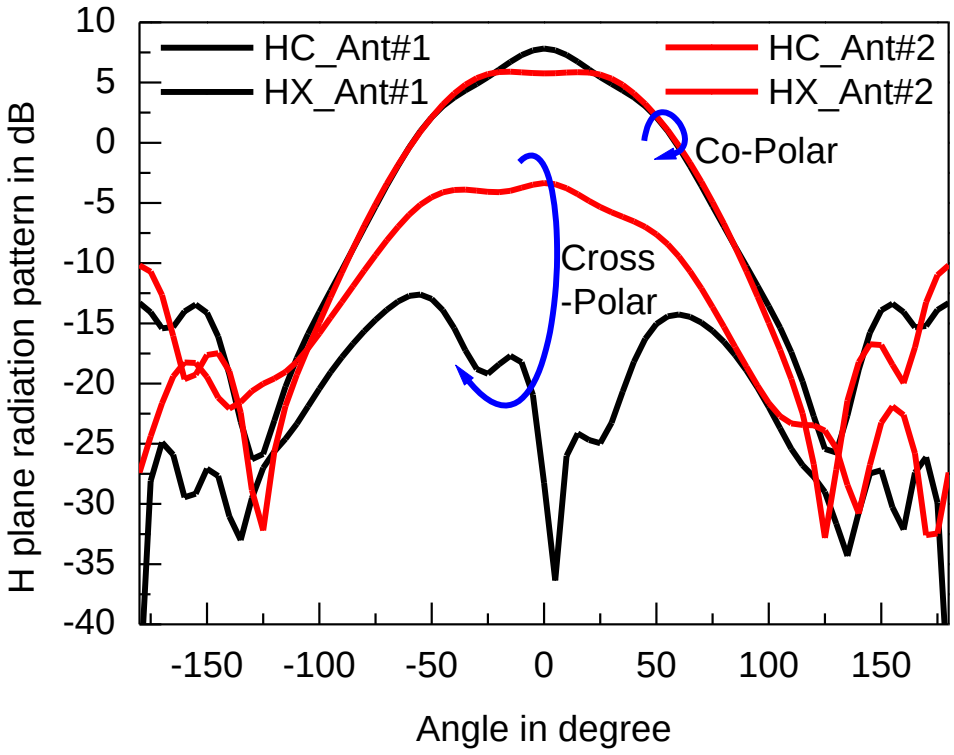
HC_Ant#1
HX_Ant#1
HC_Ant#2
HX_Ant#2
Co-Polar
Cross
-Polar
H plane radiation pattern in dB
Angle in degree
10
5
0
-5
-10
-15
-20
-25
-30
-35
-40
-150
-100
-50
0
50
100
150

(a)

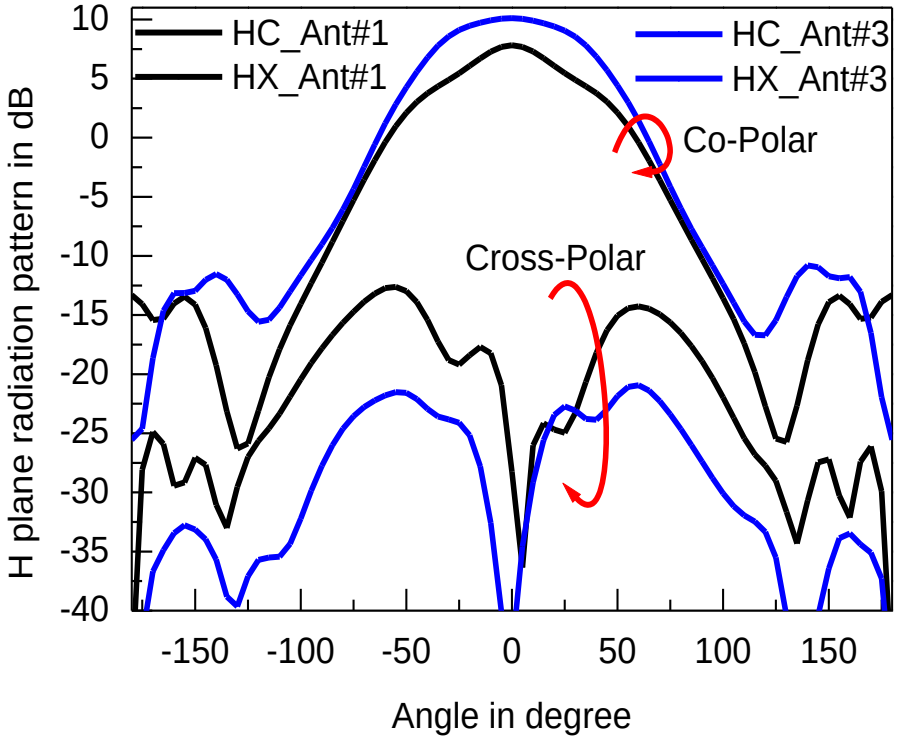
HC_Ant#1
HX_Ant#1
HC_Ant#3
HX_Ant#3
Co-Polar
Cross-Polar
H plane radiation pattern in dB
Angle in degree
10
5
0
-5
-10
-15
-20
-25
-30
-35
-40
-150
-100
-50
0
50
100
150

(b)

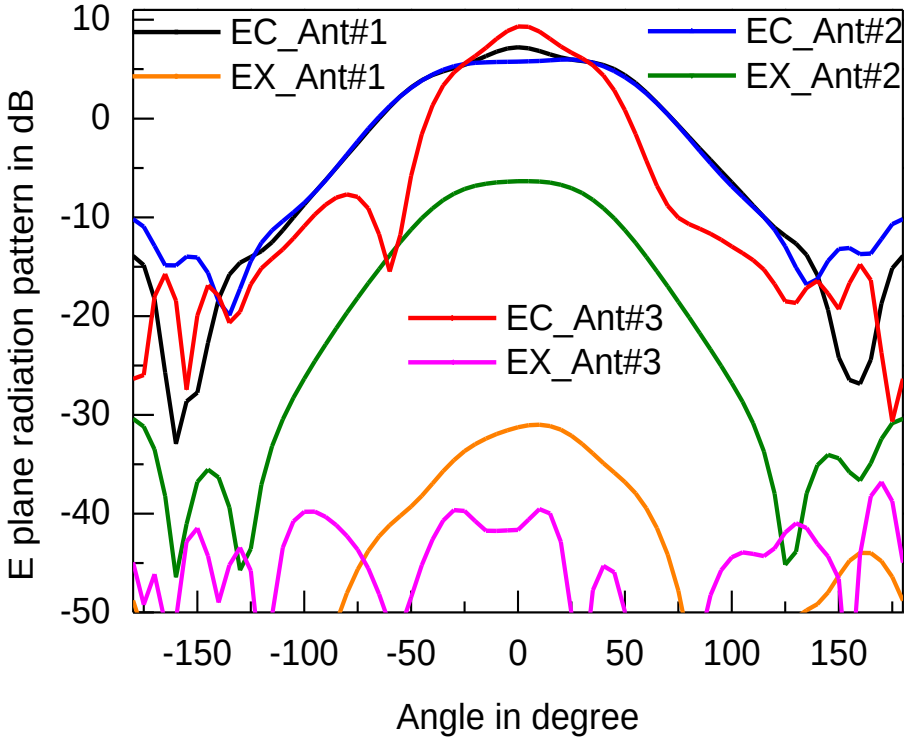

(c)

Fig. 5.6 Comparison of H plane radiation pattern(a) Antenna#1 and Antenna#2 (b)Antenna#1 and Antenna#3, (c) Comparison of E plane radiation patterns of Antenna#1, Antenna#2 and Antenna#3.

The strong radiation fields along the horizontal direction at the E plane of patch antenna is actually due to the polarization current (J_P) as,

$$\bar{J}_P = j\omega\bar{P} \tag{5.13}$$

where,

$$\bar{P} = (\varepsilon_r - 1)\varepsilon_0\bar{E} \tag{5.14}$$

Therefore, the problem of horizontal radiation in E plane is much prominent in case of patch with dielectric substrate in comparison to air substrate. In air substrate, the suppression of radiation along horizontal direction is manifested through the gain enhancement at the zenith of the patch. Contrarily, the problem of strong horizontal radiation is not the issue in H plane. In the Fig. 5.7, x-z plane is E plane while y-z plane is H plane. At the patch radiating edges (where the electric field is maximum and consequently the dielectric polarization and hence the polarization current) is counter-phased between the lower and upper half section of patch. Therefore, the effect on the horizontal radiation along H plane is cancelled while it is prominent in

E plane due to the path difference travelled by radiation field arises due to polarization current as is clear from Fig. 5.7.

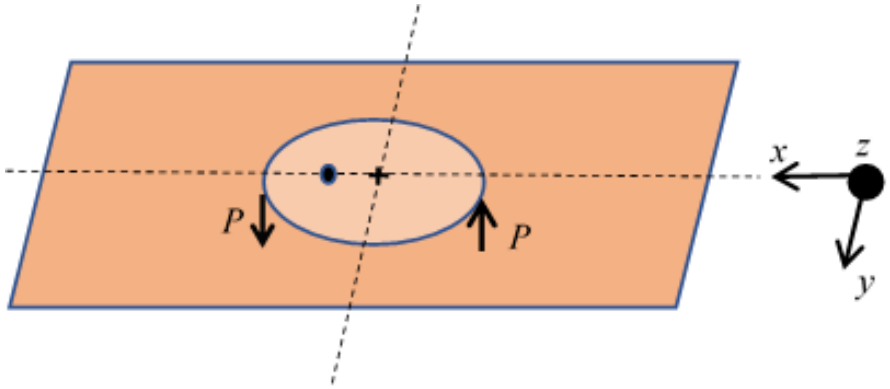

Fig. 5.7 Effect of polarization current in horizontal radiation at E plane.

Now, near the radiating edges of the patch, if shorting pins are incorporated, it compensates this polarization current by counter-phased conduction current through shorting pin. With this in view, 12 numbers of shorting pins are incorporated at four extreme sides of Antenna#2 which, gives birth to Antenna#3. Therefore, the radiation along horizontal direction becomes 20 dB down than peak co-polar gain in case of Antenna#3 while the same is only around 8-9 dBi in Antenna#1 and Antenna#2.

This, suppression of radiation field along horizontal direction in Antenna#3 in turn enhances broadside radiation and hence gain increases. The incorporation of shorting pins in Antenna#3 concentrates the fields near the radiating edges of patch structure and hence fringing increases there. This may also be attributed for higher gain in Antenna#3. Furthermore, incorporation of shorting pin reduces the effective dielectric constant of the substrate. Hence, surface wave reduces and as a result gain and efficiency increases.

It may be noted that, the incorporation of shorting pins reduces orthogonal component (y directed) of fringing electric fields as is confirmed from Fig. 5.4 in Antenna#3. In fact, because of structural modification as well as the incorporation of shorting pin, locus of current path has been modulated as is shown in Fig. 5.2(b) and Fig. 5.3(b). It results in low cross polarized radiation in the proposed Antenna#3.

5.2.5 Circuit Model Approach

A simple CMA is a parallel resonant circuit consisting of resonant input resistance *R*, patch inductance *L* and the patch capacitance *C* between two electrodes (patch and ground plane) as is shown in Fig. 5.8(a). The resonant frequency of the patch in terms of circuit theory can be written as,

$$f_r = \frac{1}{2\pi\sqrt{LC}} \tag{5.15}$$

Where approximate value of C can be the patch capacitance and may be written as,

$$C = \frac{\varepsilon_0 \varepsilon_r}{h} A_P \text{ and } L = \frac{1}{4\pi^2 f^2 C} \tag{5.16}$$

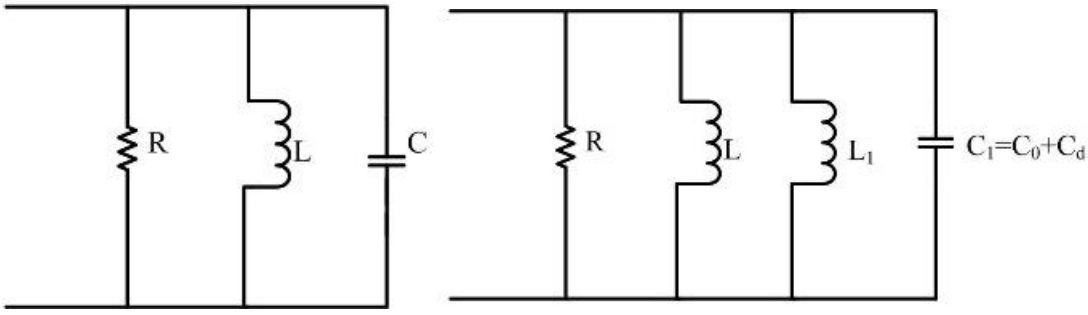

(a) (b)

Fig. 5.8 Approximate circuit model (a) Conventional CMA, (b) proposed antenna

Now, when we insert shorting pins beneath the patch plate, an inductance L_1 comes between the electrodes (patch and ground plane) of the capacitor. This L_1, comes parallel to the anti-resonant circuit of patch. Also, the incorporation of shorting pins change the dielectric constant of the substrate from ε_r to $(\varepsilon_r)_N$ as is discussed in section 5.2.3. Therefore, a new dielectric capacitance C_d has come up replacing the conventional dielectric capacitance of patch. The new dielectric capacitance C_d is the capacitance only due to the presence of new dielectric with dielectric constant $(\varepsilon_r)_N$. It may be noted that, once the shorting pins are introduced, the antenna structure (Antenna#3) is behaving like a simple circular patch of radius *a* = 7 mm irrespective of patch plate geometry as is discussed and validated in previous sections 5.2.2 and 5.2.3.

The pin inductance L_1 and the new dielectric capacitance C_d can be obtained from [179, 201] as,

$$L_1 = \frac{\mu_0}{2\pi}\left[ln\left(\frac{a}{d/2}\right) - \frac{3}{4}\right]h \tag{5.17}$$

and

$$C_d = [(\varepsilon_r)_N - 1]\frac{\varepsilon_0 \pi a^2}{h} \tag{5.18}$$

Therefore, the whole patch capacitance of Antenna#3 can be written as [179],

$$C_1 = C_0 + C_d \tag{5.19}$$

where, C_0 is the portion of patch capacitance of Antenna#3 when dielectric is removed [179]. Hence,

$$C_1 = \left[\frac{\varepsilon_0 \pi a^2}{h}\right] + [(\varepsilon_r)_N - 1]\frac{\varepsilon_0 \pi a^2}{h} \tag{5.20}$$

In the context of section 5.2.4, the current through this pin inductance L_1 must be compensated by the polarization current through new dielectric capacitance C_d. Then only, the horizontal radiation from antenna in E plane can be reduced as is discussed in section 5.2.4.

Therefore, the new equivalent circuit for Antenna#3 is as shown in Fig. 5.8(b). The equivalent inductance and capacitance of Antenna#3 can be written as,

$$L_{eq} = \frac{LL_1}{(L+L_1)} \quad \text{and } C_{eq} = C_1 \tag{5.21}$$

and the resonant frequency will be

$$f_r = \frac{1}{2\pi\sqrt{L_{eq}C_{eq}}} \tag{5.22}$$

Considering patch of radius a = 7 mm, pin diameter d = 1.2 mm, substrate thickness h = 0.787 mm and new effective dielectric constant of $(\varepsilon_r)_N$ = 1.7 (equation 5.9), patch plate area A_p = 190 mm (equations 5.6 and 5.7); the calculated f_r for Antenna#3 is 9.3 GHz which is very close to that obtained in equation (5.10). The simulated and measured resonant frequency of same antenna (10.01 GHz and 10.02 GHz respectively) is documented in results section (section 4.4, Fig. 5.10) which

shows good agreement with the predicted results by both the cavity model and circuit model approaches.

5.3 Proposed Structure

First, a simple CMA with 0.5 mm copper strip having radius a = 7 mm is chosen and two rectangular thin strips of dimension 14 mm × 3 mm are loaded at the upper and lower sections of patch as shown in Fig. 5.1(b). It is then fabricated on RT-5880 (dielectric constant ε_r = 2.2 and thickness h = 0.787 mm) substrate. The dimensions of substrate and ground plane are chosen to be 50 mm × 50 mm (~$1.5\lambda_0$ × $1.5\lambda_0$). Next, 12 shorting pins of diameter d (=1.2 mm) with center-to-center spacing d_1 (= 1.5 mm) has been incorporated at the sides of two thin rectangular strips as shown in Fig. 5.1(c). The patch is fed at 1.5 mm from the centre point (Fig. 1). An equivalent conventional CMA of radius 5.5 mm having same resonant frequency has also been fabricated on RT-5880 (dielectric constant ε_r = 2.2 and thickness h = 0.787 mm) substrate for comparison. The fabricated prototype of the proposed patch is shown in Fig. 5.9.

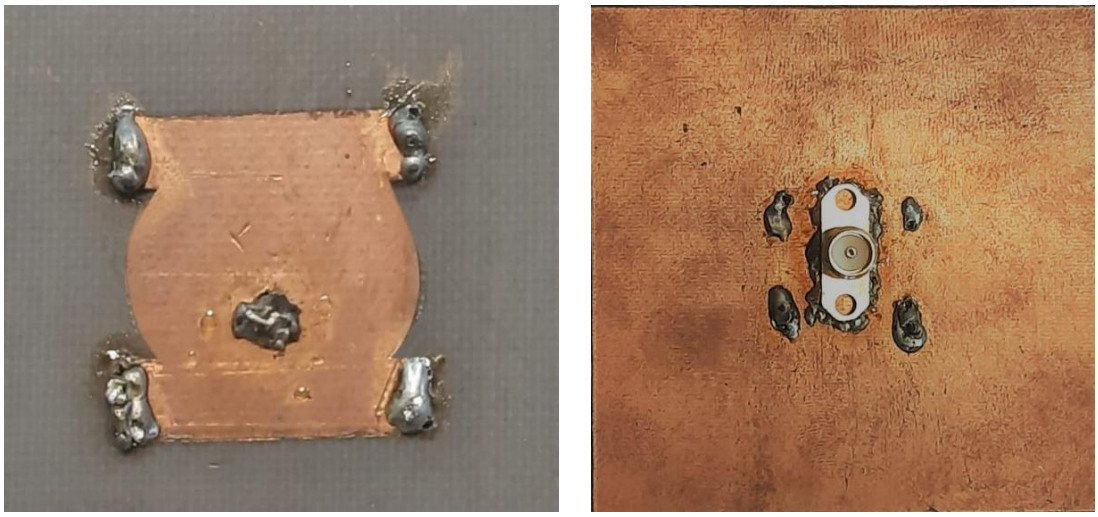

(a) (b)

Fig. 5.9 Fabricated prototype (a) Top view (b) bottom view

5.4 Results and Discussions

The fabricated prototypes (conventional CMA of radius 5.5 mm and the proposed patch) have been measured and the results are documented. In Fig. 5.10, the simulated and measured reflection coefficient profiles for the proposed antenna (Antenna#3) are

presented. The proposed antenna resonates at 10.02 GHz with an impedance bandwidth from 9.94 GHz to 10.14 GHz. The equivalent conventional CMA of radius 5.5 mm also resonates at same 10.02 GHz frequency although not shown in figure to avoid clumsy plot.

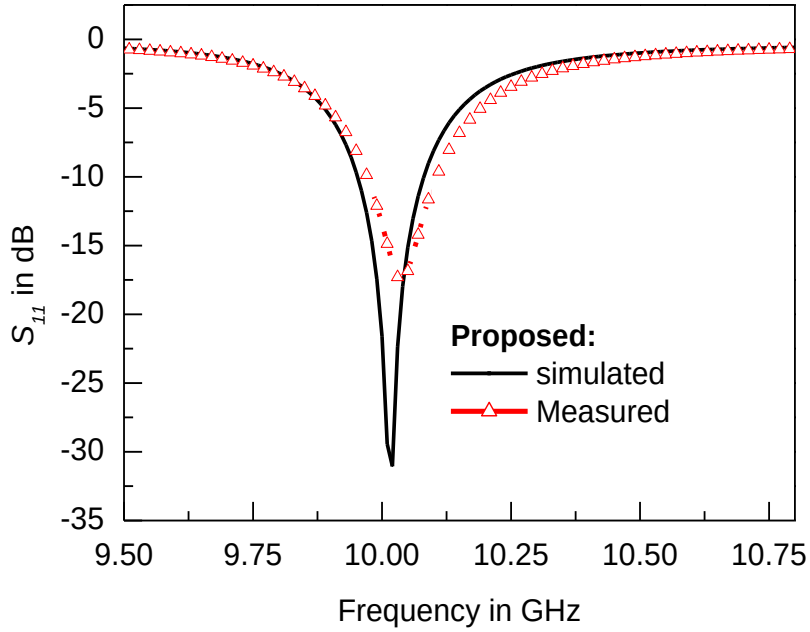

Fig. 5.10 Simulated and measured reflection coefficient profiles of proposed Antenna#3

The complete H and E plane radiation patterns of the proposed antenna has been presented in Fig. 5.11 (a) and Fig. 5.11 (b) respectively. The complete radiation pattern of equivalent conventional CMA has also been incorporated in the respective plot for comparison. Fig. 5.11 depicts that; the measured gain of the proposed antenna is 9.2 dBi while the simulated gain is 9.6 dBi. Contrarily, equivalent conventional CMA has measured gain of 6.8 dBi while the simulated one is 7.4 dBi. Therefore, 2.4 dB improvements in gain can be achieved with the proposed antenna in comparison to conventional CMA resonating at same 10.02 GHz frequency.

The simulated magnitude of electric field at the substrate shown in Fig. 5.12 reveals a high concentration of fringing fields near radiating edges of patch as is discussed in section 5.2.4. This confirms the conjecture for higher gain of the structure discussed earlier. Fig. 5.11(b) shows that, the polarization purity in E plane radiation pattern is 44 dB while the same for conventional CMA at same frequency is 35 dB. However, the polarization purity in E plane is not a major concern as it is usually below 30 dB than the peak co-polar gain always.

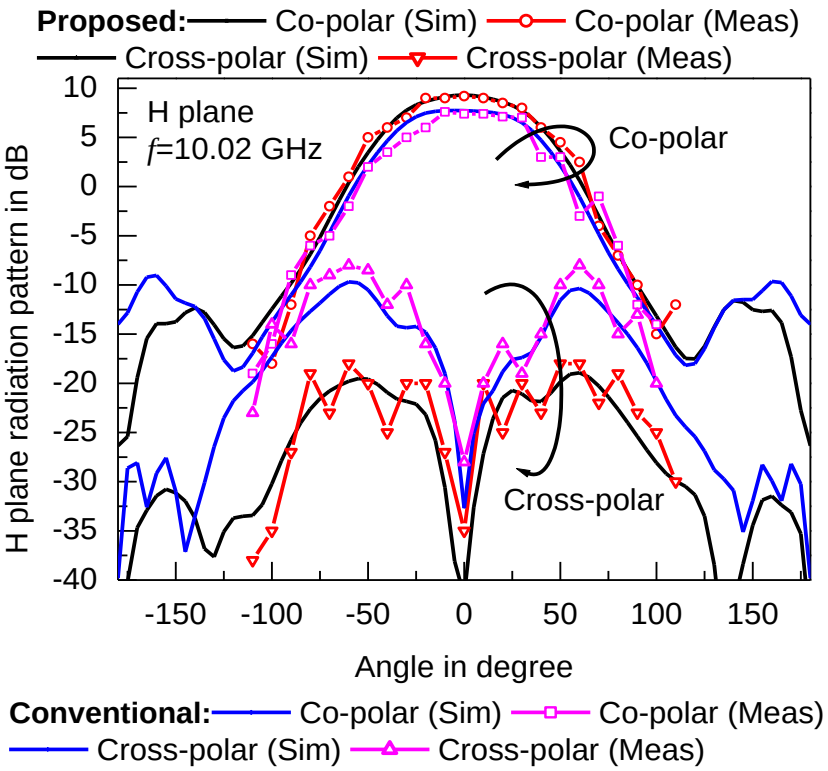

(a)

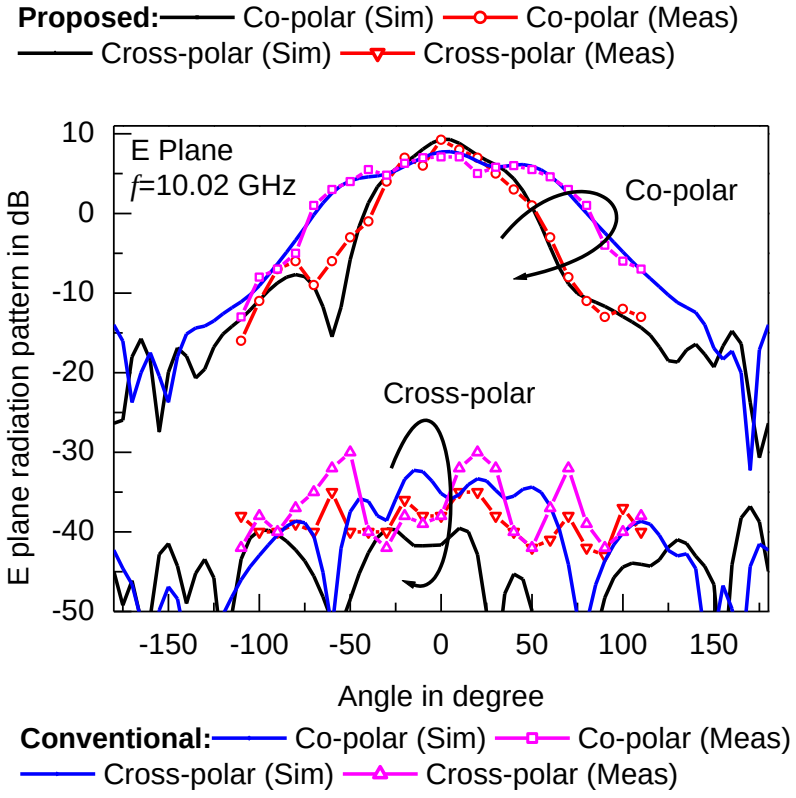

(b)

Fig. 5.11 Comparison of simulated and measured radiation patterns of conventional Antenna#1 and proposed Antenna#3 (a) H plane, (b) E plane.

On the contrary, H plane cross-polarization is a major factor for linearly polarized antenna and it is usually high in conventional CMA. Fig. 5.11(a) confirms that, the H plane polarization purity of proposed patch is 27 dB while the same for conventional CMA is only 15 dB. About 12 dB improvement in co-polar to cross-polar radiation isolation is revealed from proposed patch than conventional CMA at same frequency at H plane.

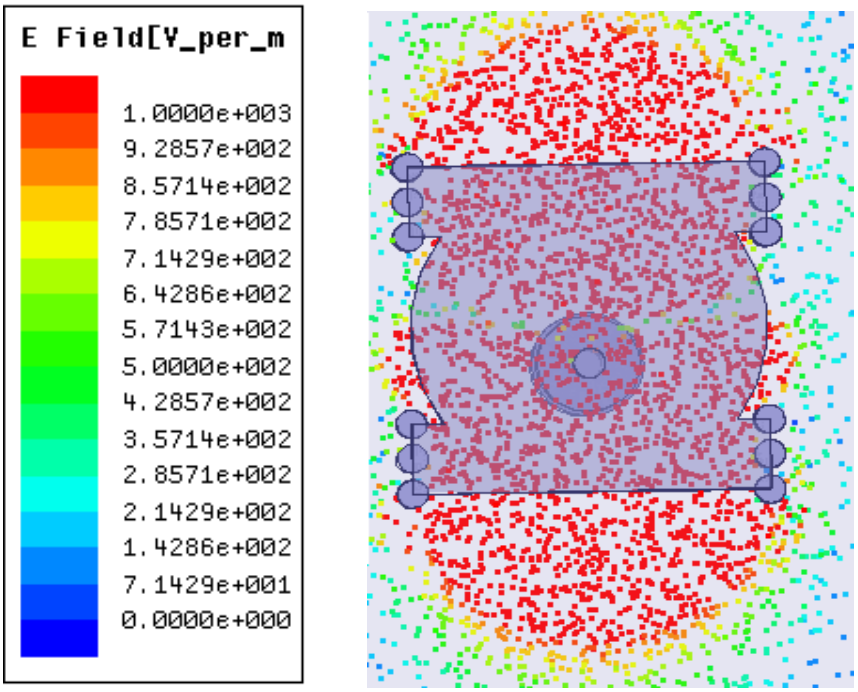

Fig. 5.12 Simulated electric field magnitude over substrate in proposed Antenna#3.

The variation of antenna gains as function of angle θ at off bore sight direction has also been examined through simulation and measurements at the operating frequency f = 10.02 GHz. The resulting plot is depicted in Fig. 5.13. The gain variation is examined within its 3 dB beam width. In E plane, the measured gain is monotonically decreasing from 9.2 dBi to 6 dBi, while the same is 10 dBi to 6.88 dBi for simulated gain within $\pm 25^0$. Contrarily, this gain decrement is comparatively slower in case of H plane where the measured gain varies from 9.2 dBi to 6 dBi within $\pm 40^0$. It may be noted that, the measured gain is around 0.8-1 dB lower than the simulated gain. This 0.8-1.0 dB decrement in measured gain is expected due to unavoidable cable and connector losses. Therefore, the 3 dB beam width of the proposed antenna is around 50^0 in E plane while the same for H plane is 80^0.

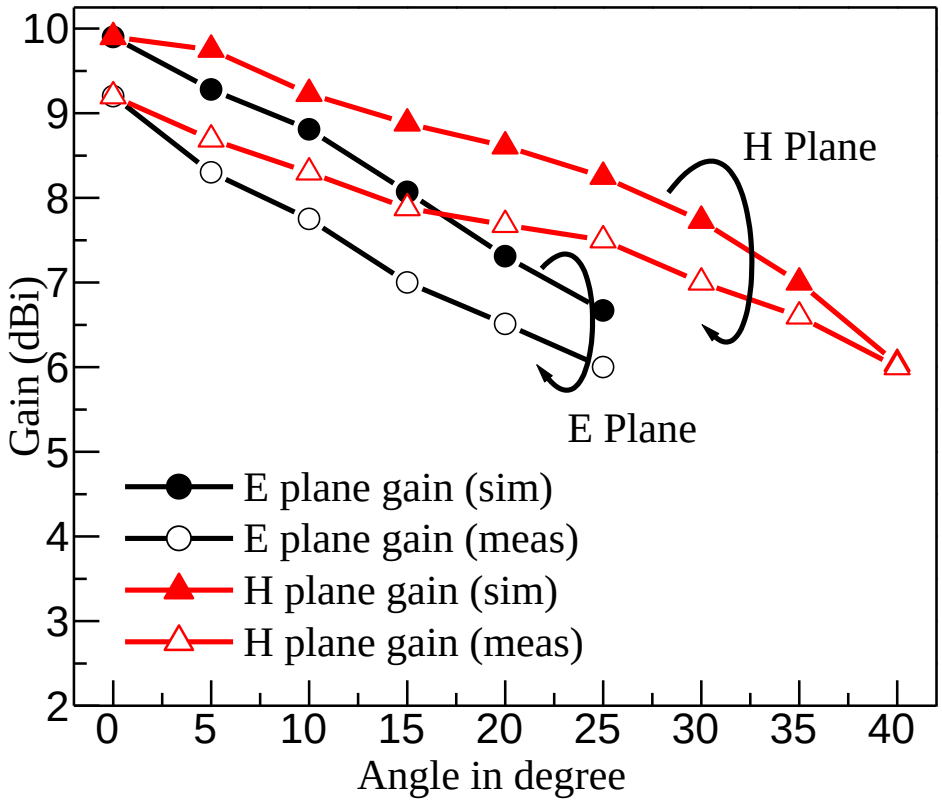

Fig. 5.13 Variation of gain of proposed antenna at both principal planes within it's 3 dB beam widths.

The measured horizonal radiation arises from lateral surface wave is 20-21 dB down than peak co-polar gain in case of proposed antenna at it's both E and H plane. On the other hand, for conventional CMA, the same is only 10 dB down than peak co-polar gain in E plane and 20 dB down in H plane.

The measured efficiencies of the proposed antenna are 92% while the same for conventional CMA is 85%. The gain and efficiency variation as a function of frequency has been presented in Fig. 5.14. Minor degradation of measured gain and efficiency both in respect to simulation results are noted and it is expected due to practical and unavoidable loss factors as discussed above. It is noted that, measured gain varies from 8-9 dBi while the measured efficiency varies from 88 to 92%. However, it may be concluded that, gain and efficiency is merely constant over the whole operating band of the proposed antenna.

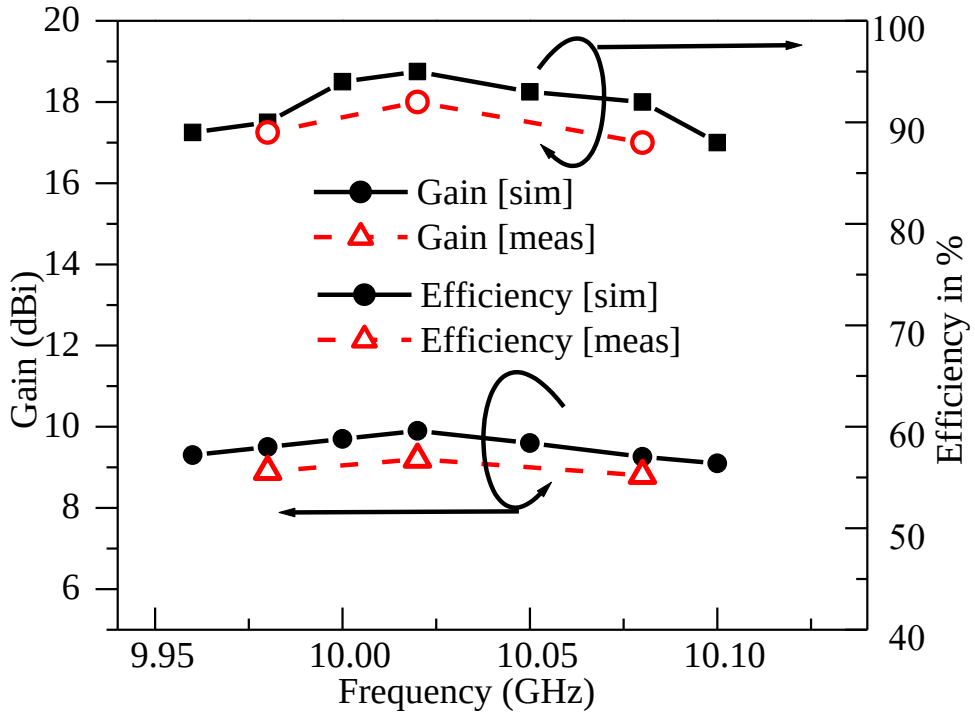

Fig. 5.14 Variation of gain and efficiencies of proposed antenna as function of frequency in the operating band.

The performance of the proposed Antenna#3 has been compared with the available relevant literatures in Table-5.2. This confirms the consistency and superiority of the present structure over others.

TABLE 5.2

Performance comparison of the present antenna with recently reported relevant works

Reference	Gain (dBi)	Minimum CP-XP Isolation (dB)	Efficiency (%)	Max radiation to horizontal radiation isolation (E plane) (dB)	Remarks
[193]	8.5	25	93	---	Simple RSW inspired circular patch with pair of shorting strips makes concurrent improvements in gain, efficiency and polarization purity.
[150]	7.8	20	---	10	Four stacked planes with complex feeding.
[170]	8	---	91	13	Use of slots, numerous vias with 3 stack ground plane makes the structure too bulky.
[152]	7.25	18	73.5	16	Complex structure integrated with branch line coupler. Dual feed RSW inspired antenna.

Reference	Gain (dBi)	Minimum CP-XP Isolation (dB)	Efficiency (%)	Max radiation to horizontal radiation isolation (E plane) (dB)	Remarks
[153]	9	13	69	10	RSW inspired simple circular patch with shorting four vias.
[137]	11	19	89	15	RSW inspired antenna with much distortion in radiation pattern and very high side lobes.
[154]	9.0	20	92	15	Use of multiple stacking with dual stacked dense dielectric circular patch make the structure too complex for manufacturing.
[155]	6.8	0	----	3	Hexadecagon circular patch with DGS makes significantly distorted radiation pattern).
[156]	7.8	----	63	7	Asymmetric E and H plane radiation beam makes the radiation property poor.
Present work	9.2	27	92	20	Simple modified CMA for reduced horizontal radiation along with high gain, excellent PP and efficiency.

5.5 Conclusion

A symmetrically modified circular microstrip antenna with a pair of thin strips has been proposed and investigated theoretically as well as experimentally. Excellent improvement in radiation performance with high gain of 9.2 dBi, 27 dB polarization purity with 92% efficiency have been obtained. Notably, a new feature of reduced horizontal radiation i.e., 21 dB down than peak co-polar gain has been achieved which is undeniably helpful for modern array or 5G MIMO configuration. The thorough investigation presented in the paper gives an insightful exploration of such new antenna structure. The proposed antenna will surely be helpful for modern scientific and research community looking for tiny planar structure with excellent radiation properties.

CHAPTER 6

Conclusion and Scope for Future Studies

In this dissertation, a detailed study on the characteristics of circular microstrip antenna (CMA) has been carried out and different techniques are imposed for the improvement in the input and radiation characteristics of such CMA. The various shortcomings of CMA such as low gain, narrow bandwidth, low efficiency, poor polarization purity and strong horizontal fields along the horizontal direction has been investigated thoroughly and different techniques to overcome such shortcomings are proposed and presented methodically.

Initially, shorting and strip loading approach has been investigated to achieve simultaneous enhancement of gain and polarization purity. Four circular microstrip antennas with a pair of shorting walls placed at the non radiating periphery of the patch, two with FR4 and two with Glass substrate having two different substrate thickness has been investigated to improve the co-polar gain and polarization purity without hampering basic radiation pattern. The proposed structure with FR4 substrate provides a CP-XP isolation (polarization purity) of 27 dB while the polarization purity with glass substrate is more than 30 dB. The polarization purity obtained from all the structures are quite higher than the conventional structures with FR4 and glass substrates. A CMA with strip loading approach has also been proposed to improve the radiation characteristics. In this approach, a CMA is designed by placing a strip at the top of the circular patch for better polarization purity in H plane as well as higher co-polar gain as compared to the conventional CMA. The co-polar gain of 7.5 dBi with 23 dB polarization purity is observed from the proposed structure. The simultaneous improvement of co-polar gain and polarization purity without

disturbing the conventional E plane radiation pattern is very much require in modern wireless communication.

Next, simultaneous enhancement of impedance bandwidth and polarization purity has been achieved using DGS Structure. A pair of rectangular defects have been deployed on the ground plane at the radiating edge of the conventional CMA on RT-Duroid substrate having dielectric constant ε_r = 2.33 and height h = 1.58 mm in order to provide concurrent improvement in impedance bandwidth and polarization purity. This structure provides impedance bandwidth of 31.5% and polarization purity of around 24 dB. Another DGS structure with a curved dumbbell shape defect deployed on the ground plane at the non-radiating edge of the conventional patch has also been investigated to provide improvement in the impedance bandwidth and polarization purity. This structure provides 25.8 dB polarization purity with 12% impedance bandwidth. This structure can be useful in the modern wireless communication field where wide impedance bandwidth and high polarization purity is required.

Next, a simple CMA with a pair of shorting strips loaded at the non radiating sides has been successfully investigated analytically based on the reduced surface wave (RSW) theorem for improving the co-polar gain, efficiency, and polarization purity simultaneously. Besides improving the gain, efficiency, and polarization purity, the proposed antenna can also successfully suppress the radiation along the horizontal direction, which is worthy of modern array and MIMO wireless applications. The proposed structure attains a Co-polar gain of 8.5 dBi, polarization purity of 25 dB and 93% efficiency. The radiation along the horizon (i.e. θ = 90°) of the proposed antenna is approximately 20 dB less than the peak CP gain.

Theoretical and mathematical analysis has been carried out to modulate the cavity fields under a conventional CMA to reduce horizontal radiations and improve the radiation profile. This is done by placing a pair of thin rectangular strip loaded at the top and bottom of a CMA. The structure is further modified by placing 12 shorting pins at the edge of the shorting strips. This structure is proposed to provide improvement in co-polar gain, efficiency and polarization purity. Excellent improvement in radiation performance with high gain of 9.2 dBi, 27 dB polarization

purity with 92% efficiency have been obtained using this structure. A new feature of reduced horizontal radiation i.e., 21 dB down than peak co-polar gain has been achieved which is undeniably helpful for modern array or 5G MIMO configuration. The proposed antenna will surely be helpful for modern scientific and research community looking for tiny planar structure with excellent radiation properties.

Further improvement in the input and radiation characteristics of CMA is always a positive choice and hence some more ideas may be implemented. In addition to different techniques of defected ground surface (DGS), defected patch surface (DPS), shorting of non-radiating edges of CMA, some other methods may be explored. Complete RSW approach as discussed in chapter 4 or quasi RSW approach as discussed in chapter 5 may be adopted in other regular and irregular geometries of patches for improvement in input and radiation performance.

References:

[1] D. D. Greig and H. F. Engleman, "Microstrip-a new transmission technology for the kilomegacycle range," *Proceedings of the IRE.*, vol. 40, pp. 1644-1650, 1952.

[2] G. A. Deschamps, "Microstrip Microwave Antennas," *Proceedings of 3rd symposium on the USAF Antenna and Research Development Program*, pp. 18-22. Oct1953.

[3] H. Gutton and G. Baissinot, "Flat Aerial for Ultra High Frequencies," French Patent No. 703113, 1955.

[4] J. Q. Howell, "Microstrip antennas," *Dig. IEEE Int. Symp. Antennas Propagat*. pp. 177-180, 1972.

[5] R. E. Munson, "Dual slot microstrip antenna device," U.S. patent No. RE29296, 1975.

[6] L. Lewin, "Radiation from discontinuities in strip lines," *Proceedings of IEEE – Part C*, vol. 107, no. 12, pp 163-170, 1960.

[7] E.G. Fubini, "Stripline radiators," *IRE Transactions on Microwave Theory and Tech.*, vol. 3, no. 2, pp. 149-156, 1955.

[8] J. A. McDonough, R.G. Malesh, and J. Kawalsky, "Recent developments in the study of printed antennas," *IRE International Convention Record*, vol.5 pp. 173-176, New York, 1957.

[9] E. J. Denlinger, "Radiation from microstrip resonators," *IEEE Transaction on Microwave Theory and Tech.*, vol. 4, pp. 235-236, 1969.

[10] T. Itoh and R. Mittra, "Analysis of microstrip disk resonator," *Arch. Elek. Ubertagung*, vol. 21, pp. 864-851, 1973.

[11] A. Derneryd, "Linearly polarized microstrip antenna," *IEEE Transaction on Antennas Propagation*, vol. 24, no. 6, pp. 864-851, 1976.

[12] G. Dubost, M. Nicholas, and H. Havot, "Theory and applications of broadband microstrip antennas," *Proc. 6th European Microwave Conference*, pp. 275-279, 1976.

[13] P. Agarwal and M. Bailey, "An analysis technique for microstrip antennas," *IEEE Trans. Antennas Propagation*, vol. 25, no. 6, pp. 756-759, 1977.

[14] W.F. Richards, Y.T. Lo, and D.D. Harrison, "Improved theory for microstrip antennas," *Electronics Letters*, vol. 15, no. 2, pp. 42-44, 1979.

[15] Y.T. Lo, D. Solomon, and W. Richards, "Theory and experiment on microstrip antennas," *IEEE Trans. Antennas Propagation*, vol. 27, no. 2, pp. 137-145, 1979.

[16] P. Hammer, D.V. Bouchaute, D. Verschraeven, and A.V.D. Capelle, "A model for calculating the radiation field of microstrip antennas," *IEEE Trans. Antennas Propagation*, vol. 27, no. 2, pp. 267-270, 1979.

[17] K. Keen, "A planar log-periodic antenna," *IEEE Trans. Antennas Propagation*, vol. 22, no. 3, pp. 489-490, 1979.

[18] D.T. Shahani and B. Bhat, "Network model for strip-fed cavity-backed printed slot antenna," *Electronics Letters,* vol. 14, no. 24, pp. 767-769, 1978.

[19] I.E. Rana and N.G. Alexopoulos, "On the theory of printed wire antennas," *9th European Microwave Conference,* pp. 687-691, 1979.

[20] A. Mulyanto and R.Vernon, " A V-shaped log periodic printed circuit antenna array for the 1 to 10 GHz frequency range," *Antennas and Propagation Society Intl. Symp.*, vol. 17, pp. 392-395, 1979.

[21] I.J. Bahl and P.Bhartia, *Microstrip Antennas*. Boston: Artech House, 1980.

[22] J. R. James, P. S. Hall and C. Wood, *Microstrip Antennas: Theory and Design*. London: Peter Peregrines, 1981.

[23] J. R. James and P. S. Hall, *Handbook of Microstrip Antennas*. London: Peter Peregrines, 1989.

[24] C.A. Balanis, *Antenna Theory: Analysis and Design*. NY: John Wiley & Sons, 1997.

[25] D.M. Pozar and D.H. Schaubert, *Microstrip Antennas*. New York: IEEE Press, 1995.

[26] R. Garg et.al., *Microstrip Antenna Design Handbook*. Boston: Artech House, 2001.

[27] G. Kumar and K.P. Ray, *Broadband Microstrip Antennas*. Boston: Artech House, 2002.

[28] R. B. Waterhouse, *Microstrip Patch Antennas: A Designer's Guide*. Boston: Kluwer Academic Publishers, 2003.

[29] J. Liang and H. D. Yang, "Radiation Characteristics of a Microstrip Patch Over an Electromagnetic Bandgap Surface," *IEEE Transactions on Antennas and Propagation,* vol. 55, no. 6, pp. 1691-1697, 2007.

[30] C. Chandan, A. Ghosh, S. K. Ghosh, and S. Chattopadhyay, "Radiation characteristics of rectangular patch antenna using air substrates," *International Conference on Emerging Trends in Electronic and Photonic Devices & Systems,* pp. 346-348, 2009.

[31] J.-F. Kiang, "Radiation characteristics of rectangular patch antennas with a laminated ground plane," *IEEE Proc.Microw. Antennas Propag.,* vol. 143, no. 2, pp. 107-112, 1996.

[32] A. Raj and Nisha Gupta, "Radiation characteristics of microstrip antenna on frequency selective surface absorbing layer," *International Journal of Microwave and Wireless Technologies,* vol.13, no.9, pp. 962-968, 2020.

[33] G. Qasim and S. Zhong, "Radiation characteristics of microstrip patch antennas with dielectric cover," *IEEE Antennas and Propagation Society International Symposium,* pp. 2208-2211, 1992.

[34] W.C. Chew and J.A. Kong, "Radiation characteristics of a circular microstrip antenna," *Journal of Applied Physics.,* vol.51, no.7, pp.3907-3915, 1980.

[35] A.K. Bhattacharyya, "Effects of finite ground plane on the radiation characteristics of a circular patch antenna," *IEEE Trans on Antenna and Propagation,* vol. 38, no. 2, pp. 152-159 1990.

[36] W. Cao, B. Zhang, A. Liu, T. Yu, D. Guo, and Y. Wei, "Broadband High-Gain Periodic Endfire Antenna by Using I-Shaped Resonator (ISR) Structures*," IEEE Antennas and Wireless Propagation Letters,* vol. 11, pp. 1470-1473, 2012.

[37] H. Wang, S. Liu, L. Chen, W. Li, and X. Shi, "Gain Enhancement for Broadband Vertical Planar Printed Antenna With H-Shaped Resonator Structures," *IEEE Transactions on Antennas and Propagation,* vol. 62, no. 8, pp. 4411-4415, Aug. 2014.

[38] Z. Han, W. Song and X. Sheng, "Gain Enhancement and RCS Reduction for Patch Antenna by Using Polarization-Dependent EBG Surface," *IEEE Antennas and Wireless Propagation Letters,* vol. 16, pp. 1631-1634, 2017

[39] S. Park, C. Kim, Y. Jung, H. Lee, D. Cho, and M. Lee, "Gain enhancement of a microstrip patch antenna using a circularly periodic EBG structure and air layer," *Int. J. Electron. Commun. (AEU),* vol. 64, no. 7, pp. 607-613, 2010.

[40] N. Llombart, A. Neto, G. Gerini, and P. de Maagt, "Planar circularly symmetric EBG structures for reducing surface waves in printed antennas," *IEEE Transactions on Antennas and Propagation,* vol. 53, no. 10, pp. 3210-3218, 2005.

[41] P. Ketkuntod, T. Hongnara, W. Thaiwirot, and P. Akkareakthalin, "Gain enhancement of microstrip patch antenna using I-Shaped Mushroom-like EBG structure for WLAN application," *International Symposium on Antenna and Propagation,* pp.1-2, 2017

[42] H. Boutayeb and T.A. Denidni, "Gain enhancement of a microstrip patch antenna using a cylindrical electromagnetic crystal substrate," *Transactions on Antennas and Propagation,* vol. 55, no. 11, pp.3140-3145, 2007.

[43] L. Lu, K. Ma, F. Meng, and K. S. Yeo, "Design of a 60-GHz Quasi- Yagi Antenna with Novel Ladder-Like Directors for Gain and Bandwidth Enhancements," *IEEE Antennas and Wireless Propagation Letters,* vol. 15, pp. 682-685, 2016.

[44] Y. Zhou, X. Cao, J. Gao, S. Li, and Y. Zheng, "In-Band RCS Reduction and Gain Enhancement of a Dual-Band PRMS-Antenna," *IEEE Antennas and Wireless Propagation Letters,* vol. 16, pp. 2716-2720, 2017.

[45] J. H. Kim, C. Ahn, and J. Bang, "Antenna Gain Enhancement Using a Holey Superstrate," *IEEE Transactions on Antennas and Propagation,* vol. 64, no. 3, pp. 1164-1167, March 2016.

[46] M. Asaadi and A. Sebak, "Gain and Bandwidth Enhancement of 2 × 2 Square Dense Dielectric Patch Antenna Array Using a Holey Superstrate," *IEEE Antennas and Wireless Propagation Letters,* vol. 16, pp. 1808-1811, 2017.

[47] A.K. Singh, M.P. Abegaonkar, and S.K. Koul, "High-Gain and High-Aperture-Efficiency Cavity Resonator Antenna Using Metamaterial Superstrate," *IEEE Antennas and Wireless Propagation Letters,* vol. 16, pp. 2388-2391, 2017.

[48] A. Kumar, S. Dwari, G. P. Pandey, B. K. Kanaujia, and D. K. Singh, "A high gain wideband circularly polarized microstrip antenna," Int. *J. Microw. Wirel. Technol.,* vol. 12, no. 7, pp. 678–687, Sep. 2020.

[49] P. Prakash, M. P. Abegaonkar, A. Basu, and S. K. Koul, "Gain Enhancement of a CPW-Fed Monopole Antenna Using Polarization- Insensitive AMC Structure," *IEEE Antennas and Wireless Propagation Letters,* vol. 12, pp. 1315-1318, 2013.

[50] R.V.S. R. Krishna and R. Kumar, "Slotted ground microstrip antenna with FSS reflector for high-gain horizontal polarization," *Electron. Lett.,* vol. 51, no. 8, pp. 599–600, 2015.

[51] A. Kumar, S. Dwari, and G. P. Pandey, "A Dual Band High-Gain Microstrip Antenna with a Defective Frequency Selective Surface for Wireless Applications," *J. Electromagn. Waves Appl.,* vol.35, no.12, pp.1637-1651, 2021

[52] J. Liu, Z. Tang, Z. Wang, H. Li, and Y. Yin, "Gain Enhancement of a Broadband Symmetrical Dual-Loop Antenna Using Shorting Pins," *IEEE Antennas and Wireless Propagation Letters,* vol. 17, no. 8, pp. 1369-1372, Aug. 2018

[53] X. Zhang and L. Zhu, "Gain-enhanced patch antenna without enlarged size via loading of slot and shorting pins," *IEEE Transaction on Antennas and Propagation,* vol.65, no 11, pp. 5702-5709, 2017

[54] X. Zhang and L. Zhu, "Gain-enhanced patch antenna with loading of shorting pins," *IEEE Transaction on Antennas and Propagation,* vol.64, no.8, pp. 3310-3318,2016.

[55] C.Y. Huang, J.Y. Wu, C.F. Yang, and K.L. Wong, "Gain-enhanced compact broadband microstrip antenna," *Electronics Letters,* vol. 34, no. 2, pp. 138-139, 1988.

[56] S. B. Yeap and Z. N. Chen, "Microstrip Patch Antennas with Enhanced Gain by Partial Substrate Removal," *IEEE Transactions on Antennas and Propagation,* vol. 58, no. 9, pp. 2811-2816, Sept. 2010.

[57] S. B. Yeap and Z. N. Chen, "Microstrip patch antennas with enhanced gain by partial substrate removal," *IEEE Transaction on Antennas and Propagation,* vol. 58, no.9, 2010.

[58] K. Mandal and P.P. Sarkar, "A compact high gain microstrip antenna for wireless applications," *International Journal of Electronics and Communications,* vol 67, Issue12, pp.1010-1014, 2013.

[59] P. K. Deb, T. Moyra, and P. Bhowmik, "Return loss and bandwidth enhancement of microstrip antenna using Defected Ground Structure (DGS)," *2nd International Conference on Signal Processing and Integrated Networks(SPIN),*pp. 25-29, 2015

[60] I. Khan, D. Geetha, K.R. Sudhindra, and F. Fakhruddin, "Review on Microstrip Patch Antennas for Bandwidth Improvement," *IJEECSE,* E-ISSN: 2348-2273, 2016.

[61] Md Mohiuddin et. al, "Analytical Review of Bandwidth enhancement techniques of microstrip patch antenna," *5th Int. conference for Convergence in Technology,* pp.1-5,2019.

[62] P. Singh and D.C. Dhubkarya, "Bandwidth improvement of S-Shaped microstrip patch antenna," *Global Jour. of researches in Engg.,* vol. 10, issue 5, 2010.

[63] K. Malakar, S.M.D. Abbas, and S. Chattopadhyay, "Stacked stair-case patch antenna for high gain and ultra wideband applications," *Int. Jour. of Electronics and Comm. Tech.,* vol. 2, issue 1, 2011.

[64] A.A. Deshmukh and G. Kumar, "Compact broadband E-shaped microstrip antennas", *Elect. Letters,* vol. 41, no. 18, 2005.

[65] M. S. Kushwaha, M. Chandan, and R.K. Prasad, "Improvement of bandwidth of microstrip patch antenna by multiple notches," *Conference on Advances in Comm. And Control Systems*. pp. 245-248, 2013.

[66] J. Loni, V. K. Singh, and S. Ayub, "Bandwidth improvement of microstrip patch antenna for WLAN Application," *Int. Jour. of Engg. And Technical Research,* pp. 44-46, 2014. ISSN: 2321-0869.

[67] T. R. Chanu and S. Rawat, "Bandwidth improvement using slotted triangular MPA," *3rd International Conference on Advanced Computing and Communication Technologies,* pp. 129-132, 2013.

[68] A. Gautam, A. Kumar, A.K. Jaiswal, and E.K. Chauhan, "Bandwidth improvement using slotted triangular microstrip patch antenna," *International Journal of Current engineering and Technology,* vol. 6, no. 3, 2016.

[69] K. Anum, S.S. Singh, R. Mishra, and G.S. Tripathi, "Bandwidth enhancement of a microstrip patch antenna for ultra-wideband applications," *AIP Conference proceedings,* vol. 1952, no. 1, 2018.

[70] S.J. Thomas and M. Fatima, "Bandwidth improvement of a microstrip patch antenna using partial ground plane," *International Journal of Engineering Research and Technology*, vol. 4, no. 5, pp. 87-91, 2015.

[71] S.J. Abdulkareem and G. Srivatsun, "Bandwidth improvement of microstrip patch antenna using hexagonal PDGS," *International Conference on Microwave Integrated Circuits, Photonics and Wireless Networks* , pp.15-18, 2019.

[72] S.K. Ghosh, A. Ghosh, D. Ghosh, S. Chattopadhyay, and S. Banerjee, "Rectangular microstrip antenna on ridge ground plane to control the resonant modes for improved bandwidth using traverse resonance method," *Journal of Electromagnetic Analysis and Applications,* vol.4, no.4, pp.206-211, 2012.

[73] K.L. Wong, C.L. Tang and J.Y. Chiou, "Broad-band probe-fed patch antenna with a W-Shaped ground plane," *IEEE Trans. on Antennas & Propagation,* vol. 50, no. 6, pp. 827-831, 2002.

[74] A.A. Ahmadi and Y.S.H. Khraisat, “Bandwidth enhancement of microstrip patch antenna,” *Applied Physics Research,* vol. 11, no. 1, pp.35-40, 2019.

[75] P.B. Parmar, B.J. Makwana, and M.A. Jajal, “Bandwidth enhancement of microstrip patch antenna using parasitic patch configuration,” *International Conference on Communication Systems and Network Technologies*, pp.53-57, 2012.

[76] C.K. Wu and K.L. Wong, “Broadband microstrip antenna with directly coupled and parasitic patches,” *Microwave and Optical Technology Letters,* vol. 22, issue 5, pp. 348-349, 1999.

[77] M. H. Reddy, R. Joany, and M. Reddy, “Bandwidth Enhancement of Microstrip Patch Antenna using Parasitic Patch,*” IEEE International Conference on Smart Technologies and Management for Computing, Communication, Controls, Energy and Materials*, pp. 295-298, 2017.

[78] A.Kandwal and S.K. Khah, “A Novel Design of Gap-Coupled Sectoral Patch Antenna,” *IEEE Antennas and Wireless Propagation Letters,* vol. 12, pp. 674-677, 2013.

[79] R.S.A.R. Abdullah, D. Yoharaaj, and A. Ismail, “Bandwidth Enhancement for Microstrip Antenna in Wireless Applications,” *Modern Applied Science*, vol. 2, no. 6, 2008.

[80] M. Ali, H. Jaafar, and A. Yusof, “Gain Enhancement of Air Substrates at 5.8GHz for Microstrip Antenna Array”, *Asia-Pacific Symposium on Electromagnetic Compatibility*, pp.477-480, 2012.

[81] A.G. Koutinos, G.A. Ioannopoulos, M.T Chryssomallis, and G.A. Kyriacou, "Bandwidth Enhancement of Rectangular Patch Antennas Using Multiple Feeding Points: A Review," *7th International Conference on Modern Circuits and Systems Technologies*, 2018.

[82] R. F. Harrington, “Effect of antenna size on gain, bandwidth, and efficiency,” *Journal of Research of the National Bureau of Standards- D. Radio Propagation,* vol. 64D, no.1, pp. 1-12, 1960.

[83] K.C. Gupta, “Broadbanding technique for Microstrip patch antennas- A Review”, *Scientific Report*, No. 98, 1988.

[84] S. Dwivedi, V. Mishra, and Y.P. Kosta, “Design and Comparative analysis of a Metamaterial included Slotted Patch Antenna with a Metamaterial Cover over Patch,” *International Journal of Recent Technology and Engineering,* vol. 1, no.6, pp. 1-6, 2013.

[85] M.A.W. Nordin, M.T. Islam, and N. Misran, “Design of a compact Ultra-Wideband metamaterial antenna based on the modified Split ring resonator and Capacitively Loaded Strips unit cell,” *PIER*, vol. 136, pp. 157-173, 2013.

[86] N. Kingsley, “Liquid crystal polymer: Enabling next-generation conformal and multilayer electronics,” *Microwave Journal*, vol.51, no.5, 2008.

[87] C.H. Lai, T.Y, Hanand, and T.R. Chen, “Broadband aperture-coupled microstrip antennas with low cross polarization and back radiation,” *Progress in Electromagnetics Research Letters,* vol. 5, pp. 187-197, 2008.

[88] S.Gao, L.W. Li, S. Leong, and T.S. Yes, "A broad-band dual-polarized microstrip patch antenna with aperture coupling," *IEEE Transactions on Antennas and Propagation,* vol. 51, no. 4, pp.898-900, 2003.

[89] K.S. Chin, J.A. Liu, C.C. Chang, and J.C. Cheng, "LTCC Differential-fed patch antenna with rat-race feeding structures," *Progress in Electromagnetics Research,* vol. 32, pp. 95-108, 2012.

[90] P. Li, H.W. Lai, K.M. luk, and K.L. Lau, "A wideband patch antenna with cross-polarization suppression," *IEEE Antennas and Wireless Propagation Letters*, vol. 3, no.1, pp-211-214, 2004.

[91] C.H.K. Chin, Q. Que, H. Wong, and X.Y. Zhang, "Broadband patch antenna with low cross-polarization," *Electronics Letters,* vol. 43, no. 3, 2007.

[92] Z.N. Chen and M.Y.W. Chia, "Broadband probe-fed plate antenna,"*30th European Microwave Conference*, IEEE, 2000.

[93] T.W. Chiou and K.L Wong, "Broad-band dual-polarized single microstrip patch antenna with high isolation and low cross polarization," *IEEE Transactions on Antennas and Propagation,* vol. 50, no. 3, pp.399-401, 2002.

[94] C.Y.D. Sim, C.C. Chang, and J.S. Row, "Dual-feed dual-polarized patch antenna with low cross polarization and high isolation," *IEEE Transactions on Antennas and Propagation,* vol. 57, no. 10, pp. 3405-3409, 2009.

[95] V.P. Sarin, M.S. Nishamol, D. Tony, C.K. Aanandan, P.M.Mohanan, and K. Vasudevan, "A wideband stacked offset microstrip antenna with improved gain and low cross polarization," *IEEE Transactions on Antennas and Propagation*, vol. 59, no. 4, pp. 1376-1379, 2011.

[96] J.S. Baligar, U.K. Revankar, and K.V. Acharya, "Broadband two-layer shorted patch antenna with low cross-polarization," *Electronics Letters*, vol. 37, no. 9, pp.547-548, 2001.

[97] D. Loffler and W. Wiesbeck, "Low-cost X-polarized broadband PCS antenna with low cross-polarization level," *Electronics Letters,* vol. 35, no. 20, pp.1689-1691,1999.

[98] J. Granholm and K. Woelders, "Dual polarization stacked microstrip patch antenna array with very low cross-polarization," *IEEE Transactions on Antennas and Propagation,* vol. 49, no. 10, pp. 1393-1402, 2001.

[99] W.H. Hsu and K.L. Wong, "Broad-band Probe-fed patch antenna with a U-shaped ground plane for cross-polarization reduction," *IEEE Transactions on Antennas and Propagation,* vol. 50, no. 3, pp.352-355,2002.

[100] K.L. Wong, S.W. Su, C.L. Tang, and S.H. Yeh, "Internal shorted patch antenna for a UMTS folder-type mobile phone," *IEEE Transactions on Antennas and Propagation,* vol. 53, no. 10, pp.3391-3394, 2005.

[101] J.S. Row and S.W. Wu, "Monopolar square patch antenna with wideband operation," *Electronics Letters,* vol. 42, no. 3, pp.139-140, 2006.

[102] H. Malekpoor and S. Jam, "Enhanced bandwidth of shorted patch antennas using folded-patch techniques," *IEEE Antennas and Wireless Propagation Letters*, vol. 12, pp.198-201, 2013.

[103] K.F. Leem, Y.X. Guo, J.A. Hawkins, R. Chair, and K.M. Luk, "Theory and experiment on microstrip patch antennas with shorting walls," *IEE Proc. Microw. Antennas Propag.*, vol. 147, no. 6, pp. 521-525,2000.

[104] D. Ghosh et. al., "Physical and Quantitative analysis of compact rectangular microstrip antenna with shorted non-radiating edges for reduced cross-polarized radiation using modified cavity model," *IEEE Antennas and Propagation Magazine*, vol.56, no. 4, pp. 61-72, 2014.

[105] R. Poddar, S. Chakraborty, and S. Chattapadhyay, "Improved cross polarization and broad impedance from simple single element shorted rectangular microstrip patch: Theory and experiment", *Frequenz*, vol.70, pp.1-9, 2016

[106] H.W. Liu, C.H. Weng, and C.F. Yang, "Design of Near-field edge-shorted slot microstrip antenna for RFID handheld reader applications," *IEEE Antennas and Wireless Propagation Letters*, vol. 10, pp.1135-1138, 2011.

[107] C. Kumar and D. Guha, "DGS integrated Rectangular microstrip patch for improved polarization purity with wide impedance bandwidth," *IET Micro. Ant. and Prop.*, vol. 8, no. 8, pp. 589-596, 2014.

[108] F.Y. Zulkifli, S.T. Lomorti, E.T. Rahardjo, "Improved design of triangular patch linear array microstrip antenna using isosceles triangular DGS," *Proc. of Asia-Pacific Microwave Conf.*, pp.1-4, 2007.

[109] F. Zulkifli, Y. E T. Rahardjo, D. Hartanto, "Radiation properties enhancement of triangular patch microstrip antenna array using hexagonal DGS," *Prog. Electromagn. Res. M*, vol. 5, pp. 101–109, 2008.

[110] R.D. Heydari and M.N. Moghadasi, "Introduction of a novel technique for the reduction of cross-polarization of rectangular microstrip patch antenna with elliptical DGS," *J. Electromagn. Wave Appl.*, Vol. 22, pp. 1214– 1222, 2008.

[111] C. Kumar, M.I. Pasha, and D. Guha, "Microstrip patch with non-proximal symmetric defected ground structure (DGD) for improved cross-polarization properties over principal radiation planes," *IEEE Antennas and Wireless Propagation Letters*, vol.14, pp. 1412-1414, 2015.

[112] S. Chakraborty and S. Chattapadhyay, "Substrate fields modulation with defected ground structure: A key to realize high gain, wideband microstrip antenna withimproved polarizationpurity in principal and diagonal planes," *International Journal of RF and Microwave Computer-Aided Engineering*, vol.26,no.2 pp. 174-181, 2015.

[113] A. Ghosh, S. Chakraborty, S. Chattapadhyay, A. Nandi, and B. Basu, "Rectangular microstrip antenna with dumbbell shaped defected ground structure for improved cross polarized radiation in wide elevation angle and its theoretical analysis," *IET Microwaves, Antennas & Propagation*, vol.10, no.1, pp. 68-78, 2015.

[114] A. Ghosh, D. Ghosh, and S. Chattopadhyay, "Rectangular microstrip antenna on slot type defected ground for reduced cross polarized radiation," *IEEE Antennas and Wireless Propagation Letters*, vol.14, pp. 321-324, 2014.

[115] C. Kumar and D. Guha, "Asymmetric geometry of defected ground structure for rectangular microstrip: A new approach to reduce its cross polarized fields," *IEEE Transactions on Antennas and Propagation,* vol.64, no.6, pp.2503-2506, 2016.

[116] A. Ghosh, S. Chattopadhyay, S. Chakraborty, and B. Basu, "Cross type defected ground structure integrated microstrip antenna: a novel perspective for broad banding and augmenting polarization purity", *Journal of Electromagnetic Waves and Applications,* vol.31, no.5, pp.461-476, 2017.

[117] H. Khouser and Y.K. Choukiker, "Cross polarization reduction using DGS in microstrip patch antenna," *IEEE Indian Conference on Antennas and Propogation,*pp. 1-4, 2017.

[118] M. Saravanan and M.J.S. Rangachar, "Design of wide beam hexagonal shaped circularly polarized patch antenna for WLAN application," *International Conference on Soft Computing and Pattern Recognition,* pp.142-150, 2016.

[119] Z. Zhang et. al., "The MIMO antenna array with mutual coupling reduction and cross-polarization suppression by defected ground structures," *Radio engineering,* vol. 27, no. 4, 2018.

[120] J. Acharjee, A.K. Singh, K. Mandal, and S.K. Mandal, "Defected ground structure toward cross polarization reduction of microstrip patch antenna with improved impedance matching," *Radio engineering,* vol. 28, no. 1, pp.33-38, 2019.

[121] A. Ghosh and B. Basu, "Triangular slotted ground plane: A key to realizing high-gain, cross-polarization-free microstrip antenna with improved bandwidth," *Turkish Journal of Electrical Engg. & Computer Sciences,* vol.27, no.3, pp. 1559-1570, 2019.

[122] B.N. Reddy, M.H. DSharani, S. Pavithra, A. Sivapradhayni, and V. Mekaladevi, "Suppression of cross polarization with various geometries of DGS in the design of microstrip patch antenna," *4th International Conference on Communication and Electronics Systems,* pp.464-467, 2019.

[123] X. Fu, C. Chen, C. Li, and W. Wang, "Wideband probe-fed rectangular patch with defected ground structure for cross polarization suppression," *Progress in Electromagnetics Research Letters,* vol. 84, pp. 31-38, 2019.

[124] A. Ghosh, S. Chakraborty, and S. Chattapadhyay, "Rectangular microstrip antenna with cross headed dumbbell defected patch surface for improved polarization purity," *International Conference on Microwave and Photonics (ICMAP),* pp.1-2, 2015.

[125] S. Poornima, R.G. Halappa and S. Chandramma, "Design of rectangular microstrip antenna with defected patch surface for improved cross-polarized radiation," *IEEE International Conference for Convergence in Engineering,* pp.345-346, 2020.

[126] W. You, H. Guo, W. Cai, and X. Liu, "A D-shaped defected patch antenna with enhanced bandwidth," *3rd IEEE International Symposium on Microwave, Antenna, Propagation and EMC Technologies for Wireless Communications,* pp.684-686,2009.

[127] A. Ghosh et. al., "Rectangular microstrip antenna with defected patch surface for improved polarization purity," *3rd International Conference on Computer, Communication, Control and Information Technology*, pp.1-5, 2015.

[128] A. Ghosh and B. Basu, "Rectangular microstrip antenna with defected patch surface for miniaturization and improved polarization purity," *Advances in computer, communication and control*, pp. 13-20, 2019.

[129] S. Chakraborty, A. Ghosh, S. Chattapadhyay, and L.L.K. Singh, "Improved cross polarized radiation and wide impedance bandwidth from rectangular microstrip antenna with dumbbell shaped defected patch surface," *IEEE Antennas and Wireless Propagation Letters*, vol.15, pp.84-88, 2015.

[130] A. Ghosh, S. Chattapadhyay, L.L.K. Singh, and B. Basu, "Wide bandwidth microstrip antenna with defected patch surface for low cross polarization applications," *International Journal of RF and Microwave Computer-Aided Engineering*, vol.27, no.8, 2017.

[131] A.A. Rakholiya and N.V. Langhnoja, "A review on miniaturization techniques for microstrip patch antenna," *IJARIIE*, vol. 3, no. 2, pp. 4281-4287, 2017.

[132] J.M. Mom, A.A. Roy and D.T. Kureve, "Investigation of the effect of various feed variation on the performance of a circular patch microstrip antenna," *International Journal of Applied Information Systems*, vol. 6, no. 5, 2013.

[133] P. Tilanthe, P.C. Sharma, and T.K. Bandopadhyay, "Gain enhancement of circular microstrip antenna for personal communication systems," *International Journal of Engineering andTechnology*, vol. 3, no. 2, 2011.

[134] E. Anusha, "Gain enhancement evaluation in circular microstrip patch with air substrate," *IJARTET*, vol.3, no. 1, 2016.

[135] I. Olumide, "Gain enhancement in microstrip patch antenna by replacing conventional (FR-4 and Rogers) substrate with air substrate," *IJIREC*, vol.1, pp.39-44, 2014.

[136] S. Upreti and S. Katiyar, "Gain enhancement of a circular microstrip patch antenna using dual-FSS superstrate layer for ISM band," *IOSR-JECE*, vol. 4, issue 3, pp. 36-40, 2012.

[137] J.H. Ou, J. Huang, J. Liu, J. Tang, and X.Y. Zhang, "High-gain circular patch antenna and array with introduction of multiple shorting pins," *IEEE Transactions on Antennas and Propagation*, vol.68, no.9, pp. 6506-6515, 2020.

[138] R. Banuprakash, S.A. Hariprasad, C.J. Dinah, and T.C. Hamsa, "Bandwidth enhancement of circular patch antenna using different feeding techniques," *International Journal of Engineering Science Invention*, no. 6, pp. 46-51, 2014.

[139] T. Prakoso et. al., "Bandwidth enhancement of circular microstrip antenna using characteristic mode analysis," *4th international Conference on Information Technology, Computer and Electrical Engineering (ICITACEE)*, pp.312-316, 2017.

[140] V. Punia, D. Rana, V. Kapoor, and A. Sonker, "Performance enhancement of circular patch by modified ground microstrip feed design," *International*

Journal of Electrical, Electronics and Data Communication, vol. 2, issue 7, 2014.

[141] D. Guha, M. Biswas, and Y.M.M. Antar, "Microstrip patch antenna with defected ground structure for cross polarization suppression," *IEEE Antennas and Wireless Propagation Letters,* vol. 4, pp.455-458, 2005.

[142] C. Kumar and D. Guha, "New defected ground structures (DGSs) to reduce cross-polarized radiation of circular microstrip antenna," *Applied Electromagnetics Conference,* pp.1-4, 2009.

[143] D. Guha, C. Kumar, and S. Pal, "Improved cross-polarization characteristics of circular microstrip antenna employing arc-shaped defected ground structure (DGS)," *IEEE Antennas and Wireless Propagation Letters,* vol. 8, pp.1367-1369, 2009.

[144] C. Kumar and D. Guha, "Nature of cross-polarized radiations from probe-fed circular microstrip antennas and their suppression using different geometries of defected ground structure (DGS)," *IEEE Transactions on Antennas and Propagation,* vol.60, no. 1, pp.92-101, 2012.

[145] S. Chakraborty and S. Chattopadhyay, "Arc-cornered microstrip antenna with defected structure for broad banding and improved cross-polarization suppression over whole skew planes," *International Journal of Microwave and Wireless Technologies,* vol.9 no.2, pp. 437-446, 2015.

[146] A. Ghosh, S.K. Ghosh, D. Ghosh, and S. Chattopadhyay, "Improved polarization purity for circular microstrip antenna with defected patch surface," *International Journal of Microwave and Wireless Technologies,* vol.8, no.1, pp. 89-94, 2014.

[147] D. Guha and Y.M.M. Antar, *Microstrip and Printed Antennas - New Trends. Techniques and Applications.* Chichester: *Wiley*, 2011.

[148] S. Chattopadhyay (Ed), *Trends in Research on Microstrip Antennas*. Rijeka, Croatia: Intech Open, 2017.

[149] K. F. Lee, K. M. Luk, and P. Y. Tam, "Cross-polarization characteristics of circular patch antennas," *Electron. Lett.,* vol. 28, pp. 587-589, 1992.

[150] S. K. Padhi, N.C. Karmakar, C. L. Law, and S.A. Aditya, "Dual Polarized Aperture Coupled Circular Patch Antenna Using a C-Shaped Coupling Slot," *IEEE Transactions on Antenna and propagation,* vol. 51, no. 12, pp. 3295-3298, 2003.

[151] Y. Yusuf, H. Cheng, and X. Gong, "Co-designed Substrate-Integrated Waveguide Filters with Patch Antennas," *IET Microwaves, Antenna & Propagation,* vol. 7, no. 7, pp. 493-501, 2013.

[152] S. Kojima, N. Shinohara, and T. Mitani, "Integration of a Via-Loaded Annular-Ring Reduced Surface Wave Antenna and a Branch-Line Coupler," *IEEE Access,* vol. 8, pp. 133645-133653, 2020.

[153] S. M. Rathod, R.N. Awale, K.P. Ray, and S.S. Kakatkar, "Directivity Enhancement of a Circular Microstrip Antenna with Shorting Post," *IETE journal of Research,* vol.68, no.1, pp. 504-513, 2019.

[154] K. Xu and J. Shi, "High-Efficiency Circular Dense Dielectric Patch Antenna with Frequency Selectivity," *Electronics Letter,* vol. 54, no. 14, pp. 861-862, 2018.

[155] K.K. Naik and P.A. Vijaya Sri, "Design of Hexadecagon Circular Patch Antenna with DGS at Ku Band for Satellite Communications," *Progress in Electromagnetics Research M,* vol. 63, pp. 163-173, 2018.

[156] M.A.K. Khan, T.A. Shaem, and M.A. Alim, "Graphene Patch Antenna with Different Substrate Shapes and Materials," *Optik,* vol. 202, 2020.

[157] A. Ghosh, S.K. Ghosh, D. Ghosh, and S. Chattopadhyay, "Improved polarization purity for circular microstrip antenna with defected patch surface," *International Journal of Microwave and Wireless Technologies,* vol. 8, no. 1, pp. 89-94, 2016.

[158] A. Ghosh, S. Ojha, Y. Rana, A. Anand, S. Kumar, and S. Chattopadhyay," Improved Cross Polarization Performance of Circular Microstrip Antenna with Arc Shaped Defected Patch Surface," *1st International Science & technology Congress 2014(IEMCONGRESS'2014), Elsevier Publication,* August 2014, Kolkata, India, pp. 87-92. [ISBN: 9789351072485]

[159] HFSS, "High-Frequency Structure Simulator", Version 14, Ansoft Corp.

[160] K. Mondal, L. Murmu, and P. P. Sarkar, "Investigation on compactness, bandwidth and gain of circular microstrip patch antenna," *2017 Devices for Integrated Circuit (DevIC),* pp. 742-746, Kalyani, India, 2017.

[161] A. Petosa, A. Ittipiboon, andN. Gagnon, "Suppression of unwanted probe radiation in wideband probe-fed microstrip patches," *Electronics Letter,* Vol. 35, No. 5, pp. 355–357, 1999.

[162] V. Schejbal, V. A. Kovarik, "Method of cross-polarization reduction," *IEEE Antennas Propagation Magazine,* vol. 48, pp. 108-111, 2006.

[163] Z. N. Chen, M. Y. W. Chia, "Broad-band suspended probe-fed plate antenna with low cross-polarization level," *IEEE Transactionon Antennas and Propagation,* vol. 51, pp. 345–346, 2003.

[164] N. C. Karmakar, "Investigations into a cavity backed circular patch antenna,"*IEEE Transaction on Antennas and Propagation,* vol. 50, pp. 1706–1715, 2002.

[165] A. K. Singh, R. K. Gangwar, and B. K. Kanaujia, "Cavity backed annular ring microstrip antenna loaded with concentric circular patch," *The 8th European Conference on Antennas and Propagation (EuCAP 2014),* pp. 2155-2158, Netherlands, 2014.

[166] P. U. Ankush, S. Chakraborty, L. Lolit Kumar Singh, and S. Chattopadhyay, "Application of Defected Ground Structure for Augmenting High-Gain Ultra-Wide Bandwidth from Rectangular Microstrip Antenna," *Electromagnetics,* Vol. 38, No. 2, pp. 123-133, 2018.

[167] U. A. Pawar, S. Chakraborty, T. Sarkar, A. Ghosh, L. L. K. Singh, and S. Chattopadhyay, "Quasi-Planar Composite Microstrip Antenna: Symmetrical

Flat-Top Radiation With High Gain and Low Cross Polarization," *IEEE Access*, Vol. 7, No. 1, pp. 68917-68929, 2019

[168] S.Chattopadhyay, J. Y. Siddiqui, and D. Guha, "Rectangular Microstrip Patch on A Composite Dielectric Substrate for High Gain Wide Beam Radiation Patterns", *IEEE Transactions on Antennas & Propagations*, Vol.57, No.10, pp.3324-3327, 2009

[169] D. Guha, S. Chattopadhyay, and J.Y.Siddiqui, "Estimation of Gain Enhancement Replacing PTFE by Air Substrate in a Microstrip Patch Antenna," *IEEE Antennas & Propagations Magazine,* Vol.52,No.3, pp.92-95, 2010.

[170] Y.Yusuf, H.Cheng, and X. Gong, "Co-designed substrate-integrated waveguide filters with patch antennas," *IET Microwave, antennas and propagation,* Vol.7, No.7, pp.493-501,2013.

[171] S.Chattopadhyay and S. Chakraborty, "A Physical Insight Into the Influence of Dominant Mode of Rectangular Microstrip Antenna on Its Cross-Polarization Characteristics and Its Improvement With T-Shaped Microstrip Antenna", *IEEE Access,* USA, Vol. 6, No. 1, 2018, pp. 3594-3602.

[172] D. Ghosh, S. K. Ghosh, and S. Chattopadhyay, "Physical and Quatitative Analysis of Compact Rectangular Microstrip Antenna with Shorted Non radiating Edges for Reduced Cross Polarized Radiation Using Modified Cavity Model," *IEEE Antennas& Propagations Magazine*, USA, Vol.56, No.4, pp.61-72, 2014.

[173] X. Zhang, and L. Zhu, "Patch Antennas With Loading of a Pair of Shorting Pins Toward Flexible Impedance Matching and Low Cross Polarization," *IEEE Transactions on Antennas and Propagation,* Vol. 64, no. 4, pp.1226-1233, 2016.

[174] N.W. Liu, L. Zhu, G. Fu, and Y. Liu, "A Low Profile Shorted-Patch Antenna With Enhanced Bandwidth and Reduced H-Plane Cross-Polarization," *IEEE Transactions on Antennas and Propagation*, Vol. 66, no. 10, pp.5602-5608, 2018.

[175] R.B. Waterhouse, "Improving the Efficiency of Microstrip Patch Antennas. In: Microstrip Patch Antennas: A Designer's Guide," pp. 167-195, *Springer, Boston, MA*, 2003

[176] A. R. Alajmi and M. Saed, "Simplified microstrip patch antenna design for reduced surface wave applications," *IEEE Antennas and Propagation Society International Symposium (APSURSI),* pp. 1849-1850, Memphis, TN, 2014.

[177] D.R. Jackson, "Reduced Surface Wave Microstrip Antennas," *Handbook of Antenna Technologies, Z. N. Chen et. al. (Eds)*, Springer 2016

[178] D.R. Jackson, J.T. Williams, A. K. Bhattacharyya, R. L. Smith, and S.A. Long, "Microstrip Patch Designs That Do Not Excite Surface Waves,"*IEEE Transactions on Antennas and Propagation,* Vol. 41, no. 8, pp.1026-1037, 1993.

[179] M.M. Nikolic, A. R. Djordjevic, and A. Nehorai, "Rectangular Microstrip Antennas with Suppressed Radiation in Horizontal directions and Reduced Coupling," *IEEE Transactions on Antennas and Propagation,* Vol. 53, no. 11, pp.3469-3475, 2005.

[180] S. I. Maslovski, S. A. Tretyakov, and P.A. Belov, "Wire Media with Negative Effective Permittivity: A Quasi-static Model," *Microwave and Optical Technology Letters,* vol. 35, no. 1, pp.47-50, 2002

[181] G.P. Gauthier, A. Courtay, and G.M. Rebeiz, "Microstrip Antennas on Sythesized Low Dielectric Constant substrate," *IEEE Transactions on Antennas and Propagation,* vol. 45, no. 8, pp.1310-1314, 1997

[182] P.Lowes, S. Scott, E. Korolkiewicz, and A. Sambell, "Quasi_satatic Capacitance and Frequency Dependent Effective Permittivity of Multilayer Microstrip Patch Antennas," *IEE Proc. Microw. Ants. Prop.,* vol. 145, no. 1, pp.75-79, 1998.

[183] R. Poddar, S.Chakraborty, and S. Chattopadhyay, "Improved Cross Polarization and Broad Impedance Bandwidth from Simple Single Element Shorted Rectangular Microstrip Patch:Theory and Experiment," *Frequenz,* Germany, Vol. 70, No. 1-2, pp. 1-9, 2016.

[184] S. F. Mahmoud and A. R. Al-Ajmi, "A Novel Microstrip Patch Antennawith Reduced Surface Wave Excitation," *Progress In Electromagnetics Research,* PIER 86, pp. 71–86, 2008.

[185] H. Boutayeb and T.A. Denidni, "Gain Enhancement of a Microstrip Patch Antenna Using a Cylindrical Electromagnetic Crystal Substrate," *IEEE Transactions on Antennas and Propagation,* Vol. 55, no. 11, pp.3140-3145, 2007.

[186] B. Roudot, C. Terret, and J.P. Daniel, "Fundamental Surface Wave Effects on Microstrip Antenna Radiation," *Electron. Lett.,* Vol. 21, no.23, pp.1112-1114, 1985.

[187] J.D. Kraus, and R.J. Marhefka, *Antennas: for All Applications,* 3rd ed: Mc Graw Hill, 2003.

[188] V. Pathak, S. Thomwall, M. Krier, S. Rowson, G. Poilasne, and L. Desclos, "Mobile Handset System Performance Comparison of a Linearly Polarized GPS Internal Antenna with a Circularly Polarized Antenna,"*IEEE Antennas and Propagation Society International Symposium. Digest.* Columbus, *OH,* vol.3, pp. 666-669, 2003.

[189] S. Chakraborty and S. Chattopadhyay, " Arc- Cornered Microstrip Antenna with Defected Ground Structure for Broad Banding and Improved Cross-Polarization over whole skew planes," *International Journal of Microwave and Wireless Technologies*, Cambridge University Press and the European Microwave Association, vol.9, no.2, pp.437-446, 2015.

[190] M. U. Khan, M. S. Sharawi, and R. Mittra, "Microstrip patch antenna miniaturization techniques: A review," *IET Microwaves, Antennas &Propagation*, vol. 9, no. 9, pp. 913-922, June, 2015.

[191] M.A. Khayat, J. T. Williams, D. R. Jackson, and S. A. Long, "Mutual coupling between reduced surface wave microstrip antennas," *IEEE Transactions on Antennas and Propagation*, vol.48, no. 10, pp.1581-1593, Oct. 2000.

[192] J.G. Yook and L. P. B. Katehi, "Micromachined microstrip patch antenna with controlled mutual coupling and surface waves," *IEEE Transactions on Antennas and Propagation*, vol.49, no. 9, pp.1282-1289, Sep. 2001.

[193] Zonunmawii, A. Ghosh, L. L. K. Singh, S. Chattopadhyay, and C.Y.D. Sim, "Reduced-Surface-Wave-Inspired Circular Microstrip Antenna for Concurrent Improvement in Radiation Characteristics", *IEEE Antenna & Wave Propagation Letter*, vol. 20, Issue 5, pp. 858-862, May. 2021.

[194] A. Nehorai, and E. Paldi, "Vector-sensor array processing for electromagnetic source localization," *IEEE Transaction on Signal Processing*, vol.42, no. 2, pp.376-398, Feb. 1994.

[195] J. Li, P. Stoica, and D. Zheng, "Efficient direction and polarization estimation with a COLD array," *IEEE Transactions on Antennas and Propagation*, vol.44, no. 4, pp.539-547, Apr. 1996.

[196] N. G. Alexopoulos, and D. R. Jackson, "Fundamental superstrate (Cover) effects on printed circuit antennas," *IEEE Transactions on Antennas and Propagation*, vol.32, no. 8, pp.807-816, Aug. 1984.

[197] S. D. Cheng, R. Biswas, E. Ozbay, S. M. C. Calmont, G. Tuttle, and K.-M. Ho "Optimised dipole antennas on photonic bandgap crystals," *Appl. Physics Letters*, vol.67, no. 23, pp. 3399-3401, Dec. 1995.

[198] R. Coccioli, T. Itoh, "Design of photonic bandgap substrates for surface wave suppression*," Proc. MTT-S Int. Microwave Symposium Digest*, pp. 1259-1262, Baltimore, MD, USA,1998.

[199] S.J. Li, J. Gao, X. Cao, Z. Zhang, and D. Zhang, "Broadband and high-isolation dual polarized microstrip antenna with low radar cross section," *IEEE Antennas and Wireless Propagation Letters*, vol.13, pp. 1413-1416, 2014.

[200] S. J. Li, Y. B. Li, H. Li, Z. X. Wang, C. Zhang, Z. X. Gao, R. Q. Li, X. Y. Cao, Q. Cheng, and T. J. Cui, "A thin self-feeding Janus metasurface for manipulating incident waves and emitting radiation waves simultaneously," *Annalen der Physik*, vol. 532, no. 5, pp. 1-13, 2020.

[201] F. E. Terman, *Electronic and Radio Engineering*. Singapore: McGraw Hill,1955.

BIO-DATA OF THE CANDIDATE

Name of Candidate	:	Zonunmawii
Date of Birth	:	12/05/1988
Contact	:	9862119935
		zonunimiller12@gmail.com
Permanent Address	:	D/O: Zothantluanga
		Vill: Zotlang
		PO: Vaivakawn
		Dist: Aizawl
		Pin: 796009, Mizoram
Married	:	Yes

Educational Details

(a) B. E.	:	Visvesvaraya Technological University, Belgaum, Karnataka, India
(b) M.Tech.	:	Electronics and Communication Engineering, Lovely Professional University, Punjab
(c) Ph. D. Course work:		SGPA of 9.00.

Present Occupation Details

Organization	:	Mizoram University
Rank	:	Assistant Professor, Department of Electronics & Communication Engineering
Job Profile	:	Teaching and management of B.Tech. and M.Tech. courses of Department of Electronics & Communication Engineering, Mizoram University

LIST OF PUBLICATION

Journal publications:

1. **Zonunmawii**, Abhijyoti Ghosh, L. L. K. Singh, Sudipta Chattopadhyay, "Cavity Field Modulation with Modulating Circular Patch Antenna Surface: A Key to Realize Reduced Horizontal Radiation and Omni-present Improvement in Radiation Performance," *IEEE Access*, Vol. 10, pp. 18434- 18444, 2022. [ISSN 2169-3536] [Impact Factor: 3.476 (Thomson Reuters)]
2. **Zonunmawii,** Abhijyoti Ghosh, L. L. K. Singh, Sudipta Chattopadhyay, Chow-Yen-Desmond Sim, "Reduced-Surface-Wave-Inspired Circular Microstrip Antenna for Concurrent Improvement in Radiation Characteristics," *IEEE Antenna & Wave Propagation Letter*, Vol. 20, Issue 5, pp. 858-862, 2021. [ISSN 1536-1225] [Impact Factor: 3.825 (Thomson Reuters)].

Conference publications:

1. **Zonunmawii**, L. Lolit Kumar Singh, Sudipta Chattopadhyay, Abhijyoti Ghosh, "Rectangular Strip Loaded Circular Patch Antenna for Simultaneous Improvement of Co polar Gain and Co Polarization to Cross Polarization radiation Separation," *2022 2nd International Conference on Artificial Intelligence and Signal Processing (AISP)*, February, 2022, pp.1-4, Vijayawada, India. (**Paper presented**)
2. **Zonunmawii**, L. Lolit Kumar Singh, Sudipta Chattopadhyay, Abhijyoti Ghosh, "Circular Microstrip Antenna with Shorting Walls for Improved Radiation Performance," *International Conference on Emerging Electronics and Automation, National Institute of Technology*, Silchar, 17th -19th December, 2021. (**Paper presented**)
3. **Zonunmawii**, Manoj Sarkar, L. Lolit Kumar Singh, Sudipta Chattopadhyay, Abhijyoti Ghosh, "Enrichment of Impedance Bandwidth and Co-Polarization to Cross Polarization Isolation of Circular Patch Antenna with Rectangular DGS structure," *International Conference on Intelligent Computing Systems and Applications (ICICSA 2022)*, National Institute of Technology, Silchar, Assam, September 23-24, 2022. (**Paper presented**)
4. **Zonunmawii**, Manoj Sarkar, L. Lolit Kumar Singh, Sudipta Chattopadhyay, Abhijyoti Ghosh, "Curved Shaped Defected Ground Structure: A way to achieve high Polarization Purity, Wide Bandwidth and Stable Gain," *International Conference on Intelligent Computing Systems and Applications (ICICSA 2022)*, National Institute of Technology, Silchar, Assam, September 23-24, 2022. (**Paper presented**)

IEEE Access
Multidisciplinary | Rapid Review | Open Access Journal

Received November 8, 2021, accepted November 21, 2021, date of publication November 25, 2021,
date of current version February 18, 2022.

Digital Object Identifier 10.1109/ACCESS.2021.3130914

Cavity Field Modulation With Modulating Circular Patch Antenna Surface: A Key to Realize Reduced Horizontal Radiation and Omni-Present Improvement in Radiation Performance

ZONUNMAWII, ABHIJYOTI GHOSH, LOUREMBAM LOLIT KUMAR SINGH, AND SUDIPTA CHATTOPADHYAY
Department of Electronics and Communication Engineering, Mizoram University, Aizawl 796004, India
Corresponding author: Abhijyoti Ghosh (abhijyoti_engineer@yahoo.co.in)

ABSTRACT Although, the circular microstrip antennas are the most popular tiny planar antennas, increased horizontal radiation in the E plane imposes a severe limitation in case of modern applications such as array or 5G MIMO configurations. Further, low broadside gain, high H plane cross polar radiation reduces the efficiency of antenna for different wireless applications. Therefore, in order to cope up with the ubiquitous development of tiny and efficient wireless communication devices, antenna structure is to be judiciously modified. Symmetrical modification on patch structure by loading a pair of thin strip on circular patch with shorting posts germinates a modified circular patch with excellent radiation performances. High gain of around 9.2 dBi with excellent polarization purity of 27 dB has been achieved with such structure. Further, an excellent radiation characteristic of reduced horizontal radiation (21 dB down than peak co-polar gain) with 92% efficiency has been revealed from the present antenna. A clear physical insight in to the observed characteristics has been thoroughly documented. The antenna is simple, easy to manufacture and measured results are in close agreement with simulated results.

INDEX TERMS Gain, horizontal radiation, microstrip antenna.

I. INTRODUCTION

Circular microstrip antenna (CMA) on dielectric substrate is well known tiny antenna and the most popular genre of printed antennas although it suffers from poor gain, low efficiency and poor polarization purity (PP). However, this circular microstrip antenna is still be the first choice for use in industry because of its simple design procedure and well-developed theory [1]. Beside these shortcomings, another major but less investigated shortcoming of such CMA is a strong radiation fields along horizontal direction i.e., along ground plane. This radiation is undeniably undesirable for many applications like 5G MIMO, array [2]–[4] configuration or in vector sensors [5], [6]. The far field coupling of antenna elements in an array is mainly due to the strong patch radiation along horizontal direction. Therefore, this can be only minimized by judicious design of antenna structure with reduced horizontal radiation.

The gain enhancement in circular patches has been investigated in [7]–[14]. The technique such as slot-loading with aperture coupling [7] and the use of 3 stacked ground plane with slot and shorting vias [8] have been adopted to achieve around 7.8 dBi gain with no improvement in PP (Co-polar to cross-polar radiation isolation). To further increase the gain from 7.2 dBi to 9 dBi with PP of 18-19 dB only, the annular ring antenna in [9] was loaded with shorting vias (with branch line couplers), while numerous shorting vias beneath the circular patch have been reported in [10]. Notably, a structure similar to [8]–[10] has been reported in [11], and it can achieve high gain of 11 dBi but suffers from poor polarization purity of 17 dB and a much-distorted radiation pattern with a high side-lobe level. To attain high gain of around 6.8 dBi to 8 dBi for patch antenna, various techniques have been investigated, such as the adaptation of circular dual-stacked dense dielectric patch [12], replacement of circular patch

The associate editor coordinating the review of this manuscript and approving it for publication was Tutku Karacolak.

Reduced-Surface-Wave-Inspired Circular Microstrip Antenna for Concurrent Improvement in Radiation Characteristics

Zonunmawii, Abhijyoti Ghosh, L. Lolit K. Singh, Sudipta Chattopadhyay, *Member, IEEE*, and Chow-Yen-Desmond Sim, *Senior Member, IEEE*

***Abstract*—Classical microstrip patch antenna fabricated on a dielectric substrate suffers from poor gain, efficiency, and high cross polarization due to the automatic excitation of TM_0 surface wave. It also radiates strong fields along the horizon which is susceptible to multiple-input–multiple-output (MIMO) or array configurations. In view of this, a separate class of circular microstrip antenna known as the reduced surface wave (RSW) circular patch antenna has been proposed with a pair of shorting strips. Unlike earlier RSW-inspired antennas that mainly confirmed their ability for the successful reduction in the mutual coupling between array elements, here, and the enhancement of radiation properties is considered.**

***Index Terms*—Cross polarization, microstrip antenna, reduced surface wave (RSW).**

I. Introduction

THE circular microstrip antenna (CMA) based on reduced surface wave (RSW) theorem is a typical category of microstrip antennas (MA) that extremely reduces the surface wave fields than conventional CMA. Therefore, such RSW-inspired CMA is immensely preferable as they have reduced horizontal radiation. Moreover, the fundamental TM_0 surface wave causes increased mutual coupling, which is undesirable for any array or multiple-input–multiple-output (MIMO) configuration. Furthermore, the lateral radiation arises due to the surface wave usually interact with other associated circuitry or the supporting structure of hand-held equipment. However, such TM_0 surface wave elimination is impossible in conventional design (as it has zero cutoff frequency) until a special surface wave mitigation technique has been employed.

In the last several years, many works have been reported to enhance the gain of MA [1]–[5] by employing composite antenna topology or composite substrate. The gain and efficiency enhancement in CMA have been investigated in [6]–[13]. Different techniques [6]–[13] have been employed to yield maximum 7–8 dBi gain with maximum 73% efficiency. Notably, all these techniques fail to address the issue of copolar radiation (CP) to cross-polar radiation (XP) isolation (CP-XP isolation). Furthermore, the structures are complex, bulky and difficult to manufacture.

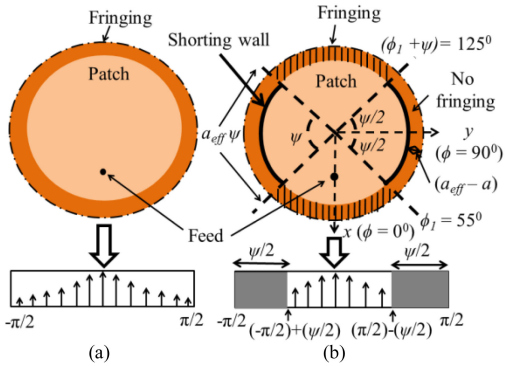

Fig. 1. Schematic representation of patch. (a) Conventional CMA. (b) Proposed antenna with field distribution at lower radiating slots for conventional and proposed antenna.

Numerous efforts have also been given [14]–[19] to maximize CP-XP isolation (22–23 dB) with no improvement in gain and efficiency. Moreover, none of the studies are reported to reduce horizontal radiation arises from the surface wave that can mutilate the antenna performances [20]. Therefore, the isolation between boresight gain (BG) to horizontal direction gain (HG) (BG-HG isolation) is a crucial factor to determine in case of GPS receiving antenna [21] or base transreceiver station antenna for microcellular system [20]. In order to address the lacunae of the earlier studies, a CMA with a pair of shorting strip (shown in Fig. 1) has been proposed based on RSW theorem.

In the present investigation, a simple RSW antenna using only a pair of shorting strips has been employed for simultaneous improvement in gain, efficiency, and polarization purity. The proposed RSW antenna can also successfully suppress the radiation along the horizontal direction. Radiating and nonradiating slot aperture fringing field is judiciously modulated to yield high aperture efficiency. Detailed analysis is provided to facilitate antenna designers.

II. Theoretical Insight

The present antenna excites the dominant mode similar to conventional CMA with a frequency shift toward the higher side of the spectrum. This is due to the modified permittivity of

Manuscript received February 2, 2021; revised March 8, 2021; accepted March 8, 2021. Date of publication March 17, 2021; date of current version May 5, 2021. *(Corresponding author: Sudipta Chattopadhyay.)*

Zonunmawii, Abhijyoti Ghosh, L. Lolit K. Singh, and Sudipta Chattopadhyay are with the Department of Electronics and Communication Engineering, Mizoram University, Aizawl 796004, India (e-mail: zonunimiller12@gmail.com; abhijyoti_engineer@yahoo.co.in; llksingh@yahoo.co.in; piyalirekha@yahoo.com).

Chow-Yen-Desmond Sim is with the Department of Electrical Engineering, Feng Chia University, Taichung 40724, Taiwan (e-mail: cysim@fcu.edu.tw).

Digital Object Identifier 10.1109/LAWP.2021.3065677

PARTICULARS OF THE CANDIDATE

NAME OF CANDIDATE	:	ZONUNMAWII
DEGREE	:	Ph.D.
DEPARTMENT	:	ELECTRONICS AND COMMUNICATION ENGINEERING
TITLE OF THESIS	:	INVESTIGATION OF CIRCULAR MICROSTRIP ANTENNA WITH IMPROVED INPUT AND RADIATION CHARACTERISTICS
DATE OF ADMISSION	:	26th JULY 2019
APPROVAL OF RESEARCH PROPOSAL:		
1. DRC	:	3rd MARCH 2020
2. BOS	:	22nd APRIL 2020
3. SCHOOL BOARD	:	13th MAY 2020
MZU REGISTRATION NO.	:	1904972
PH. D REGISTRATION NO. & DATE	:	MZU/PH.D./1618 of 26.07.2019
EXTENSION	:	NO

_____

Head

Department of Electronics and Communication Engineering

ABSTRACT

INVESTIGATION OF CIRCULAR MICROSTRIP ANTENNA WITH IMPROVED INPUT AND RADIATION CHARACTERISTICS

AN ABSTRACT SUBMITTED IN PARTIAL FULFILLMENT OF THE REQUIREMENTS FOR THE DEGREE OF DOCTOR OF PHILOSOPHY

ZONUNMAWII

MZU REGN NO: 1904972

PH. D REGN NO: MZU/Ph.D./ 1618 of 26.07.2019

DEPT. ELECTRONICS & COMMUNICATION ENGINEERING
SCHOOL OF ENGINEERING AND TECHNOLOGY

AUGUST 2022

INVESTIGATION OF CIRCULAR MICROSTRIP ANTENNA WITH IMPROVED INPUT AND RADIATION CHARACTERISTICS

BY

Zonunmawii
Department of Electronics & Communication Engineering

Name of Supervisor : Dr. Abhijyoti Ghosh
Name of Joint Supervisor : Prof. Sudipta Chattopadhyay

Submitted

In partial fulfillment of the requirement of the Degree of Doctor of Philosophy in Electronics & Communication Engineering of Mizoram University, Aizawl

In the present wireless world, the requirement of designing a small, compatible and affordable antenna continues to grow. A circular microstrip antenna (CMA) is one of the most popular small antennas and is a good contender in the field of communication engineering due to its small size, less cost and light weight. Further, such antenna is very attractive due to its ease of fabrication with active devices like monolithic microwave integrated circuits (MMICs), hybrid microwave integrated circuits (HMICs) and microelectromechanical systems (MEMSs). The easy design techniques and established theory makes CMA a primary choice of industry for different communication systems. The required redial dimension of circular microstrip patch antenna is smaller than rectangular microstrip patch antenna. Therefore, in the present wireless world where miniaturized antennas are of great demand, circular microstrip patch antenna will be more effective for tiny and compact electronic devices. So out of the different geometries of a patch Circular Patch is chosen for present investigation.

Some other advantages of circular patch geometry are given below:

i. have smaller dimension that are related with the operating frequency.

ii. offers a number of radiation pattern options that are not readily implemented using a rectangular patch.

iii. the fundamental mode TM_{11} of a circular microstrip yields a radiation pattern comparable to the lower order modes of a rectangular patch antenna

iv. In a circular microstrip antenna, the only parameter that can be varied for the structure design is the patch radius. So, this makes the circular patch more popular and widely used.

From the reason stated above it is concluded that circular microstrip patch antenna is more advantageous than the other geometries.

Beside the advantages of CMA, it has several disadvantages such as narrow impedance bandwidth, poor polarization purity, poor co-polar gain and less efficiency. Microstrip antenna (MA) fabricated on a dielectric substrate suffers from

high cross polarization (XP) due to the excitation of TM_0 surface waves. Strong radiation fields along the horizontal direction are also radiated which is susceptible to MIMO and array configurations.

A CMA emits linearly polarized broad side fields in TM_{11} mode which is the dominant mode of a CMA. The linearly polarized broadside fields occurred due to the fringing fields that reside at the radiating edges of the patch. However, when a CMA emits broad side fields, a few handful amount of fringing fields are also emitted from the non-radiating edge. These orthogonal fields are undesirable and these unwanted fields are called as cross polarization (XP) radiation. The orthogonal resonance field of TM_{11} along with higher orthogonal excitation mode TM_{21} is mainly responsible for producing high XP radiation. Due to high XP radiation the polarization purity becomes very poor which limits the use of CMA for different wireless applications. Increased horizontal radiation in E plane also imposes a severe limitation in case of modern applications such as 5G MIMO and array configurations.

In this dissertation, an investigation has been carried out for improvement of the input and radiation characteristics of a CMA. The inherent disadvantages of a CMA such as low co-polar gain, low efficiency, poor polarization purity, narrow impedance bandwidth and increased horizontal radiation in E plan has been investigated and different techniques are proposed to enhance the shortcomings.

Initially, the introduction of CMA along with its technical details has been discussed. The first chapter contains an exclusive literature survey on existing techniques to enhance the co-polar gain, bandwidth and polarization purity of a CMA.

After thorough literature review, shorting and strip loading approach to improve the co-polar gain and polarization purity have been studied. The investigation has been started by incorporating shorting walls at the non-radiating edge along the periphery of a CMA. FR4 and glass substrate with two different substrate thicknesses are considered for detailed study. It has been observed that all the proposed structures provide simultaneous improvement in co-polar gain and polarization purity

as compared to a conventional CMA. After this, strip loading approach has been investigated by placing a thin rectangular strip at the top of a conventional CMA. This proposed structure provides a co-polar gain of 7.5 dBi and a polarization purity of 23 dB. Simultaneous enhancement of co-polar gain and polarization purity has been achieved without disturbing the conventional E plane radiation pattern which is very much required for the modern wireless communication.

After this, defected ground structure (DGS) approach has been investigated for wideband CMA. Two DGS structures are proposed to provide enhancement in impedance bandwidth and polarization purity. First, a curved dumbbell shape defect deployed on the ground plane at the non-radiating edge has been proposed. A polarization purity of 25.8 dB with 12% impedance bandwidth is achieved with this structure. Next, a DGS structure with a pair of rectangular defects placed on the ground plane at the radiating edge of a conventional CMA has been investigated. This structure provides enrichment in impedance bandwidth and polarization purity. Impedance bandwidth of 31.5% and a polarization purity of 24 dB have been achieved with this structure. The proposed structures provide enhancement in impedance bandwidth and polarization purity and will be useful in modern wireless communication field where high polarization purity and wide impedance bandwidth is required.

After this, a less investigated shortcoming of a CMA which is strong radiation field along the horizontal direction is investigated along with low co-polar gain, low efficiency and poor polarization purity. A co-polar gain of 8.5 dBi, polarization purity of 25 dB and efficiency of 93% is achieved using a simple reduced surface wave (RSW) antenna using only a pair of shorting strips at the non-radiating edge of a CMA. The proposed antenna also successfully suppresses the radiation along the horizontal direction. This improvement will be helpful for 5G MIMO and array configurations.

Lastly, a CMA has been symmetrically modified by placing a pair of thin rectangular strips at the top and bottom of the patch. Further, 12 shorting pins are symmetrically placed at the corners of the rectangular strip. This structure is proposed to eliminate the surface wave, provides improvement in co-polar gain,

polarization purity, efficiency and to suppress the horizontal radiation in E plane. Excellent improvement in the radiation performance with polarization purity of 27 dB, efficiency of 92% and a high co-polar gain of 9.2 dBi has been obtained. The horizontal radiation is 21 dB down than the peak co-polar gain which shows a reduction in the horizontal radiation. This proposed antenna will be helpful for modern research and scientific community looking for tiny planar structure with excellent radiation properties. It will also be useful for modern array and 5G MIMO configuration.